The Hong Kong Polytechnic University

Department of Health Technology and Informatics

THE EFFECT OF THE SUBTALAR ORIENTATIONS ON THE PLANTAR FOOT GEOMETRY

LEE KA LAI

A thesis submitted in partial fulfillment of the requirements for the degree of Master of Philosophy

January 2008

Certificate of Originality

I hereby declare that this thesis is my own work and that, to the best of my knowledge and belief, it reproduces no material previously published or written, nor material that has been accepted for the award of any other degree or diploma, except where due acknowledgement has been made in the text.

_____

LEE Ka Lai

Date: 8/4/09

The Effect of the Subtalar Orientations on the Plantar Foot Geometry

Abstract

Foot alignment control is regarded as one of the most important elements in the impression procedure in foot orthosis. Keeping the subtalar joint in its neutral position by palpating the joint congruity and keeping the plane of the forefoot parallel to the plane of the heel are recommended. However, results of gait analyses showed that the subtalar joint is in an everted position for over 60% of the stance phase in normal walking. The rationale of keeping the subtalar joint in a neutral position during the foot impression procedure is questionable. This study aimed at investigating the effect of the subtalar orientations on the plantar foot geometry three-dimensionally. Twenty adults with normal foot type participated in this study. Bilateral foot impressions were taken with the subtalar joint angles ranging from 2° inversion to 4° eversion. The plane of the forefoot at the metatarsal heads region was kept perpendicular to the calcaneal bisection line. Positive plaster models were generated from these impressions and scanned with a three dimensional laser imaging system. Custom computer software was designed to quantify the plantar foot geometry in terms of foot parameters such as projection volumes at different foot regions, medial-lateral cross-section slopes, arch heights, and etc. It was

observed that the projection volume and the medial-lateral slopes of the medial longitudinal arch were the lowest at 2° eversion. On the other hand, the projection volume under the medial forefoot region became the highest at 4° eversion. Although these were significant differences found in the projection volume under the medial midfoot regions among various subtalar joint orientations, the changes in the arch heights were 0.1 - 0.6 mm (p = 0.05). This implied that the changes were concentrated at the soft tissue margin medial to the medial longitudinal arch. Thus it is suggested that the subtalar neutral position during foot impression procedure should not be over emphasized. Investigation on the effect of the forefoot alignment control on the plantar geometry is recommended in further studies.

Acknowledgements

I would like to express my deepest gratitude to Dr. Aaron Leung, my chief supervisor, for his guidance, encouragement and continual support throughout this study. His enthusiastic attitude towards the foot orthotics impressed me deeply.

I must thank Dr. Ming Zhang, my co-supervisor, and Dr. Ameersing Luximon, for their valuable advices in computer programming for analysis the foot models. I would also like to thank Dr. Daniel Chow, for his kindly advice in data analysis and continual encouragement.

Sincere appreciation is expressed to all the subjects. Without their voluntary participation in this study, this study could not be completed.

Last but not the last, I am indebted to my husband and my sisters for their loving support and patience during the course of the work.

Table of Content

List of figures

List of tables

List of Appendices

Glossary:

1. **Movement along the sagittal plane**

Sagittal plane divides the body into sinister and dexter (left and right) portions

Dorsiflexion: the distal body segment moving towards the proximal body segment in the sagittal plane

Plantarflexion: the distal body segment moving away the proximal body segment in the sagittal plane

2. **Movement along the transverse plane**

Transverse plane divides the body into cranial and caudal (head and tail) portions

Abduction: moving away from the body midline in the transverse plane

Adduction: moving towards from the body midline in the transverse plane

3. **Movement along the frontal plane**

Frontal plane divides the body into dorsal and ventral (posterior and anterior, or back and front) portions

Inversion: moving towards from the body midline in the frontal plane

Eversion: moving away from the body midline in the frontal plane

4. **Subtalar joint angle**

Tibial bisection line: the midline on the posterior surface of the lower one third of the leg. Clinically, it is done by connecting the two midpoints of the

widths at the distal one third of the tibia and at the position just proximal to the malleoli.

Calcaneal bisection line: the midline on the posterior surface of the calcaneus. Clinically, it is done by defining the two midpoints of the widths at the level just distal to the malleoli and at the level of the turning point of the curvature at the distal calcaneus.

Subtalar joint angle: the angular deviation of the parallel orientation of the calcaneal bisection line to the tibial bisection line. It is usually quantified by the inversion/eversion component of the subtalar joint. ***Subtalar inversion*** means the calcaneal bisection line moves towards the midline of the body while ***Subtalar eversion*** means the calcaneal bisection line moves away from the midline of the body.

The motion of the subtalar joint: Subtalar joint is a triplanar joint. ***Subtalar pronation*** includes dorsiflexion, eversion and abduction. ***Subtalar supination*** includes plantarflexion, inversion and adduction.

5. <u>Forefoot-to-rearfoot angle</u>

Plane of the forefoot: the imaginary plane of the first and the fifth metatarsal heads in the plantar forefoot region.

Forefoot-to-rearfoot angle: the angular deviation of the perpendicular orientation of the plane of the forefoot to the calcaneal bisection line in the frontal plane. It quantifies the midtarsal joint orientation. ***Forefoot varus*** means the plane of the forefoot rotates towards the midline of the body while ***forefoot valgus*** means the plane of the forefoot rotates away from the midline of the body respective to the calcaneal bisection line.

Chapter 1. Introduction

1.1. Research problems

The subtalar joint is the articulation between the talus and the calcaneus. Its orientation is usually represented by the inversion/eversion angle between the bisection lines of the posterior lower one third of the tibia and the posterior calcaneus in the frontal plane. Results of cadaveric studies showed that the subtalar joint orientation would affect the range of the motion of the forefoot through the midtarsal joint (Phillips and Phillips, 1983; Blackwood et al., 2005).

The subtalar joint neutral position is always emphasized in the foot examination and impression procedure in foot orthotics. The concept was based on the observations of Wright et al. (1964) and Root et al. (1971 and 1977). Root and his associates (1971 and 1977) claimed that the calcaneal bisection line of a normal person was vertical during standing, and suggested that the foot orthosis generated from the subtalar joint neutral impression procedure would help to achieve normal subtalar joint movement in a person with foot deformity. However, results of recent biomechanical studies deviated from these concepts. Statically, the angle between the calcaneal bisection line and the imaginary vertical line in relaxed standing (also known as relaxed calcaneal stance position (RCSP)) was everted (Gheluwe et al., 2002; Sell et

al., 1994; Sobel et al., 1999; Payne et al., 2001); dynamically the subtalar joint angle during midstance was in an everted position (Perry and Laotune., 1995; McPoil and Cornwall, 1996a; McPoil and Cornwall, 1996b; Mannon et al., 1997; Torburn et al., 1998). The orthosis generated from subtalar neutral position during impression procedure might impose a hidden supinatory force on the foot (Ball and Afheldt, 2002a). The concept of the subtalar joint neutral position remains one of the key controversial issues in foot orthotics (McPoil and Hunt, 1995; Menz, 1997; Ball and Afheldt, 2002a and 2002b).

The reliability of the clinical measurement of foot parameters such as the relaxed calcaneal stance position (RCSP), the subtalar joint neutral position (STJN) and the forefoot-to-rearfoot angle were low (Ghelvwe et al., 2002; Evans et al., 2003). Thus, the reliability to achieve the subtalar joint neutral position during foot impression procedure is questionable.

Although the underlying mechanism of orthoses in tackling foot disorders is unclear (Nigg, 2000; Payne and Chuter, 2001), the concepts of subtalar joint neutral position in the foot impression procedure has been widely used. The impression procedure

was regarded as an art rather than a science (Sobel and Levitz, 1997). Variations in foot impression procedure such as the casting positions (McPoil et al., 1989) and the different extent of weightbearing (Tsung et al., 2003; Guldemond et al., 2006) were performed with the subtalar joint in neutral position. No similar studies were performed with other subtalar joint orientations.

To conclude, as there would be some variations in the measurement of the subtalar joint neutral position on the same subject by different clinicians, the subtalar joint neutral position achieved in the foot impression procedure in current clinical practice exists as a range of angles, rather than a particular value. Biomechanical studies showed that the foot orthoses made by this approach was satisfactory to tackle foot problem. There is question about the acceptable range of the subtalar joint neutral position during foot impression procedure.

1.2. Objectives of the study

This study aimed at investigating the importance of the accurate control of the subtalar joint position during foot impression procedure. The plantar geometry of plaster models originated from different subtalar orientations were compared through

three-dimensionally analysis. However, it should be emphasized that this study was not aimed at defining an ideal impression position, which involves many factors, such as the design of the foot orthoses, materials used, patho-mechanisms of different deformities and etc.

The null hypothesis was that there was no significant difference in foot parameters among different subtalar joint angles.

1.3. Clinical significance of the study

Based on the clinical observation, the change in the plantar geometry affected by the subtalar joint orientation is not obvious. Moreover, foot orthosis can only capture one particular combination of joints angles of the foot, but our feet are not rigid and there are many foot joints movements during walking. Thus, some degree of tolerance in the accuracy of the foot orthosis should be considered. However, subtalar neutral position is always emphasized during impression procedure in teaching, clinical practical and research studies (Richie, 2007; Scherer et al., 2006). Foot alignment control during impression taking includes the subtalar joint,

forefoot-to-rearfoot angle, the plantargrade/slightly dorisflexion in ankle joint and forefoot adduction. Better understanding the effect of the alignment controls on the plantar foot geometry would improve the accuracy of the foot impressions, especially for those clinicians not specified in foot orthotics.

If the subtalar joint orientation does affect the plantar foot geometry, variation in the geometry of the foot orthoses may alter the plantar pressure distribution and affect the lower limb alignments during different phases of gait cycle. Further studies study should be carried out to distinguish which particular orientation is more suitable for the impression procedure. It would help to improve the biomechanical function of the foot orthoses and the user compliance.

Chapter 2. Literature review

This section is divided into five main parts:

- The subtalar joint
- The midtarsal joint
- Classification of foot types
- Foot impression procedure
- Custom-made foot orthosis.

* * * * * * * *

2.1. The subtalar joint

2.1.1. Anatomy of the subtalar joint

The subtalar (talocalcaneal) joint is the articulation between the talus and the calcaneus. It is one of the most important joints of the lower extremity. It is responsible for the conversion of the rotatory forces of the lower extremity. The mechanics of the subtalar joint also dictate the movements of the midtarsal joint and the forefoot (Root et al., 1977).

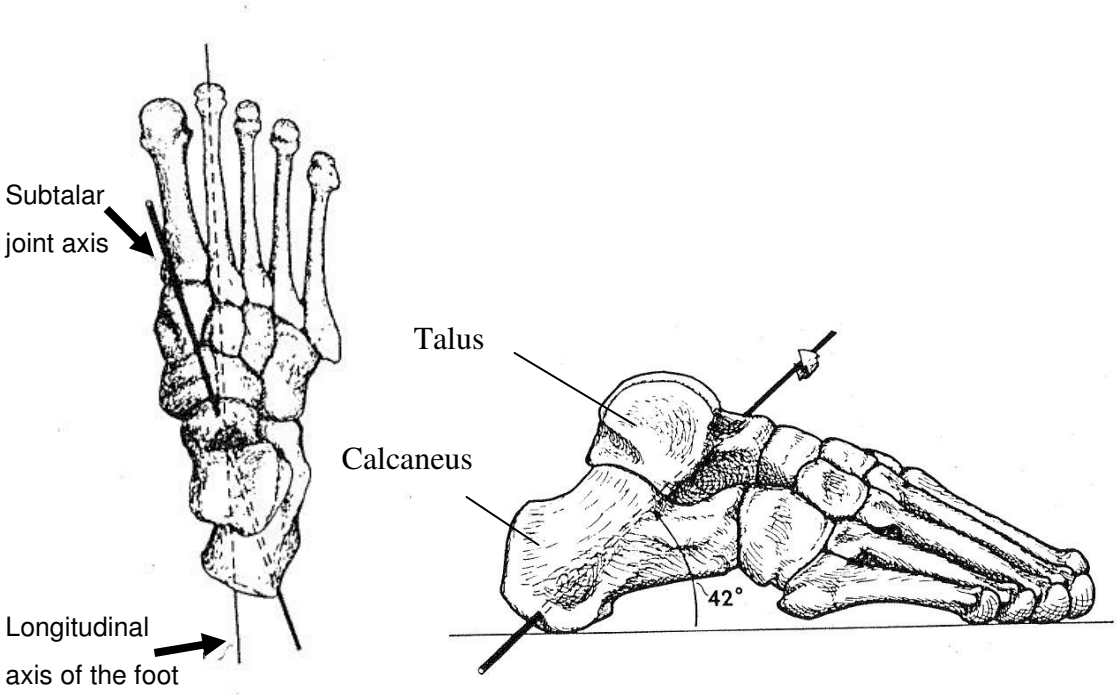

Figure 2.1.1-1 The axis of the subtalar joint defined by Root et al. (1977). (left) the top view, (right) the side view

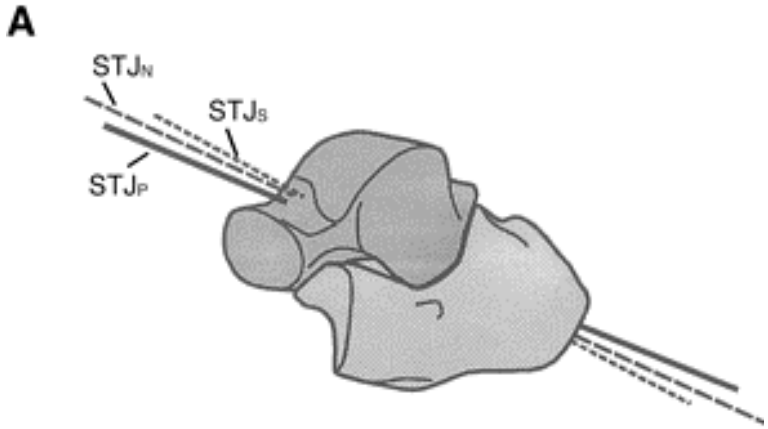

STJ pronated

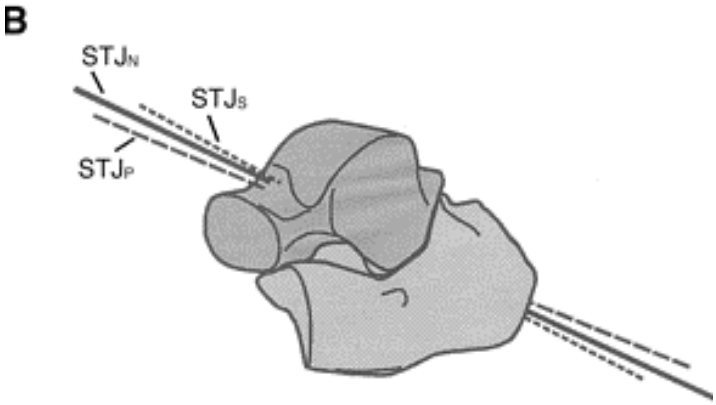

STJ neutral

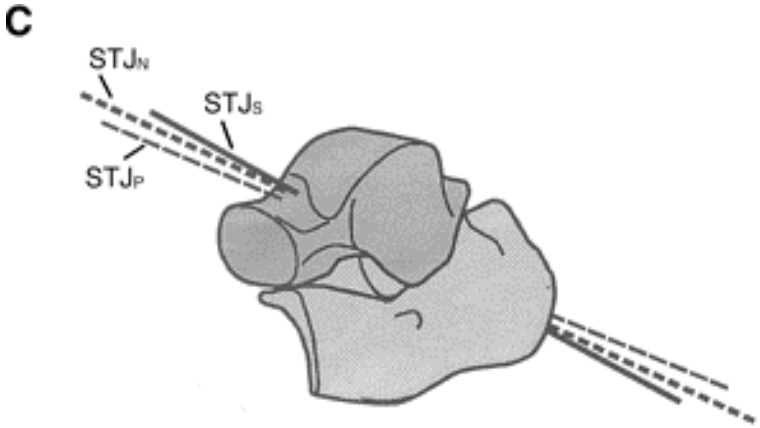

STJ supinated

Figure 2.1.1-2 The subtalar joint axis is a continuously moving axis and is better represented as a bundle of axes passing through the talocalcaneal joint.

Here are examples of how the subtalar joint axis may have different spatial locations in relation to the talus and calcaneus while in the A, the subtalar joint pronated position (STJ_P); B, subtalar joint neutral position (STJ_N); and C, the subtalar joint supinated position (STJ_S). (adopted from Kirby (2001))

Based on the clinical observations and measurements, the imaginary subtalar joint axis is oblique, passing through the neck of the talus antero-medially and the calcaneus postero-laterally. The average inclination of the axis rose 41-42° up from the horizontal plane (Inman, 1976; Root et al., 1977; McPoil and Knecht, 1985) and medially deviated 16°-23° (Inman, 1976; McPoil and Knecht, 1985) from the midline of the foot (Figure 2.1.1-1). Later, some authors suggested that the joint motion should be determined by the morphology of the articulating surfaces of the talus and the calcaneus and roentgen stereophotogrammetry was utilized to locate the spatial location of the subtalar joint axis. Roentgen stereophotogrammetry is the implantation of metallic beads into both the talus and the calcaneus and followed by taking standardized x-rays of the feet in two cardinal planes. They found that the subtalar joint axis is not a solitary axis but rather is better described as a number of discrete axes of rotation that form a bundle of axes passing through the talocalcaneal joint (Van Langelaan, 1983; Benink, 1985; Lundberg and Svensson, 1993) (Figure 2.1.1-2). Slight translation of the talus on the calcaneus was observed too (Kirby, 1989).

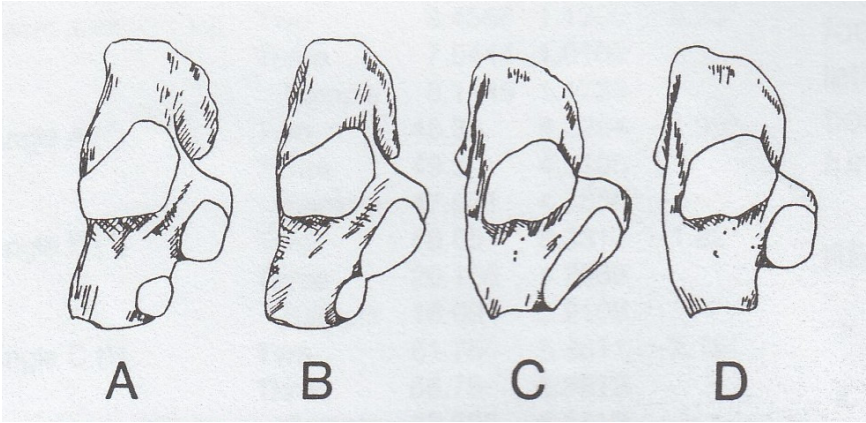

Figure 2.1.1-3 Superior view of right calcaneus depicting variations in subtalar joint face number. A, three-facet configuration; B, transitional two-facet configuration; C, simple two-facet configuration; D, special two-facet configuration. (from Bruckner, 1987)

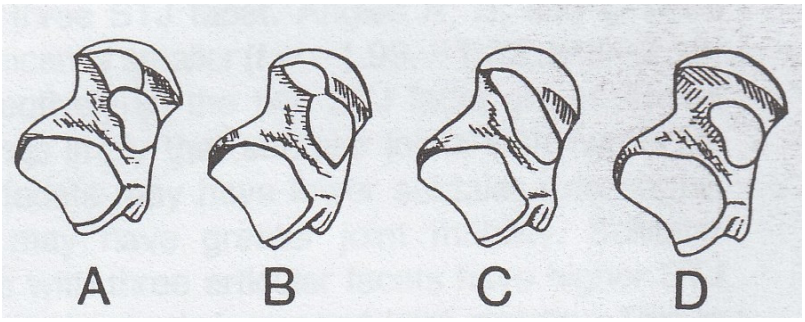

Figure 2.1.1-4 Inferior views of right talus depicting variations in subtalar joint facet number. A, three-facet configuration; B, transitional two-facet configuration; C, simple two-facet configuration; D, special two-facet configuration. (from Bruckner, 1987)

The osseous variations in the human subtalar joint affect the mobility of the joint. Bruckner (1987) studied 32 sets of dry adult human talus and calcaneus bones and observed that some feet had two subtalar joint articulation surfaces while others had three (Figure 2.1.1-3 and Figure 2.1.1-4). They suggested that a subtalar joint with two articulation surfaces might have a less inclined subtalar axis and greater joint mobility while subtalar joints with three articulation surfaces might have a more

inclined subtalar axis and smaller joint mobility. These were consistent with their clinical observations.

The motion of the subtalar joint is triplanar, which means that the subtalar joint motion involved all of the three anatomical planes (i.e. the frontal, sagittal and transverse planes). The subtalar joint motion is described as pronation or supination. The directions of the movements of the talus and calcaneus during subtalar pronation or supination depend on the open and closed kinetic chain conditions.

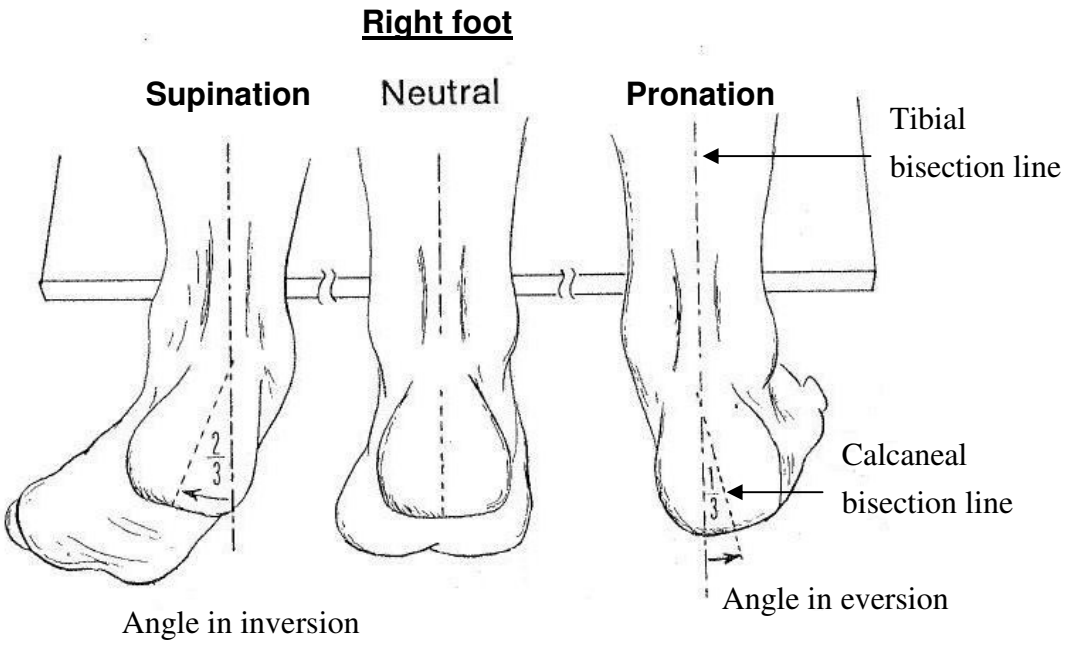

Figure 2.1.1-5 Open kinetic chain subtalar joint supination, neutral and pronation (adopted from Root et al., 1971)

In the open kinetic chain motion of subtalar joint, usually at non-weightbearing condition, there is no external force applied at the foot. The talus is relatively stationary. The calcaneus and the forefoot move in different planes. The open kinetic chain subtalar pronation is composed of calcaneal dorsiflexion, abduction and eversion while the subtalar supination is composed of calcaneal plantarflexion, adduction and inversion (Figure 2.1.1-5).

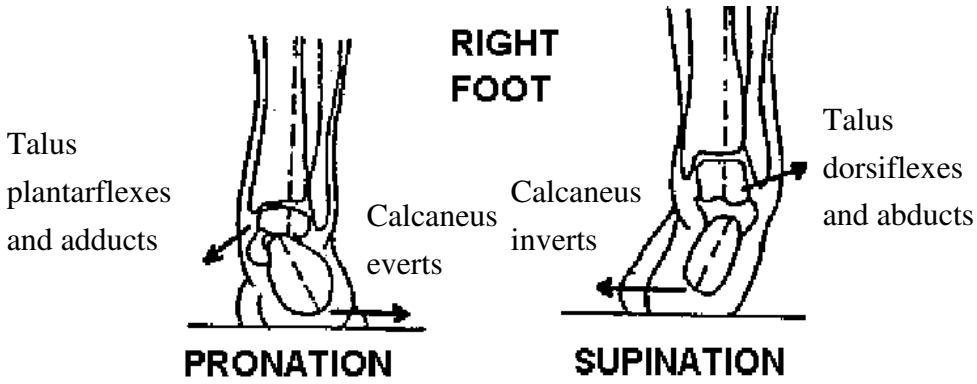

Figure 2.1.1-6 Closed kinetic chain subtalar pronation and supination (adopted from http://moon.ouhsc.edu/dthompso/gait)

In the closed kinetic chain motion of the subtalar joint, an external force, usually by the ground reaction force, is applied at the foot (Figure 2.1.1-6). The talus is mobile while the calcaneus and the forefoot are relatively fixed by its contact with the ground. In subtalar pronation, the calcaneus is relatively stable and everts, and the mobile talus plantarflexes and adducts. At the meantime, the tibial rotates internally

and the knee would flex. The motions are in opposite directions for the closed kinetic chain subtalar supination.

2.1.2. Measuring the subtalar joint angle in non-weightbearing condition

The subtalar joint supination and pronation are measured clinically by the amount of inversion and eversion respectively. It is determined by the angle between the tibial and the calcaneal bisection lines drawn on the posterior skin surfaces of the distal one third of the tibia and the calcaneus respectively. Inversion is referred to the converging movement of the two bisection lines towards the body midline, and eversion is referred to the diverging movement (Figure 2.1.1-5, page 11). Root and his associates (1971) described the ratio of inversion to eversion as one to two. They also suggested 10° inversion and 20° eversion as the range of motion of the subtalar joint of a normal foot. Other studies obtained similar ratio of subtalar joint inversion to eversion (Lattanza et al., 1988; Astrom and Arvidson, 1995).

In non-weightbearing condition, the subtalar joint neutral position (STJN) can be determined either by the palpation method (Wernick and Langer, 1971) or by the calculation method (Root et al., 1971). The palpation of the maximum congruity of the subtalar joint under the neck of the talus is commonly adopted as a simple procedure to assess the subtalar joint in clinical environment. Slight difference, ranging from 1º inversion to 2º eversion, in the mean subtalar joint neutral position determined by palpation in prone lying normal subjects were reported (Smith-Oricchio and Harris, 1990; Astrom and Arvidson, 1995; Pierrynowski et al., 1996). The coefficients of the intra-rater reliability ICC (3,1) and the inter-rater reliability ICC (2,1) were 0.35 to 0.91 and 0.02 to 0.60 respectively. Mathematically, the STJN is at the lateral one third of the total range of eversion to inversion. Astrom and Arvidson (1995) reported that the mean STJN obtained by the palpation method was 2° everted with an intra-rater reliability ICC (3,1) from 0.63 to 0.93. The mean STJN achieved by the mathematical approach was 1° inverted with an intra-rater reliability the ICC (3,1) from 0.35 to 0.91. Other studies demonstrated opposite results (Elverus et al., 1988; Smith-Oricchio and Harris, 1990). It is unclear which approach of defining STJN is more reliable.

2.1.3. Measuring the subtalar joint angle in weightbearing condition

The subtalar joint angle is defined as the angle between the tibial and calcaneal bisection lines. There are special terms to describe the angles between the tibial bisection line and the imaginary vertical reference line as well as the angles between the calcaneal bisection line and the imaginary vertical reference line at different instants. During relaxed double leg standing, the angle between the tibial bisection line and the imaginary vertical reference line is referred as the tibial stance. The angle between the calcaneal bisection line and the imaginary vertical line is referred as the relaxed calcaneal stance position (RCSP) (Figure 2.1.3-1). When the subtalar joint is in its neutral position, the angle between the calcaneal bisection line and the imaginary vertical line is referred as the neutral calcaneal stance position (NCSP). Mathematically, subtalar joint angle is usually represented as

Tibial stance + subtalar joint angle = RCSP or NCSP

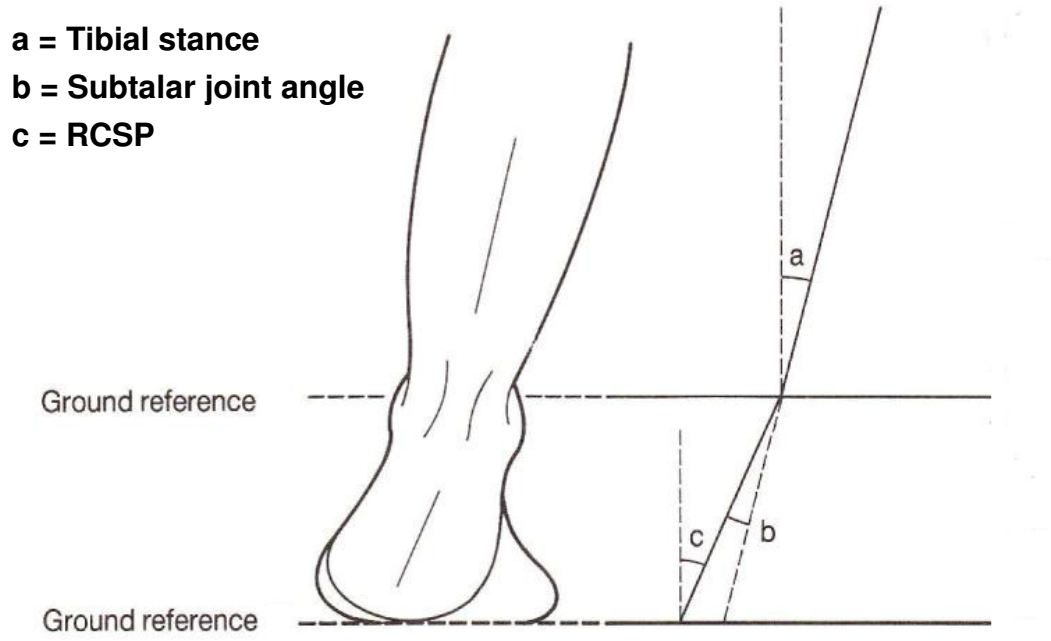

Figure 2.1.3-1 Definitions of the tibial stance and calcaneal stance

(adopted from Philps (1990))

The RCSP was found to be 4° more everted than the NCSP (Sell et al., 1994; Evans et al., 2003). This proved that the statement, "the subtalar joint is in neutral position during standing" by Root and his associates (1977) was not accurate. The inter-rater reliability ICC (2,k) of the NCSP was low, 0.21 to 0.33 (Gheluwe et al. , 2002 and Evans et al., 2003). The intra-rater reliability ICC (3,1) of the NCSP was 0.53 to 0.93 (Sell et al., 1994; Gheluwe et al., 2002 and Evans et al., 2003).

Goniometric measurements of the subtalar joint angle and the tibial stance in standing condition were seldom reported, usually only RCSP were measured. Astrin

and Arvidson (1995) observed that tibial stance was 6 ± 2° inverted and the RCSP was -7 ± 4° inverted. Various RCSP of normal subjects were reported: 0 ± 3.2° by Sell and his associates (1994); 1.8° valgus by Evans and his associates (2003); 6.07 ± 2.71° valgus by Sobel and his associates (1999); and 7 ± 4° valgus by Astrom and Arvidson (1995). The inter-rater reliability (ICC (2,k) = 0.53 to 0.68) and inter-rater reliability (ICC(3,1) = 0.61 to 0.97) of RCSP were better than those of the NCSP. In two dimensional kinematic studies, the STJN was reported as 1.6° inverted (McPoil and Cornwall, 1996a) and 3.7 ± 3.6° inverted (McPoil and Cornwall, 1996b).

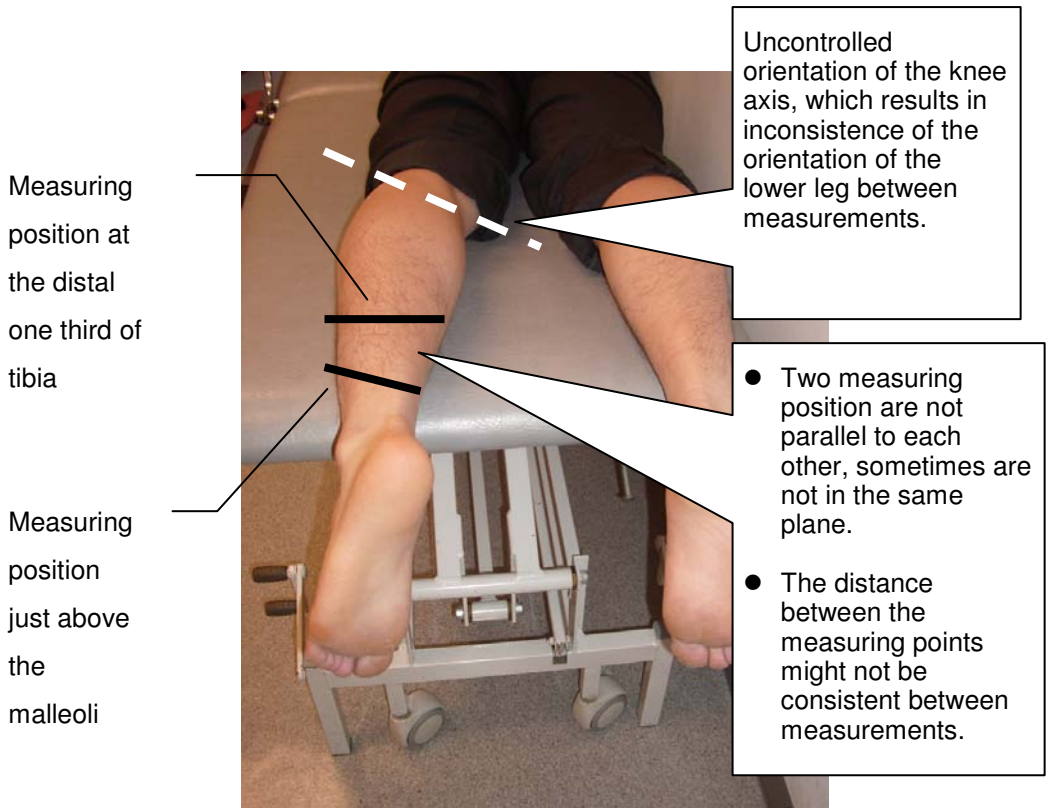

Figure 2.1.3-2 Possible errors of marking the tibial bisection line with caliper or ruler only.

The reliability of drawing the tibial and calcaneal bisection lines is very important for the measurement of subtalar joint angle and the RCSP. The coefficient of intra-rater reliability of achieving the subtalar joint neutral position varied extremely among different studies and ranged from 0.35 to 0.91 (Elverus et al., 1988; Lattanza et al., Smith-Oricchio and Harris, 1990; Astrom and Arvidson, 1995; Pierrynowski et al., 1996) and the inter-rater reliability ICC (2,1) of clinicians with different experience were ranging from 0.35 to 0.91 and 0.02 to 0.60 respectively (Smith-Oricchio and Harris, 1990; Astrom and Arvidson, 1995; Pierrynowski et al, 1996). Goniometer (Elveru et al., 1988), inclinometer (Payne and Richardson., 2000), digital caliper (LaPointe et al., 2001), and other special designed devices were used. However, very few articles described the measuring procedure clearly. The reliability was affected by the examiner's skills including the accurate positioning of the lower limb and the measuring device, as well as the effect of skin movement in motion (Figure 2.1.3-2). There is a need to develop positioning and measuring devices to improve the reliability.

2.1.4. Subtalar joint movement during walking

Subtalar joint is one of the most important joint involved during walking. In the beginning of the stance phase, the tibia rotates internally, the talus plantarflexes and adducts. The talus converts the rotation of the tibia in the transverse plane to the movement of the calcaneus in the sagittal and transverse planes. The calcaneus simultaneously rolls into eversion in the transverse plane to complete the torque conversion. This is the closed kinetic chain pronation. During the end of the stance phase, the tibia rotates externally, pushing the talus into dorsiflexion and abduction. Simultaneously the calcaneus inverts to complete the torque conversion. This is the closed kinetic chain supination. Root and his associates (1971) recommended that foot orthoses should keep the subtalar joint as closely as possible to the neutral position, to allow necessary amount of supination and pronation during the stance phase.

Investigations on subtalar joint motion during walking (Perry et al., 1995; McPoil and Cornwall, 1996a; McPoil and Cornwall, 1996b; Mannon et al., 1997; Torburn et al., 1998) showed a similar pattern of joint motion: (1) eversion begins as part of loading response immediately after the heel contacts with the floor; (2) peak eversion

is reached by mid stance or late stance phase; (3) the subtalar joint then gradually inverts throughout terminal stance. However the magnitudes of the maximum inversion and eversion varied due to the variation of equipments used and the non-standardized definition of zero subtalar joint angle.

There was no significant difference between two-dimensional and three-dimensional kinematics analysis in the measured subtalar angles during the initial 8-60% of the stance phase (McPoil and Cornwall, 1995). At the initial 6% of the stance phase, the subtalar angle could not be accurately measured with a two-dimensional video system. There was significant difference to the measurement from a three-dimensional system (McPoil and Cornwall, 1995). As the tibia rapidly externally rotates after heel off at 60-70% of the stance phase and hence this was inadequate to measure the subtalar joint movement by the two-dimensional analysis at that period (Mannon et al. 1997). Unlike the heel strike angle and the time to reach heel-off, the maximum pronation angle and the time to reach the maximum pronation found in the two-dimensional analysis were frequently used to determine the extent of pathology, the course of treatment and the efficacy of therapeutic intervention. Moreover, electromagnetic motion analysis system (Mannon et al.,

1997) and electrogoniometer (Torburn et al. 1998) were regarded as adequate to perform the analysis on the two-dimensional subtalar joint motion.

Subtalar joint movement during the stance phase

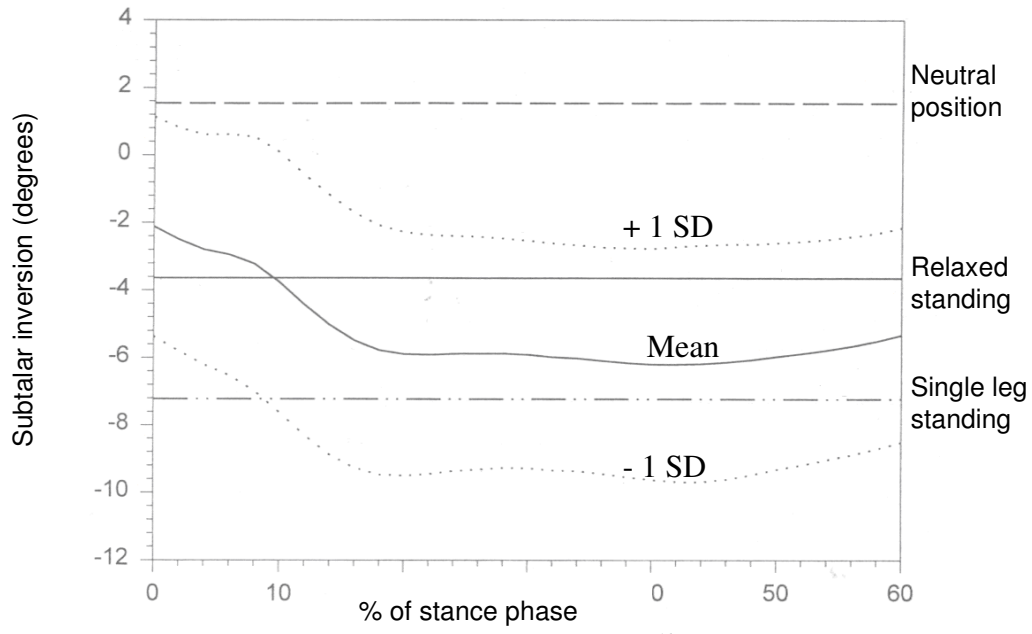

Figure 2.1.4-1 The relationship between subtalar joint movement and static subtalar joint angles at the neutral position, relaxed standing and single leg stand.
(adopted from McPoil and Cornwall, 1996a)

McPoil and his associates (1996a) showed that the mean path of subtalar joint motion during walking was more everted than the subtalar joint neutral position, and the peak eversion of normal subjects during midstance was between the subtalar joint angles at relaxed double leg standing and single leg standing (Figure 2.1.4-1). Therefore, the relaxed calcaneal stance position (RCSP) and the inclined angle of the

calcaneus in the frontal plane during single leg standing (SLS) were recently regarded as static indicators of the maximum eversion of the foot during walking (McPoil and Cornwall, 1996a; Toburn et al., 1998), rather than STJN.

* * * * * * * *

2.2. The midtarsal joint

2.2.1. Anatomy of the midtarsal joint

The midtarsal joint is composed of the calcaneo-cuboid and the talo-navicular joints. Its main functions are to adapt to irregular terrain by keeping the forefoot in contact with the ground and stabilizing the forefoot on the rearfoot by its locking mechanism, as well as absorbing rotations of the rearfoot.

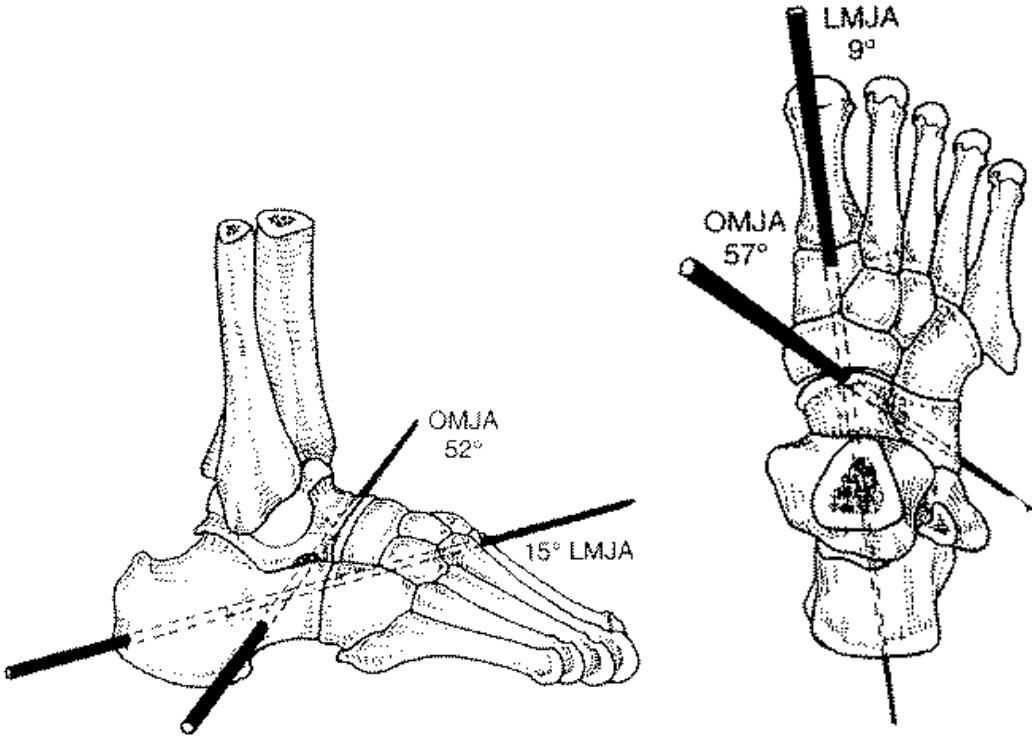

Figure 2.2.1-1 The longitudinal midtarsal joint axes (LMJA) and oblique midtarsal joint axes (OMJA)
(adopted from http://www.latrobe.edu.au/podiatry/Midtarsaljoint.html)

According to the two-axis model of the midtarsal joint, it has two oblique axes of motion: the longitudinal axis and the oblique axis. Both axes pass obliquely through the foot in an anterior, medial and dorsal direction. The average longitudinal axis angles 15° from the transverse plane and 9° from the sagittal plane whereas the average oblique axis angles 52° from the transverse plane and 57° from the sagittal plane (Manter, 1941) (Figure 2.2.1-1). The midtarsal joint movement is also described as supination and pronation. The longitudinal axis allows predominantly

forefoot inversion or eversion in the frontal plane and thus mainly responsible for absorbing rotation of the rearfoot and adapt to irregular terrain. The oblique axis allows predominantly dorsiflexion or plantarflexion in the sagittal plane and abduction or adduction in the transverse plane. It is responsible for stabilizing the forefoot on the rearfoot by locking the midtarsal joint during the pronation of the oblique axis.

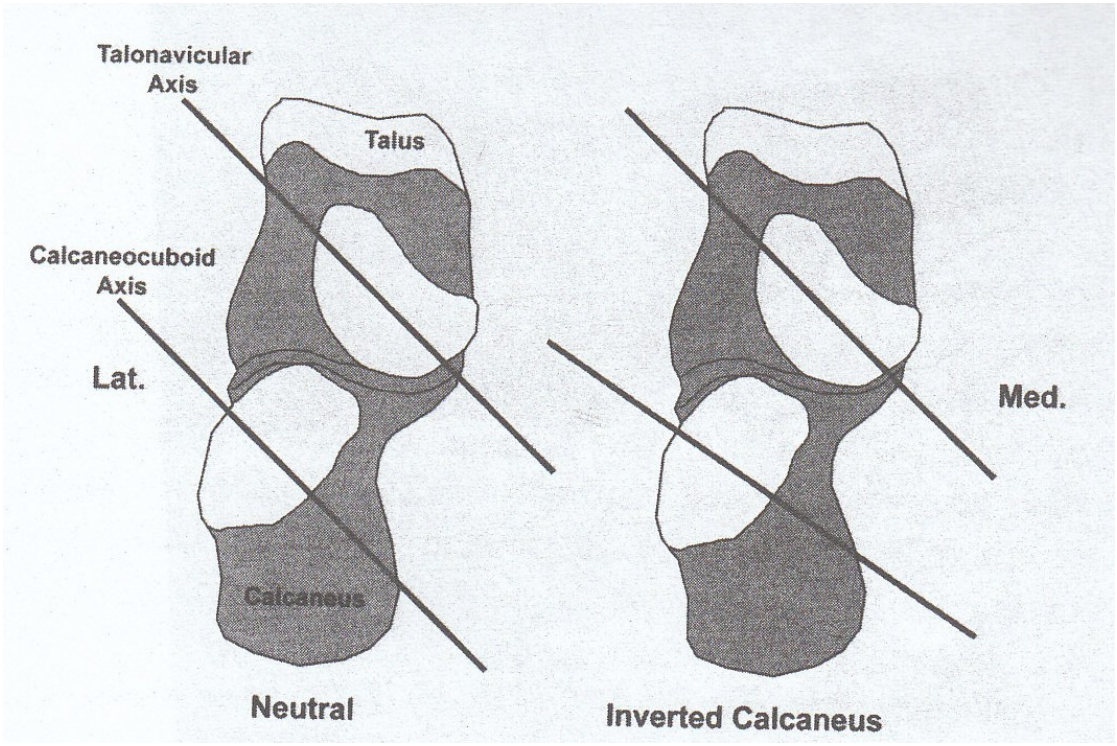

Figure 2.2.1-2 The frontal plane view of the midtarsal joint of a right foot.
The articulation of the talar head and navicular, and the calcaneus and cuboid are shown. The talonavicular and calcaneocuboid axes are shown in parallel with the calcaneus in neutral position (left) and convergent with the calcaneus inverted (right).
(adopted from Blackwood et al., 2005)

Subtalar joint motion would affect that of the midtarsal joint. Subtalar joint pronation increases the range of the motion at the midtarsal joint (Phillips and Phillips, 1983; Blackwood et al., 2005). Subtalar pronation was suggested to cause the midtarsal axes to become more parallel and hence increase the mobility of the joint. Subtalar supination would cause the midtarsal axes to become non-parallel and restrict the midtarsal joint motion (Elftman, 1960) (Figure 2.2.1-2). The forefoot locks against the rearfoot when the normal midtarsal joint is fully pronated and the normal subtalar joint is neutral, the plantar surface of the forefoot is parallel with that of the rearfoot (Root et al., 1977).

Recently, photometric studies (the tracking of metal pellets inserted into bones) showed that the mid-tarsal joint did not function about an oblique and longitudinal axis (Van Langelaan, 1983; Benink, 1985). Multiple axes of rotation could be calculated indeed (Nester et al., 2002; Nester and Findlow, 2006). Although the two-axis model of the midtarsal joint is invalid to describe reality, it is considered useful in understanding and teaching (Payne, 2000).

2.2.2. Measurement of the midtarsal joint angles

Clinically, the midtarsal joint orientation is usually reflected by the forefoot-to-rearfoot angle. It is measured on prone lying subject with the subtalar joint in neutral position by palpating the maximum joint congruency under the head of the talus. A dorsiflexion force is applied to the distal portion of the fourth and the fifth metatarsal heads to lock the midtarsal joint (Root et al., 1971).

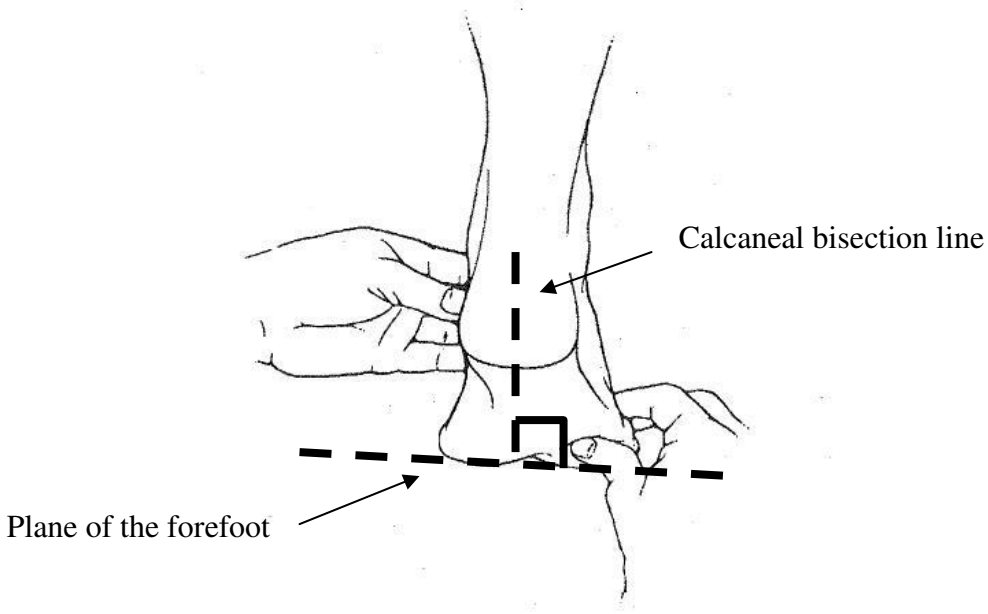

Figure 2.2.2-1 The definition of the zero forefoot-to-rearfoot angle

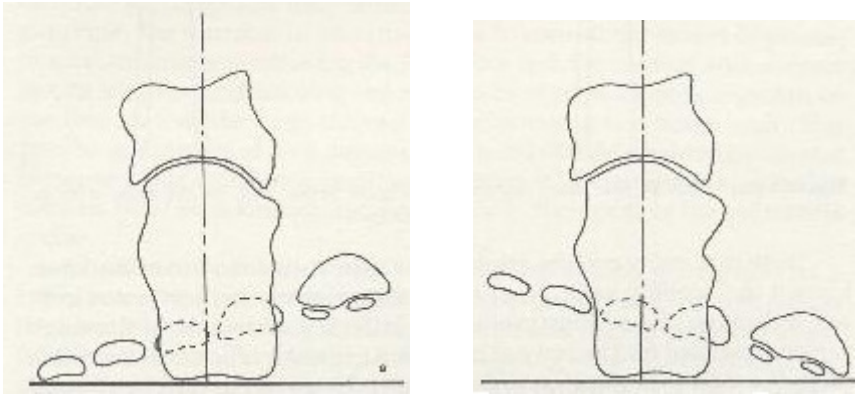

Figure 2.2.2-2 Forefoot varus (left) and forefoot valgus (right)
(adopted from http://bodyfix.net/4cycling.html)

The zero position of the forefoot-to-rearfoot angle means the plane of the plantar forefoot at the metatarsals region perpendicular to the calcaneal bisection line (Figure 2.2.2-1); the forefoot varus is referred as the plantar forefoot region facing towards the body midline whereas the forefoot valgus is referred as the plantar forefoot region facing away from the body midline (Figure 2.2.2-2). The mean forefoot-to-rearfoot angle of normal people was found to be 2.0 ± 1° varus (Evans et al., 2003) and 6 ± 4° varus (Astrom and Arvidson, 1995). The coefficient of inter-rater reliability ICC (2,k) of various studies was around 0.61 to 0.70 and the coefficient of intra-rater reliability ICC (3,1) was 0.82 to 0.99 (Astrom and Arvidson, 1995; Gheluwe et al., 2002 and Evans et al., 2003). The reliability of the forefoot-to-rearfoot angle is affected by the reliability of positing the subtalar joint

neutral. These investigators reported the standard error of measurements as about 1 to 2°.

* * * * * * * *

2.3. Classification of foot types

Minor variations in the anatomical structure of human feet would result in differences in foot type. Understanding the foot types of the subjects and their functional characteristics would be beneficial for interpreting the research results.

Human feet are usually classified into three types: normal feet, excessively pronated feet and excessively supinated feet. “Pes planus” and “pes cavus” only describe the abnormality in the medial longitudinal arch morphology (Franco, 1987; Ledoux and Hillstrom, 2002; Song et al., 1995; Subotnick, 1980 and 1981). They do not reflect the abnormalities in other foot part of the excessively pronated or supinated foot such as calcaneal eversion or inversion and forefoot abduction or adduction (Tiberio, 1987; Dahle et al., 1991; Menz et al., 1998; Aquino and Payne, 2001).

Excessively pronation could be resulted from general excess laxity of ligament or is compensated for the foot deformities like forefoot varus, accessory navicular, tight Achilles tendons and etc. (Subotnick, 1981, Franco, 1986). The excessively pronated feet are hypermobile and susceptible to a large degree of pronation during stance and/or prolonged pronation into the period of propulsion (Cavanagh, 1980). Over time, these functional deformities may develop into a chronic structural deformity like plantar fasiciitis (Subotnick, 1981) and patellofermoral symptoms (Tiberio, 1987) and etc. On the contrary, excessively supinated feet are usually associated with ankle instability, digital contracture deformities, mechanically induced metatarsalgia and heel pain due to the high plantar pressure at the forefoot and heel regions (Song et al., 1995). This foot type also demonstrates with inflexibility and poor shock absorption (Cavanagh, 1980). Both excessively pronated and supinated feet have been reported to be more prone to injury during physical activities (Root et al., 1977; Razeghi and Batt, 2002).

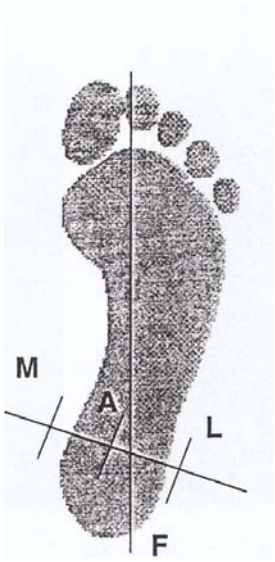

Figure 2.3-1 Malleolar Valgus index = (LA – LF) / LM x 100, where
LA = the distance between the lateral malleolus (L) and the malleoli bisection (A)
LF = the distance between the lateral malleolus (L) and the foot bisection (F), and
LM = the distance between the lateral malleolus and the medial malleolus (M)
(Adapted from Song et al., 1996)

Static assessments like anthropometric measurements, footprint indices and radiographic evaluation of the foot are widely investigated for quantifying foot morphology.

- Anthropometric measurements include:
  - arch height (Hawes et al., 1992), which is the distance from the highest point along the soft tissue margin of the medial planar curvature to the supporting surface);

- Feiss line (Norkin and Levangie, 1983), which is the angle formed by a line connecting the medial malleolus to the navicular tuberosity and a line connecting the navicular tuberosity to the most medial aspect of the first metatarsal head;
- subtalar inversion/eversion angle (Root et al., 1977),
- navicular drop and drift (Brody, 1982) which is the vertical and horizontal displacements of the navicular tuberosity from minimal weight bearing with subtalar joint neutral to 50% weight bearing at relaxed standing respectively, and
- malleolar valgus index (Song et al., 1996) (Figure 2.3-1).

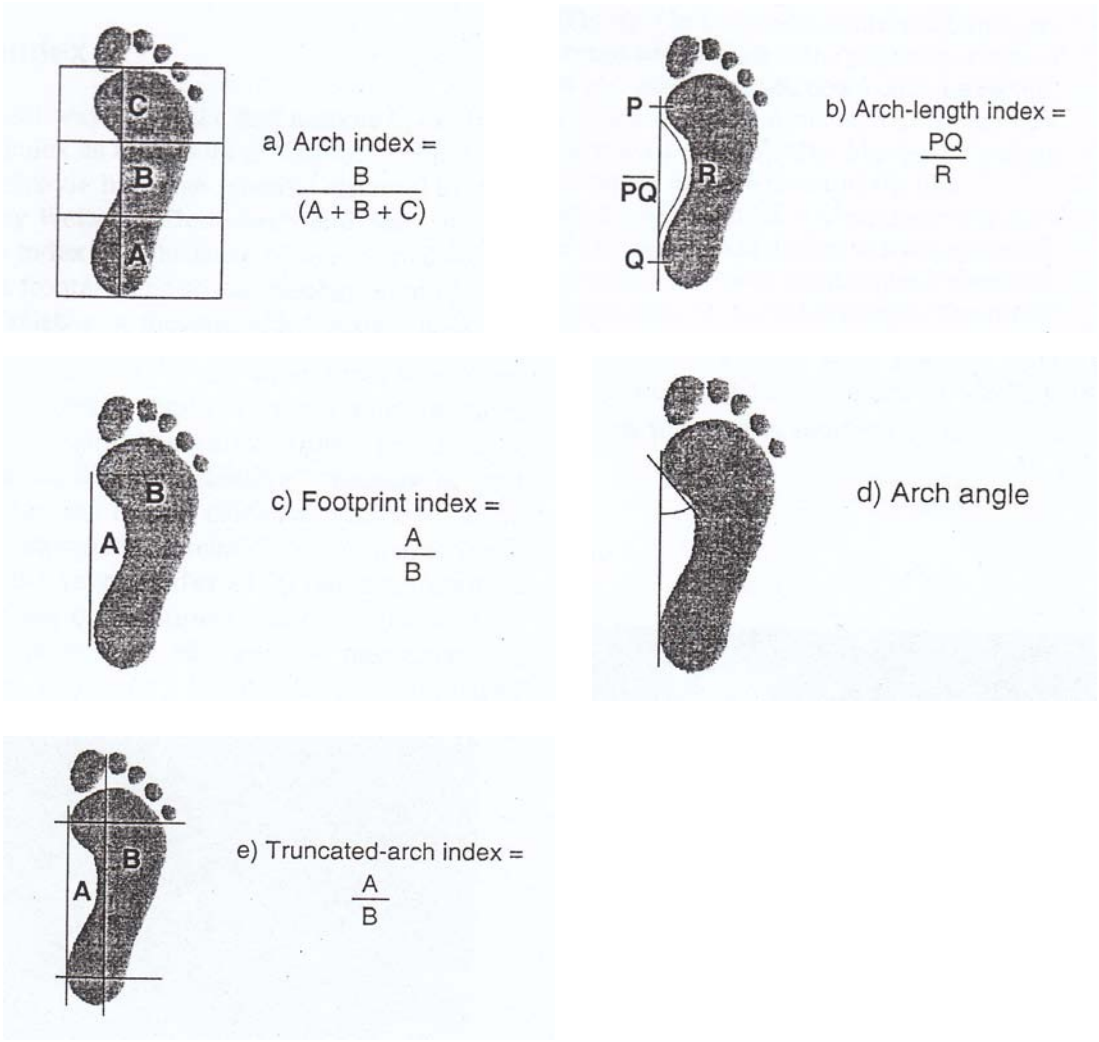

Figure 2.3-2 Definition of different foot print indices

- Footprint indices are provided by simple ink pad or pressure transducers.
  - The arch index (Cavanagh and Rodgers, 1987) (Figure 2.3-2a) is defined with the footprint orientated according to the imaginary axis connecting the second toe and the center of the heel. The footprint is then divided into three equal parts perpendicular to that imaginary

axis. The arch index is the ratio of the midfoot area to the area of the entire foot excluding the toes.

- The arch length index (Hawes et al., 1992) (Figure 2.3-2b) is the ratio of the direct distance between the most medial point of the first metatarsal to the most medial point of the heel to the length of the curvature of the medial border of the arch, extending from the most medial point of the first metatarsal to the most medial point of the heel.
- The footprint index (Irwin, 1937) (Figure 2.3-2c) is the ratio of the non-contact area of the foot print to the contact area of the foot print (excluding the toes), where the non-contact area is bounded by the medial border of the medial longitudinal arch and a reference line drawn at the most medial points of the first metatarsal and the heel.
- The arch angle (Clarke, 1933) (Figure 2.3-2d) is the angle between the two reference lines drawn on the footprint: (1) the first line joining the most medial points of the heel and the first metatarsal, and (2) The second line is drawn from the most lateral point on the medial arch border to the most medial point of the metatarsal head region and

- The truncated-arch index (Hawes et al., 1992) (Figure 2.3-2e) is the ratio of the arch area to the truncated footprint area. The arch area is the part between the medial border line (connecting the most medial points of the metatarsal and the heel) and the medial footprint outline at the arch region. The truncated footprint area was the footprint area bounded by the two lines perpendicular to the medial border line of the footprint through the most medial points of the metatarsal and the heel regions respectively.

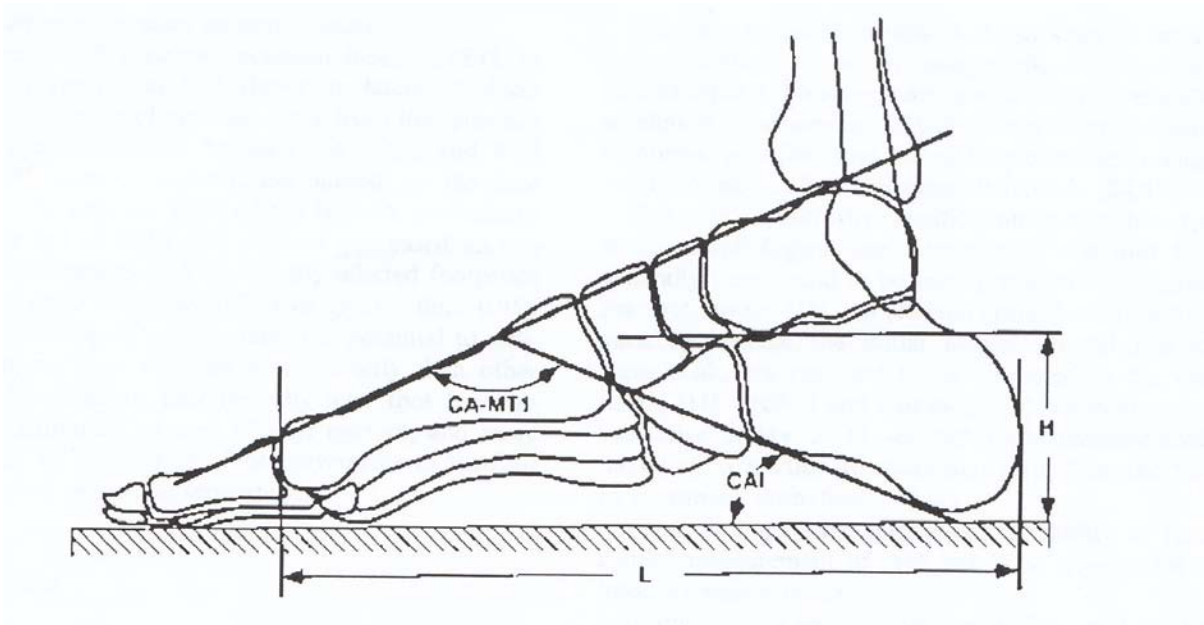

Figure 2.3-3 Radiographic measurement to quantify foot morphology.
CIA = calcaneal inclination angle
H/L = Height to length ratio
CA-MT1 = Calcaneal – first metatarsal angle
(Adapted from Razeghi and Batt, 2002)

- Radiographic parameters such as calcaneal inclination angle (Simkin et al., 1989), height to length ratio (Simkin et al., 1989) and calcaneal-first metatarsal angle (Saltzman et al., 1995) were illustrated in Figure 2.3-3.

There has been no absolute assessment method used to classify the foot type. Researchers usually measure the desired parameters with a big sample size in the population and the "normal" group is usually within the range of the mean of the parameters plus and minus two standard deviations (Aquino and Payne, 2001). Making comparison of the results from different methods and drawing sound conclusions is difficult. Static lower extremity measures had limited value in predicting dynamic lower extremity function (Hamill et al., 1989). Combining the dynamic loading function of the foot to the static measurements would be more closely to the functional behavior of the foot (Razeghi and Batt, 2002).

Dynamic foot function assessment always involves expensive instruments, such as electrogoniometer, plantar pressure measuring system and motion analysis system that may not be available in some clinical settings. Investigators attempted to find out simple and static clinical measurement that could predict the dynamic foot

function. McPoil and Cornwall (1996b) suggested navicular drop as the only the parameter that was able to predict maximum rearfoot pronation during walking. Other static measurements like hip internal and external rotation, ankle plantarflexion and dorsiflexion, first metatarsophalangeal joint extension, tibiofibular varum, navicular tuberosity height in relaxed standing and in subtalar neutral, subtalar joint inversion and eversion, subtalar joint neutral, first ray position, forefoot position and malleolar torsion, were poor predictors to maximum pronation during walking. This was also supported by other studies (McPoil and Cornwall, 1994; Mathieson et al, 2004; Menz, 1998). However, the RCSP was still widely used as an indicator to classify foot types (Aquino and Payne, 2001; Ledoux and Hillstrom, 2001 and 2002; McClay and Manal, 1998).

* * * * * * * *

2.4. Foot impression procedure

The basic principles of the orthotic intervention for different foot types are similar. Understanding the factors affecting the results of the foot impression procedure would help to enhance the experimental design. Also, the advantages of the two-dimensional and three-dimensional evaluations of foot models will be compared in this section.

2.4.1. Variables in Foot impression procedure

The function of foot orthosis is to put the foot in the desired alignment, interfering the weight loading pattern so as to relieve pain or/and enhance function. An appropriate impression position is essential for effective foot orthotic intervention (Root et al., 1971; Schuter, 1976; McPoil et al., 1989; Payne et al., 2001; Laughton et al., 2002; Chuter et al., 2003). Besides, the clinicians' experience, there are other variables affecting the foot impression, such as the weightbearing condition, the materials used and the foot alignment control.

2.4.1.1. Weightbearing conditions

Both non-weightbearing and semi-weightbearing impression procedures are used in clinical practice. The position of the patient for the non-weightbearing impression procedure is usually prone lying, with their feet hanging outside the edges of the examination table for impression taking with plaster of Paris bandage. The semi-weightbearing impression procedure is usually done with the patient being seated and a foam box is put under the patient's foot for the foot impression.

Using the foam box for foot impression is faster and neater than using the plaster bandage. Also, the semi-weightbearing impression procedure allows the heel pad and other plantar soft tissues expand. It would save the effort of putting extra plaster at the edges of the plaster models during the plaster rectification procedure of the posted foot orthosis (Schuster, 1976; Payne et al., 2001). However, the density of the foam available from the market is usually too high. The weight of the foot is not enough to immerse itself with the adequate depth in the foam box for the fabrication of the foot orthoses. Therefore, external pressure is applied by the clinician over the patient's knee and dorsal forefoot area to immerse the foot in the foam box. This has the potential to place the first ray, the functional metatarsal unit consisting of the first

metatarsal and the first cuneiform, in an artificially dorsiflexed position (Payne et al., 2001). This eliminates the plantarflexion of the first ray for normal metatarsophalangeal joint dorsiflexion to establish the windlass mechanism[1]. The forefoot-to-rearfoot angle of the impression obtained from non-weightbearing impression procedure was significantly different from that obtained from semi-weightbearing impression procedure (McPoil et al., 1989). Song et al., (1996) observed that the forefoot-to-rearfoot angles of the non-weightbearing foot impression were closer to the actual measurement of the subjects. Therefore, the non-weightbearing impression method was adopted in this study as it facilitated the control of the forefoot-to-rearfoot angle (Valmassy, 1979; Payne et al., 2001).

2.4.1.2. Impression materials for non-weightbearing foot impressions

Plaster bandage is commonly used for taking non-weightbearing foot impression. With the subtalar joint kept neutral during the impression procedure, the rearfoot width, forefoot width and the forefoot-to-rearfoot angle of the plaster foot impression were in good agreement with those of clinical measurements (Laughton et al., 2002). The mean deviation of the width measurements and the angular measurement found

[1] Windlass mechanism: as the first metatarsophalangeal joint dorsiflexes upon heel left, this has the effect of "winding" the plantar aponeurosis around the first metatarsal head, elevating the arch and inverting the rearfoot, to facilitate push-off (Hicks, 1954).

by their study were about 2 mm and 0.1° respectively. However, it is questionable that the arch height of the plaster foot impression obtained in that study was significantly lower than that of the non-weightbearing laser scanning by 14 mm.

A polycarprolactone based low temperature thermoplastic material, Orfit^{TM}, was suggested to replace the plaster bandage as the impression material (Leung et al., 2004). The self-bonding and elastic properties of the materials were utilized to control the geometry of the soft tissue of the foot. Good inter-rater and intra-rater reliability were attained by well-trained professionals. By evaluating the forefoot width, the ICC (3,1) intra-rater reliability by the experienced orthotist was 0.95 (CI 0.82-0.99) while the ICC(2,1) inter-rater reliability by two experienced orthotist was 0.95 (CI 0.82-0.99). By evaluating the navicular height measurement, the ICC (3,1) intra-rater reliability by the experienced orthotist was 0.83 (CI 0.46-0.96) while the ICC(2,1) inter-rater reliability by two experienced orthotist was 0.83 (CI 0.48-0.95).

2.4.1.3. Foot alignment control

The impressions material is not an important factor of the foot alignment control: the working time of the plaster bandage is about 5-10 minutes, while the working time of the Orfit plastics is about 2-3 minutes. An experienced clinician is able to take a foot impression with satisfactory alignment control by either material. The time for impression taking is not the main issue. In contrast, clinicians' skill was the main concern for the good alignment control, which is reflected by the low reliability of the subtalar neutral measurement by clinicians with less experience.

Wright and his associates (1964) defined the subtalar joint neutral position as the relaxed calcaneal foot position. They stated that *"the neutral position was the position of the ankle and subtalar joint when the subject was standing relaxed with the knees full extended, the arms at the side, feet six inches apart and comfortable amount of toeing out"*. Menz (1997) and Sobel and Levitz (1997) commented that the subtalar joint neutral position defined by Root and his associates (1971 and 1977) was actually the inverted subtalar joint neutral position stated by Wright et al (1964), and therefore they argued the validity of the application of the Root's concept on the

subtalar joint neutral position. However there was no study found for investigating difference subtalar joint orientation during foot impression procedure.

It has been widely accepted that the midtarsal joint should be locked at its fully pronated position by applied dorsiflexory and abductory forces at the distal portion of the fourth and fifth metatarsal heads (Root et al., 1971), so that the foot is converted from a mobile adapter to a rigid level for propulsion (Brown and Smith, 1976; Burns, 1977). Valmassy (1979) suggested that although the dorsiflexory force keeps the midtarsal locked, it is possible for the forefoot to supinate unless an abductory force is applied. Baltimore (1993) commented that the abductory force at the lesser metatarsals aimed at maintaining the talonavicular congruency in a position that the head of talus is slightly more palpable on its medial side. The inter-rater reliability of the measurement of the forefoot-to-rearfoot angle on the subjects' feet was moderate (ICC (2,1) = 0.61 to 0.70) (Astrom and Arvidson, 1995; Gheluwe et al., 2002; Evans et al., 2003). The intra-rater reliability ICC (3,1) coefficient of the forefoot-to-rearfoot angle of the plaster impressions was ranged from 0.83 to 1.0 in different studies (McPoil et al., 1989; Laughton et al. 2002;

Chuter et al., 2003). However, Cox and his associates (1999) pointed out that the ideal forefoot-to-rearfoot angle for the control of foot alignment was not sure.

Besides, Chuter and his associates (2003) compared the effect of applying abductory and adductory force at the lateral forefoot to pronate and supinate midtarsal joint respectively during non-weightbearing foot impression procedure. They found that there was no difference found in the forefoot-to-rearfoot angle. On the contrary, Kogler and his associates (1995 and 1996) recommended to applying adductory force at the lateral forefoot to ensure the maximum height of the medial longitudinal arch and stabilize the apical bony structure of the arch to reduce the strain in the plantar aponeurosis. This showed the reduction on the stain on the plantar fascia of the cadavers.

2.4.2. Three-dimensional evaluation of the plantar foot geometry

A common way to evaluate the foot impression procedure is to measure the plaster models directly with hand tools such as rulers and goniometers. However, the measurements obtained have been limited to angular measurement such as the inclination of the calcaneal bisection line to the supporting surface, and

two-dimensional measurements such as metatarsal width or heel width (Chuter et al., 2003; Laughton et al., 2002; McPoil et al., 1989; Payne et al., 2001). This approach ignores the variations in the medial arch geometry. The result of these two-dimensional measurements would not be reflected the actual geometric changes.

Digitization of the irregular foot shape into numerous pixels allows the quantification of some foot parameters, such as the slopes and volumetric measurements of various segments which are difficult to be measured by hand tools. The consistency of labeling reference point such as the highest soft tissue margin at the medial arch area to define the arch height can be improved (Laughton et al., 2002).

Although CAD/CAM technology has been used in the fabrication of prostheses and orthoses since 1990's, only a few studies (Foulston et al., 1990; Laughton et al., 2002; Tsung et al., 2003) utilized a computer system to quantify and compare the geometric shape of foot impressions. Foulston and his associates (1990) measured the surface slopes of the transverse cross-section of non-weight bearing foot impressions with relaxed forefoot in inverted position and perpendicular

forefoot-to-rearfoot relationship. They observed significant differences between these two conditions at the regions between the metatarsals and the midheel. Laughton and his associates (2002) compared foot impressions obtained by different impression methods, namely non-weightbearing plaster impression, partial weightbearing foam impression, partial and non-weightbearing laser scanning, through measuring arch height, forefoot width and forefoot-to-rearfoot angle. Tsung and his associates (2003) compared arch height, arch angle, and other width and length measurements during different weight bearing conditions.

The coordinate systems used in previous studies were depended on the manual labeling of at least three anatomical landmarks to the image of the foot impression. This manual labeling method might introduce variations in different scanning trials. In this study, the reference axes for measurement relied solely on the geometric shapes of the foot models.

* * * * * * * *

2.5. Custom-made foot orthoses

Both the posted foot orthosis and the total contact foot orthosis are commonly applied in clinical practice. Although the foot impression procedures are the same, the plaster modification and fabrication procedures are different. This would affect the experimental design of the study. This section will compare the properties of these two orthotic designs.

Root and his associates (1971 and 1977) modified the previous methods and documented the prescription criteria for various foot deformities. The principle of the posted orthoses was to maintain the subtalar joint neutral during the midstance. The magnitude and the direction (medial or lateral) of the forefoot and rearfoot postings aimed at accommodating the measurements of the calcaneal inversion/eversion and forefoot-to-rearfoot varus/valgus, at subtalar neutral, of the individuals.

Figure 2.5-1 The posted foot orthosis
(adopted from http://www.bi-op.com/bi-op-en/orthotics-prosthetics-brace/)

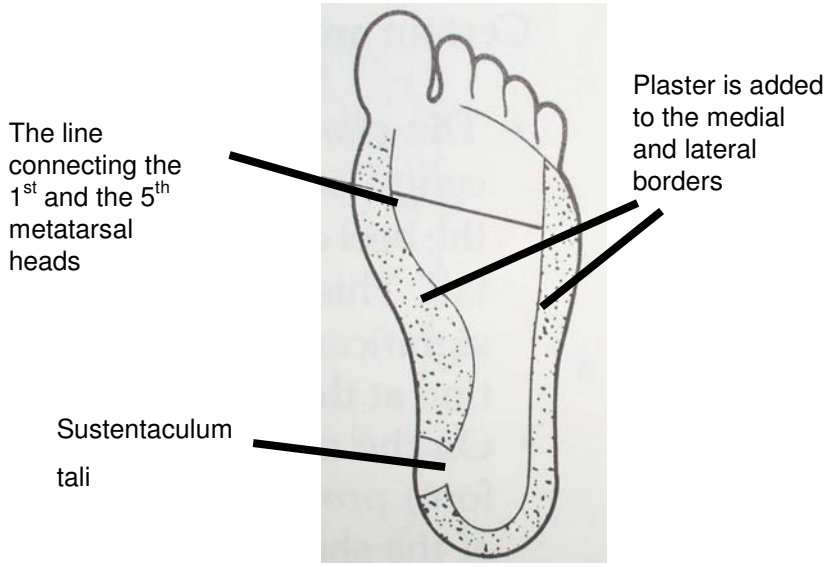

Figure 2.5-2 Plaster is added to the medial and lateral borders of the plaster model of the Root-type posted foot orthosis
(adopted from Philps (1990))

The trimline (i.e. the cutting edge during fabrication process) of the posted foot orthosis is relatively low. To avoid impingement from the edge of the orthosis to the plantar soft tissue, plaster is added along the edge area of the plaster model (Philps, 1995) before using it for the fabrication of the orthosis (Figure 2.5-1 to Figure 2.5-3).

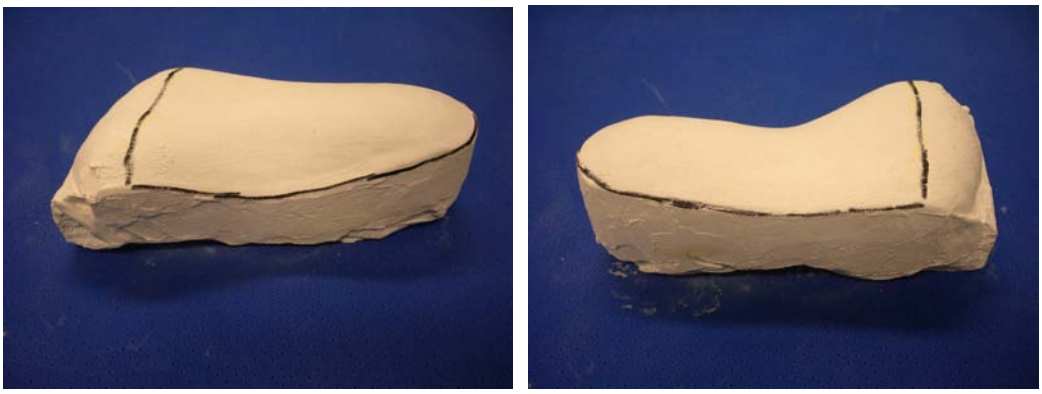

Figure 2.5-3 The medial (left) and the lateral (right) view of the plaster model of the Posted foot orthosis

Medially or laterally posted foot orthoses were reported as beneficial biomechanically (Johanson et al., 1994; Mundermann et al., 2003; Nester et al., 2003; Tillman et al., 2003). Nester and his associates (2003) found that the medially posted orthoses reduced rearfoot pronation and increased laterally directed ground reaction force, as well as reduced shock attenuation. Laterally posted orthoses provided the opposite effects. Mundermann and his associates (2003) also observed that the medially forefoot and rearfoot posted foot orthosis reduced foot inversion, but increased ankle eversion and knee external rotation moments.

The user compliance of the posted foot orthosis was questionable. Relatively high number of patients required modifications or reductions to the postings of the Posted orthoses (Basque et al., 1989). Twenty-five percent of 266 foot orthoses users

commented that their polypropylene custom-made Posted foot orthoses only met 0-40% of their satisfaction in the relief of their symptoms (Walter et al., 2004).

Johanson and his associates (1994) performed gait analysis to compare the effect of foot orthoses with three different posting approaches (forefoot posting alone, rearfoot posting alone and the combined forefoot and rearfoot postings) and non-posted foot orthosis on controlling abnormal subtalar pronation. They found that all the orthotic conditions significantly decreased the maximum pronation and the non-posted foot orthoses had similar effect as all other posting conditions (within 1° of difference). Mündermann and his associates (2003a) also observed that the effect of molded foot orthosis without postings was similar to those with postings in their kinematics, kinetics and EMG analysis. Mündermann and his associates (2003b) recommended that custom moulded foot orthoses without posting were more comfortable than posted orthosis. The concept of posting should be de-emphasized.

Figure 2.5-4 The total contact foot orthosis

Figure 2.5-5 The medial (left) and lateral sides (right) of the plaster model of the total contact foot orthosis

Figure 2.5-6 The University of California Biomechanical Laboratory (UCBL) foot orthosis

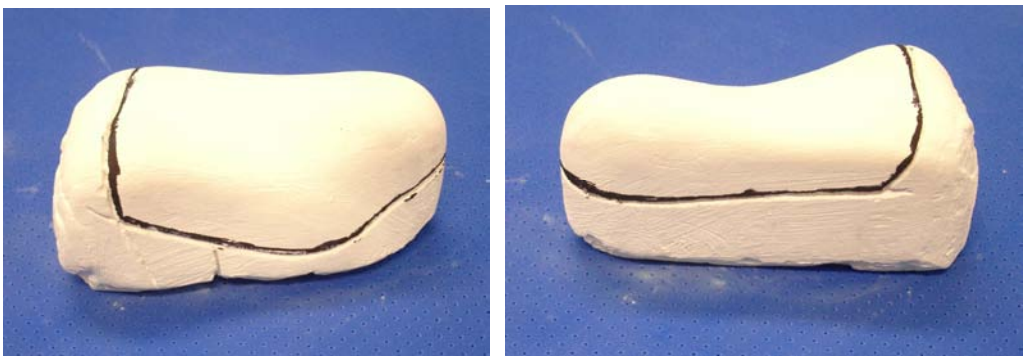

Figure 2.5-7 The medial (left) and lateral (right) sides of the plaster model of the UCBL foot orthosis

The total contact foot orthoses has a high requirement of the originality of the plantar foot geometry in order to provide support and to redistribute the high plantar pressure under the heel and the metatarsal regions (Chen et al., 2003; Guldemond et al., 2006). Only minimal plaster rectification procedure of the total contact foot model is required. No plaster should be added at the medial and lateral borders of the plaster models. The trimline is usually located above the turning point of the lateral borders of the plaster models and reaches the navicular tuberosity medially (Figure 2.5-4 and Figure 2.5-5). The total contact foot orthoses is usually made of semi-rigid materials such as Ethylene vinyl acetate (EVA) foam plastics with different density. The University of California Biomechanics Laboratory (UCBL) (Henderson and Campbell, 1969) foot orthosis is another kind of the total contact foot orthosis, which is made from more rigid plastics such as polypropylene (Figure 2.5-6 and Figure

2.5-7). It is usually used for children with flexible flat feet (Bleck and Berzins, 1977; Leung et al, 1998).

Cornwall and McPoil (1992) investigated that semi-rigid total-contact foot orthosis reduced forefoot loading, and an additional 6° rearfoot varus post had no effect on the results. Mueller (1994) recommended that the total contact foot orthosis was an effective device to control pronation. Kogler and his associates (1995) found that the UCBL orthosis and the semi-rigid total contact foot orthosis were more effective to reduce the strains on plantar aponeurosis, while the strain conditions with a prefabricated orthosis and the custom-made posted foot orthosis was just similar to that with barefoot. Kitaoka and his associates (1997) and Aquino and Payne (1999) explained that the relatively higher arch support of the custom design stabilized the apical structures of the arch, and minimized soft tissue strain. The arch support is an essential element of the foot orthosis to prevent collapsing of the medial longitudinal arch.

2.6. Summary

Foot alignment control was one of the key factors affecting the foot impression procedure. The concept of the subtalar joint neutral position has been widely applied since Root and his associates (1971). However, instrumented gait analysis showed that the subtalar joint was everted and beyond the subtalar joint neutral position during normal walking (Perry et al., 1995; McPoil and Cornwall, 1996a; McPoil and Cornwall, 1996b; Mannon et al, 1997; Torburn et al., 1998). The rationale of getting the subtalar joint neutral position during impression procedure was unclear. Moreover, the reliability of clinical measurement of the subtalar joint neutral position (STJN) were not satisfied (Ghelvwe et al., 2002; Evans et al., 2003). This study aimed at investigating the effect of controlling the subtalar joint during the foot impression procedure, through comparing the plantar geometry of the foot impressions originated from different subtalar joint angles in a three-dimensional approach.

Chapter 3. Methodology

The aim of this study was to compare the plantar foot geometry of the foot impressions within a selected range of subtalar joint orientations. The investigation was divided into three main parts:

1. Development of the measuring devices for quantifying the subtalar joint angle,
2. Foot impression procedure, and
3. Development of computer software for quantifying the plantar foot geometry.

The plantar geometry of the foot impressions originated with different subtalar joint orientations were compared by the statistical software, SPSS.

3.1. Subjects

Twenty adult subjects (8 males and 12 females) aged between twenty-two and forty-six (mean 28.3 years old) participated in this study as similar rearfoot motion pattern was observed in the age group within 20-49 (Ball and Johnson, 1993). The subjects worked in the Department of Health Technology and Informatics. There

were 28 subjects examined and only 20 of them have normal foot type and proceeded with the experiment. All subjects did not have foot pain or other lower limb injuries in twelve months before the date of the experiment. Preliminary assessment was carried out to ensure that the subjects were free from lower limb deformities, such as leg length discrepancy, hallux valgus, forefoot adductus and etc. Navicular drop and relaxed calcaneal stance position (RCSP) were measured to classify foot types. People with excessively pronated or supinated foot were excluded.

Human ethical approval was obtained from The Hong Kong Polytechnic University. Details of the study were explained to the subjects and consent forms were signed by them before the experiment. The consent form and the information sheet were attached in Appendices I and II respectively.

3.2. Equipment

3.2.1. Three-dimensional foot scanner

Figure 3.2.1-1 The INFOOT Foot Shape Scanner with the plaster model

Foot impressions were taken using Orfit^{TM} which is a polycarprolactone based low temperature thermoplastic material to generate positive plaster foot models. The models were then scanned by the INFOOT Foot Shape Scanner (I-Ware lab, Japan) (Figure 3.2.1-1) which consists of eight CCD cameras and four laser projectors. The scanner is capable of scanning a three-dimensional foot image in 20 seconds

with resolution of 0.5 mm, which is the highest resolution that the scanner can achieve.

3.3. Development of the measuring devices for quantifying the subtalar joint angle

3.3.1. The design

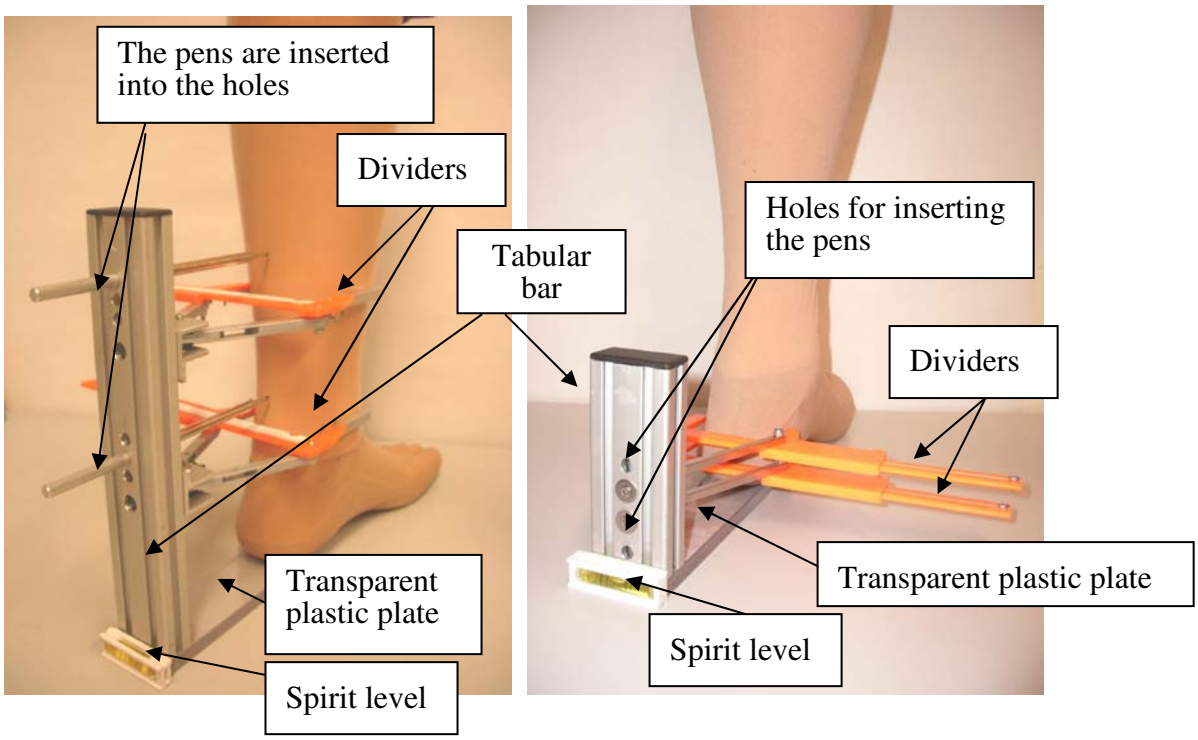

Figure 3.3.1-1 The tibial bisecting and marking device (left) and the calcaneal bisecting and marking device (right)

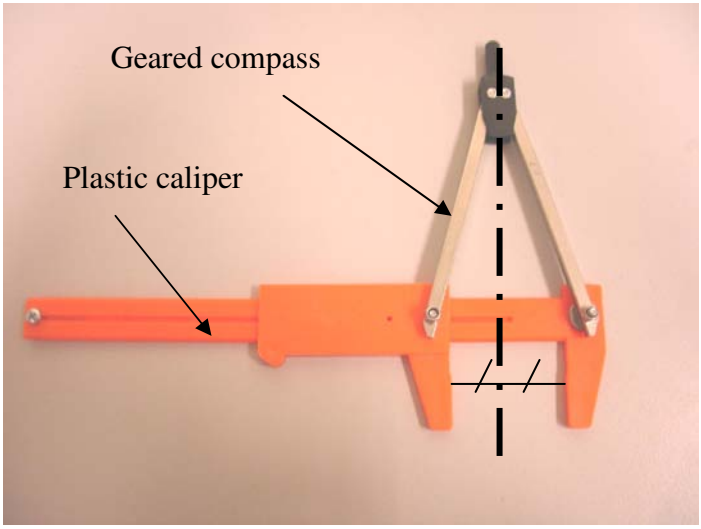

Figure 3.3.1-2 The divider was constructed of a plastic caliper and a geared compass.

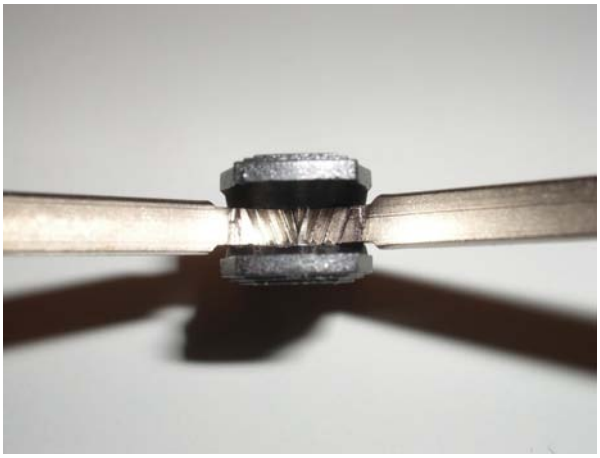

Figure 3.3.1-3 The gear of the geared compass

Tibial and calcaneal bisecting and marking devices were designed and fabricated for the consistency of bisecting and marking the tibial and calcaneal bisection lines (Figure 3.3.1-1). Its design was further developed based on the design of the calcaneal bisector of Lau and Leung (US Patent No.: US 7, 331117B2). The bisection device consisted of a tabular bar which connected two dividers. A small

level gauge was attached to the tabular bar for monitoring the orientation of the device. The two dividers were perpendicularly connected to the tabular body to a way that they were parallel to each other. There were two holes along the axis connecting the central gear of the two dividers on the tabular bar. A pen could be inserted through the holes to mark the mid point between the two measuring jaws. There was a piece of transparent plastic plate connected to the lower end of the tabular bar. Each divider consisted of a compass which had its two arms connected to the measuring jaws of a plastic caliper (Figure 3.3.1-2). The central gear structure allowed the two arms of the compass to have the same degree of angular movement whenever they moved (Figure 3.3.1-3). Therefore, the connecting point of the two arms always located at the mid point between the two measuring jaws of the caliper.

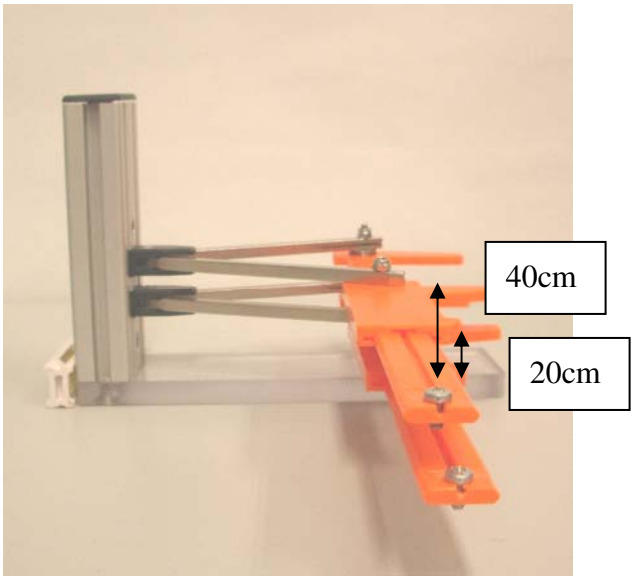

Figure 3.3.1-4 The distances between the dividers and the transparent plastic plate of the calcaneal bisecting and marking device is indicated

LaPointe and his associates (2001) examined multiple non-weightbearing radiographs of the heels and found that the posterior calcaneus was found to be approximately trapezium in shape at the levels 20 mm to 40 mm above the supporting surface. The dividers of the calcaneal bisecting and marking device were thus designed to be 20 mm and 40 mm away from the transparent plastic plate respectively (Figure 3.3.1-4).

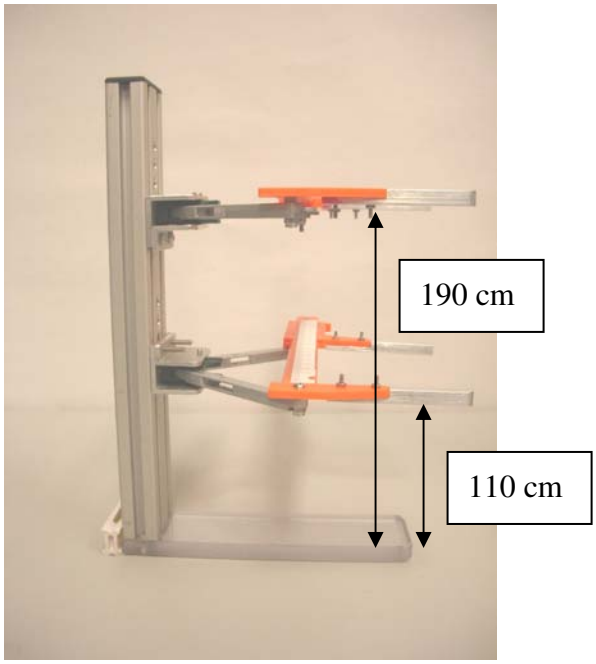

Figure 3.3.1-5 The distances between the dividers and the transparent plastic plate of the tibial bisecting and marking device is indicated

According to a study on the foot dimensions of the Chinese population by the Scientific Research Institute for the Shoe Making Industry of the China National Light industry Council (中國輕工業部制鞋工業科學研究院) (1984) and the Chinese National Standard GB 10000-88 of Human Dimension of the Chinese Adult (China National Technical Committee for the Standardization of Ergonomics, 1988), the dividers of the tibial bisecting and marking device, were located 110 mm and 190 mm away from the transparent plastic plate respectively (Figure 3.3.1-5). These two measurements were referred to the distance from the point just above the malleoli and the lower one third of the tibial to the bottom of the heel respectively.

Figure 3.3.1-6 The u-shaped cushioned ankle support attached to the examination table for stabilizing the lower leg at the knee joint axis horizontal.

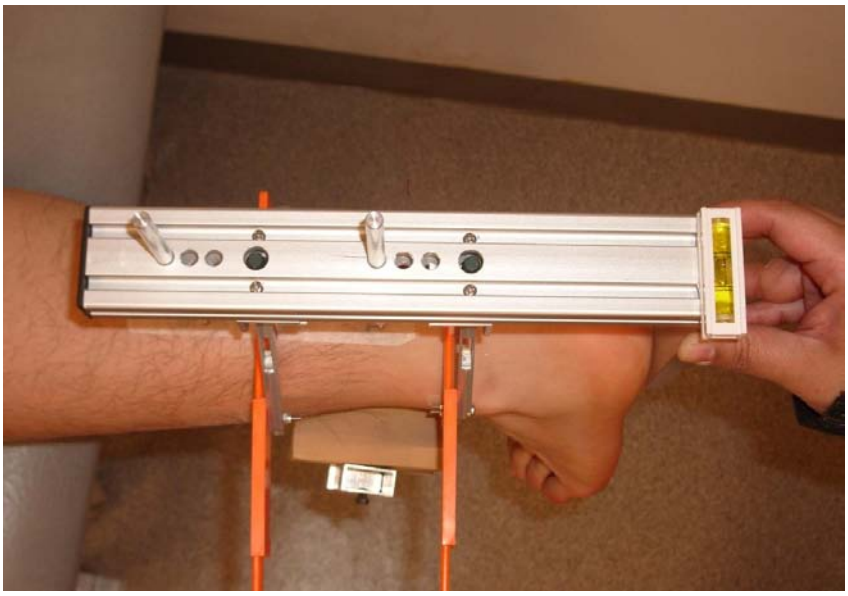

Figure 3.3.1-7 The top view of the application of the tibial bisecting device. The level gauge should be kept horizontal.

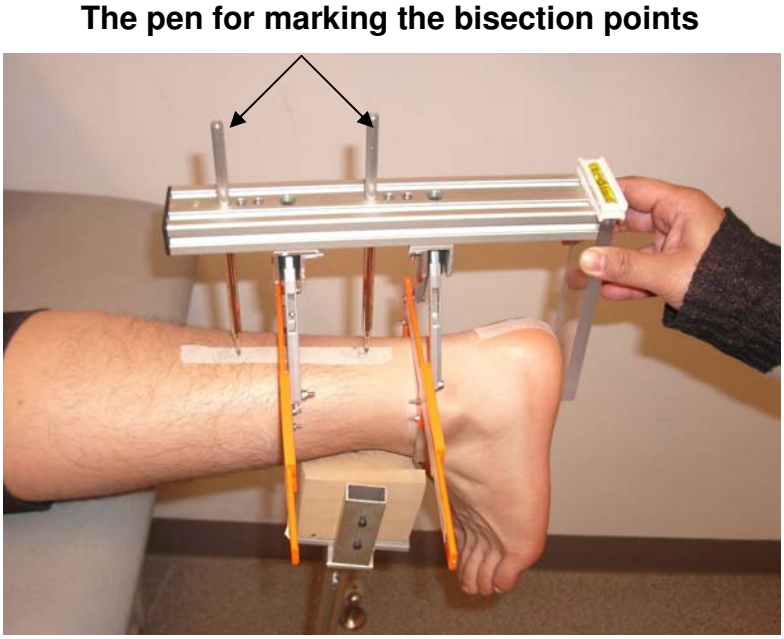

Figure 3.3.1-8 The side view of the application of the tibial bisecting device.
Two pens (indicated by the arrows) were inserted for marking the bisection line.

The dorsiflexion-plantarflexion position of the ankle might induce skin movement. In order to keep the ankle position consistent during the bisecting and marking procedures, the ankle should be kept plantargrade. A u-shaped cushioned ankle support attached to the examination table was used to stabilize the lower leg and keep the knee joint axis horizontal to the ground (Figure 3.3.1-6). The plantar heel surface should be placed to contact with the transparent plastics plate in the way that the skin just bleached (Figure 3.3.1-7). The jaws of the dividers were adjusted to just contact with the skin. The small level gauge was attached to the tabular bar for monitoring the orientation of the device. The two inserted pens marked two points

for the marking of the bisection line (Figure 3.3.1-8). Reliability tests for the devices were conducted.

3.3.2. Reliability tests of the bisecting and marking devices

To verify the reliability of the tibial and calcaneal bisection lines marked by the devices, the bisection lines were also marked by common clinical method (with ruler and pen only). The corresponding measurements of the tibial stance and the relaxed calcaneal stance (RCSP) by the devices and the clinical method were compared. Only the right feet were examined. For the intra-rater reliability test, two trials of each marking method were carried out randomly by the orthotist who carried out the foot impression procedure. Ten subjects participated. For the inter-rater reliability test, one trial was carried out for each marking method by two orthotists (the previous orthotist and another orthotist with three-year experience in foot orthotics). Five subjects were recruited.

Since the measurements of the tibial stance and RCSP would vary with the toe-in/toe-out angle and the distance between the heels, a standing template (modified from that of McPoil and his associates (1988)) was used to standardize the

toe-out angle and the heel distance between different trials of each subject (detailed procedures were listed in Appendix III).

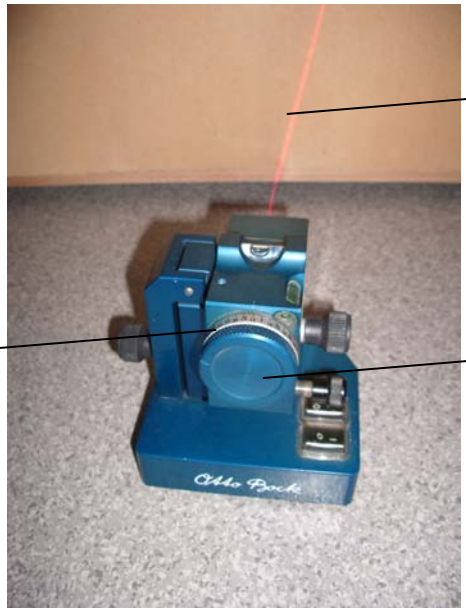

Figure 3.3.2-1 Otto Bock laser line apparatus

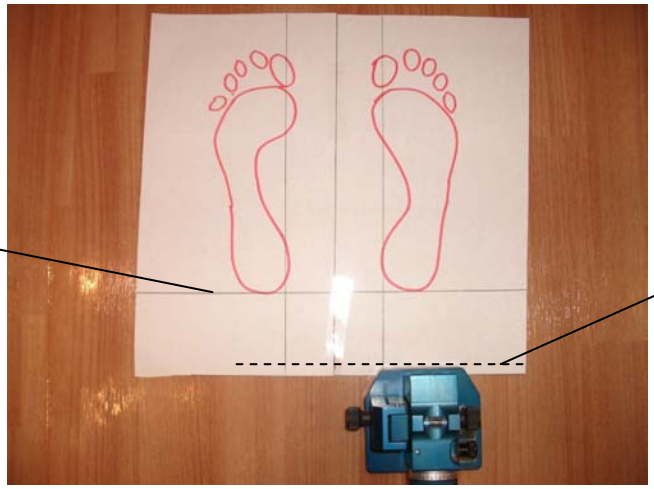

Figure 3.3.2-2 The anterior border of the laser line apparatus was parallel to the frontal plane during the measurement.

With the subject standing on his/her own standing template, the tibial stance and the relaxed calcaneal stance position were measured with the Otto Bock laser line apparatus, which had the accuracy of 1° (Figure 3.3.2-1). The anterior border of the laser line apparatus was kept parallel to the frontal plane for each measurement (Figure 3.3.2-2).

3.4. The experiments

3.4.1. Examination of foot types

The relaxed calcaneal stance position (RCSP) and the navicular drop of each subject were measured. During the navicular drop measurement, two sets of electronic balance were put under the feet to monitor the weightbearing condition. A plumb line was dropped from the 7^{th} cervical spinous process to the gluteal cleft to monitor the trunk movement. Every subject should fulfill the following conditions to ensure that their foot type is normal:

- Navicular drop of the normal arches should not be more than 15 mm (Brody, 1982).

- RCSP of the neutrally aligned foot should be between 2° inversion and 2° eversion (Song and Hillstrom, 1997).

However, the severity of the foot problem, e.g. pronation, was not quantified by the navicular drop and RCSP measurements.

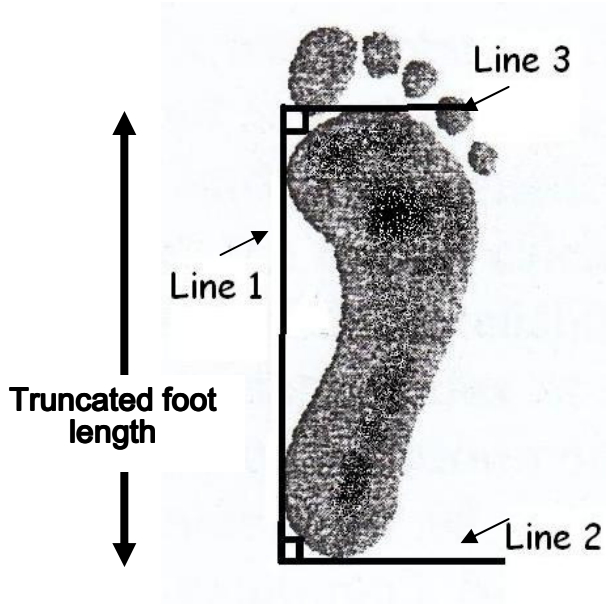

Figure 3.4.1-1 The truncated foot length

Bilateral inked footprints were taken for the measurement of the truncated foot length, which was required for the calculation of the foot parameters. The detail procedure was listed in Appendix IV.

3.4.2. Selected range of subtalar joint orientations for investigation

The subtalar joint orientations within the range of the subtalar joint neutral position (STJN) and the relaxed calcaneal stance position (RCSP) on the plantar foot geometry were selected for investigation, as RCSP was suggested as a predictor of maximum pronation during walking (McPoil and Cornwall, 1996a; Toburn et al., 1998). The mean STJN was found to be 1° inversion to 2° eversion (Smith-Oricchio and Harris, 1990; Astrom and Arvidson, 1995; Pierrynowski et al., 1996) while the mean RCSP was 0° to 7° eversion (Sell et al., 1994; Astrom and Arvidson, 1995; Sobel et al., 1999; Evans et al., 2003). However it was found that it was difficult to manipulate the subtalar joint eversion more than 4° with the subject prone lying during the pilot study. Therefore, the selected range of subtalar joint orientations for investigation was from 2° inversion to 4° eversion.

3.4.3. The foot impression procedure

Foot impressions were taken at four different subtalar joint orientations: 4° eversion (-4°), 2° eversion (-2°), 0° inversion (0°) and 2° inversion (2°) respectively. The forefoot-to-rearfoot angle was kept perpendicular for all subtalar joint orientations. Foot impressions of both feet of each subject were taken using low-temperature

thermoplastic Orfit^{TM} with the above subtalar joint orientations in random sequence. All the impressions were taken by an orthtoist specialized in foot orthotics.

The foot impression procedure was as the following:

1. The subjects were in prone lying position during the whole process. The dorsum of the ankle rested on the U-shape cushioned support with slight knee flexion (about 30°). This was to reduce the tension of the calf muscles to facilitate the plantargrade position or slight dorsiflexion of the ankle (Figure 3.4.3-1).

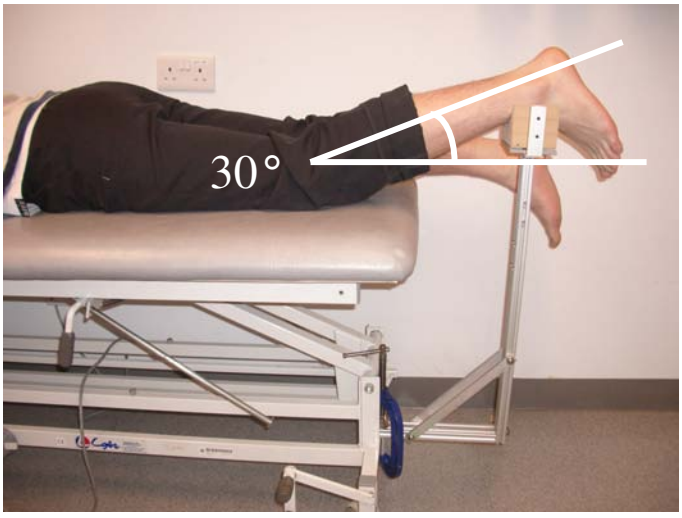

Figure 3.4.3-1 The knee was kept at 30° flexion, adjusted by the height adjustable examination table

2. The knee axis was kept horizontal. It was confirmed by a pure sagittal plane movement of the lower leg during the repeatedly and passively flexion and extension of the knee. To measure the knee flexion angle, one of the arms of the goniometer was aligned to the imaginary axis linking the greater trochanter and the knee joint axis, while the other arm was aligned parallel to the imaginary axis linking the fibular head and the lateral malleolus. Although the U-shaped cushioned ankle support has a fixed height, the knee angle could be adjusted by changing the height of the electronic examination table.

3. The tibial and calcaneal bisection lines were drawn with the aid of the bisecting and marking devices. The subtalar joint was manipulated to its neutral position by palpating the maximum joint congruity.

4. Orfit^{TM}, a low-temperature thermo-plastic, was heated to 65°C in a heating water bath and moulded at room temperature about 24°C. It becomes semi-transparent during the softened stage and thus the calcaneal bisection line was visible under the plastic material (Figure 3.4.3-2). The moulding

of the material should be carried out when it is heated and still transparent in plastic stage. The material should not be undersized to prevent excessive stretching during the moulding process (about 120% foot length and 140% of the metatarsals width). In order to control the pressure uniform between the foot impressions with different subtalar orientations, the size of the material used for each individual subject was the same and the material should be transparent, i.e. in plastic stage, during moulding. One mold was made for each condition.

Figure 3.4.3-2 The calcaneal bisection line was visible under the semi-transparency of the softened Orfit™ low-temperature thermoplastic

5. The subtalar joint angle was monitored by checking the angle between the bisection lines with a goniometer attached to the top of u-shaped cushioned support. For the foot impression of the right foot, the left hand of the orthotist supported the ankle dorsally while the right hand applied controlling force approaching from the lateral forefoot region, just distal to the metatarsal head (Figure 3.4.3-3). The index and thumb applied controlled forces across the metatarsal heads on the dorsal and plantar surface respectively. The subtalar joint angle was manipulated to the desired subtalar joint angle by applying clockwise or counterclockwise force in the frontal plane. The ankle was controlled at plantargrade position.

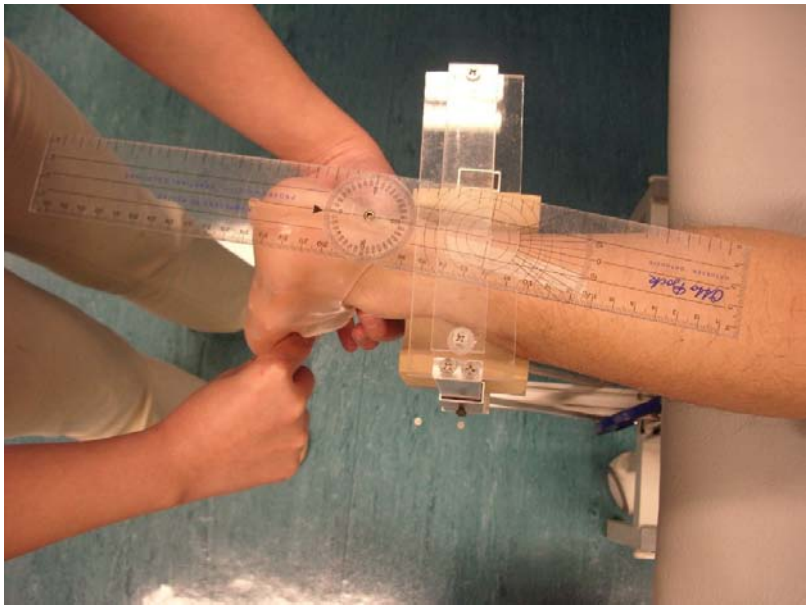

Figure 3.4.3-3 Manipulation for the subtalar joint orientation.
The left hand was used to support the ankle while the right hand was applying controlling forces at the forefoot region of the right feet.

6. In order to keep the forefoot-to-rearfoot angle perpendicular, dorsiflexory or plantarflexory force would be applied by the same hand at the medial or lateral forefoot regions.

7. When the plastic foot impression cooled down in room-temperature, it became non-transparent and the impression could be removed from the foot.

8. The forefoot-to-rearfoot angle of the plastic foot impression was evaluated by standing it on a table. If the calcaneal bisection line of any impression was deviated from the imaginary vertical line bigger than 1°, it should be neglected. Another impression with same subtalar joint orientation would be taken again from the subject's foot.

9. The impression was filled with plaster of pairs. The plastic impression was removed and the positive plaster model was dried in an oven and prepared for scanning. Although a flat Orfit sheet is quite flexible, the contour of the negative foot impression made by Orfit is rigid enough and would not be distorted after removed from the foot and during the negative cast filling. In addition, four layers of plaster bandage were wrapped outside the Orfit impression during cast filling.

10. The dried plaster model was scanned by the INFOOT laser scanner.

Figure 3.4.3-4 An L-frame helped to locate the plaster models in the same position on the scanning platform for each scanning

i. The glass of the scanning platform was cleaned and free from dust and plaster powder.

ii. An L-frame was located on the scanning platform, with the corner of the frame matching with the left corner of the scanning platform while scanning the right plaster model, and vice versa for the left plaster model.

iii. The medial edge of the plaster model was aligned with the longer edge

of the L-frame and the heel of the plaster model was in contacted with the shorter edge of the L-frame.

iv. The L-frame was carefully removed from the scanning platform, without moving the plaster model. (Figure 3.4.3-4)

v. The glass of the scanning platform was checked again, to ensure that it was free from dust or plaster powder.

vi. The cover of the INFOOT scanning was put back properly, to avoid any light source entering the scanning environment.

vii. The plaster model was scanned. The 3D image was checked immediately through the INFOOT software. If there were noises or irregularities on the image, the plaster model should be scanned again, by removing the plaster model on the scanner first and repeating steps i-vii.

3.5. Development of the custom-written computer program for quantifying the plantar foot geometry

3.5.1. Aim

During the foot impression procedure, orthotists usually palpate and mark the body landmarks on the skin surface by indelible pencil and then take the foot impression by impression materials like plaster bandage. The marking position of the body landmarks might vary from time to time. The accuracy of the position may be further reduced after the landmarks transferred from the skin surface to the plaster bandage, mainly due to the skin movement and the ink of the indelible pencil burred. Thus the parameters defined in this study would not rely on palpated landmarks. All of them depended on the capability of the software to recognize the geometrical features on the plaster model.

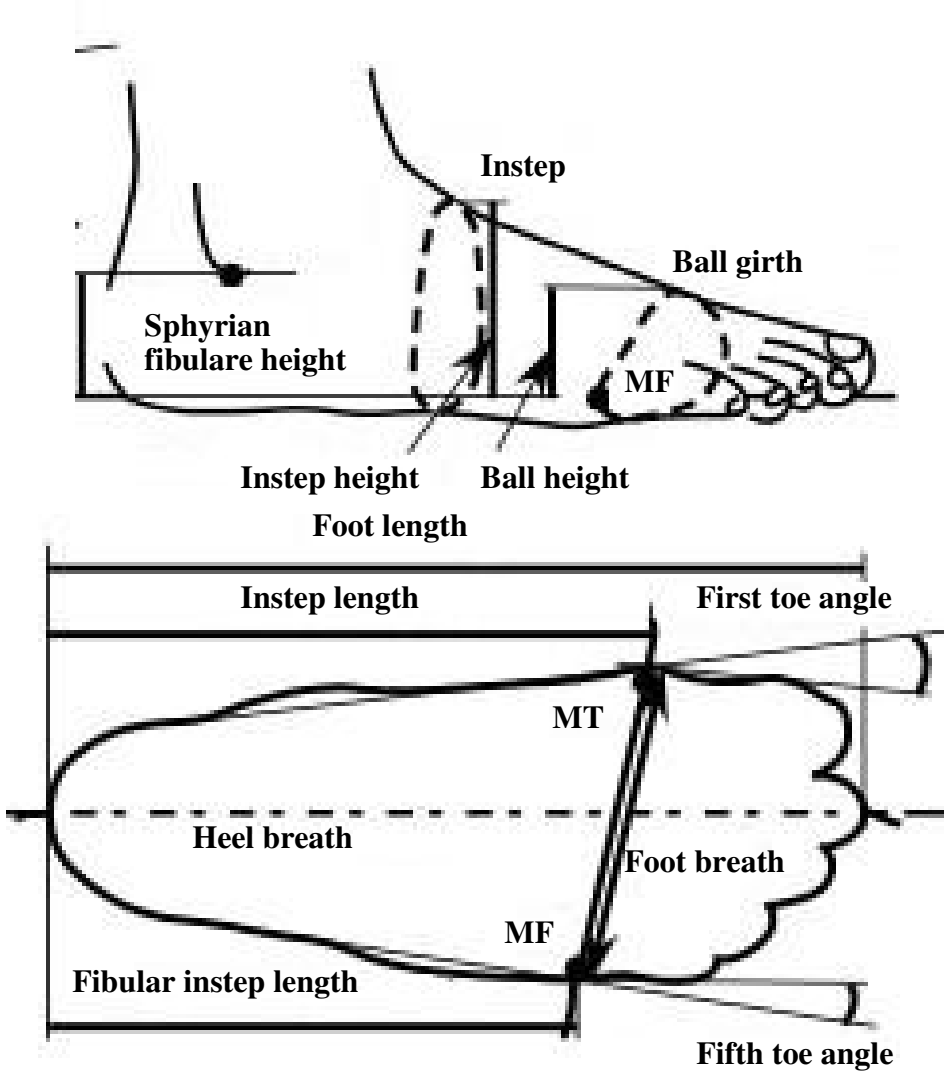

Figure 3.5.1-1 The dimensions measured by its built-in program of the INFOOT scanner

The resolution of the INFOOT scanner was set to be 0.5 mm in this study. The 3-D Cartesian co-ordinates of the scanned points were stored in the commas separated values (.csv) file format. There was a built-in software with the INFOOT scanner to generate foot parameters (Figure 3.5.1-1). However, these parameters relied on the markers stuck manually on the object before scanning. Some of the marker positions

were missing on the plaster foot model. Also palpation of landmarks on rigid plaster models might not be accurate. Thus the dimensions from the built-in program were not used. Custom-written software in Visual Basic programming language was developed and operated in Cartesian coordinates.

3.5.2. Definition of the reference axes

3.5.2.1. The z-axis (the inferior-superior axis)

The vertical orientation of the scanned plaster models was defined as z-axis, as the same as the INFOOT software.

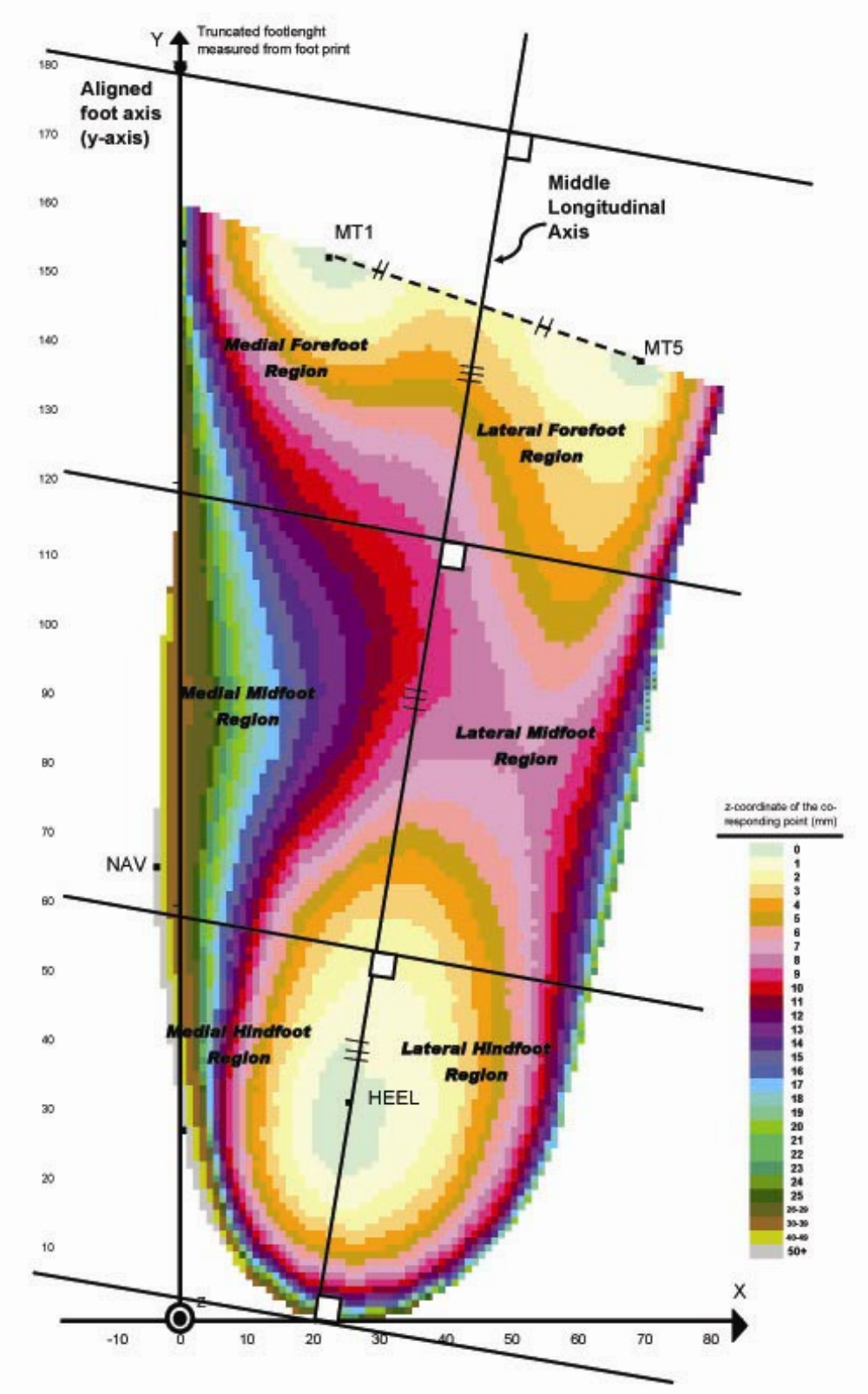

Figure 3.5.2.1-1 Definition of axes, reference points and the six foot regions.

MT1: first metatarsal contact point, MT5: fifth metatarsal contact point, HEEL: heel contact point, NAV: navicular

3.5.2.2. The y-axis (the posterior-anterior axis)

The y-axis of the foot was defined as the line connecting the most medial point at the forefoot region and the most medial point on the hindfoot region of the plaster model (Figure 3.5.2.1-1). This definition was also applied by Robinson and Frederick (1989) and Liu and his associates (1999). As the scanned image directly output from the INFOOT scanner was not aligned like this definition, the foot image was first transformed to align with the desired y-axis. It was by rotating the whole co-ordinate system along the x-y plane anti-clockwisely until the x-coordinate of the most medial point of the forefoot (allocated within the anterior 1/3 of the truncated foot length[2]) was equal to the x-coordinate of the most medial point of the hindfoot (allocated within the posterior 1/3 of the truncated foot length). The medial protrusion of the navicular (allocated within the middle 1/3 of the truncated foot length) was ignored.

3.5.2.3. The x-axis (the medial-lateral axis)

The x-axis was orthogonal to the y- and z-axes.

[2] Truncated foot: the entire foot area without counting the toes.

3.5.2.4. Directions of the axes

The plantar image was then shifted such that the most medial points of the forefoot region were zero in the x-coordinate, the most posterior points were zero in the y-coordinate and the most inferior points were zero in their z-coordinate. As both feet of the subjects were investigated, all left foot images were mirrored as the right side for the ease of comparison. The positive x-axis was pointing to lateral direction, the positive y-axis pointing anterior and the positive z-axis pointing superiorly.

3.5.3. Reference points of the image

As the foot impression might not cover the entire foot, the truncated foot length was determined by the inked footprints of the subject as described in section 3.4.1 (page 66). The image was temporarily divided into three equal parts along the y-axis according the truncated foot length. They were forefoot, midfoot and hindfoot regions. The medial and lateral forefoot regions were temporarily defined by dividing the forefoot width of the foot image into halves parallel to the y-axis. The reference points and lines of the foot image were defined as the following:

- ***The first metatarsal contact point (MT1) and the fifth metatarsal contact point (MT5)*** on the supporting surface were defined as the central point of the points

cluster with z-coordinate equal to zero at the medial forefoot and lateral forefoot regions of the image respectively.

- ***The heel contact point (HEEL)*** was located at the center of the point cluster with zero z-coordinate at the hindfoot region of the image.
- ***The midline of the foot image*** was passing through the heel contact point (HEEL) and the midway between the first and fifth metatarsal contact points (MT1 and MT5).
- ***The metatarsal line*** was the line joining the MT1 and MT5.
- ***The navicular (NAV)*** was defined as the point with highest negative value of the x-coordinate in the midfoot region of the aligned foot image in the x-y plane. ***Navicular height*** is the z-coordinates of the NAV while the ***Navicular protrusion*** was the x-coordinates of the NAV.

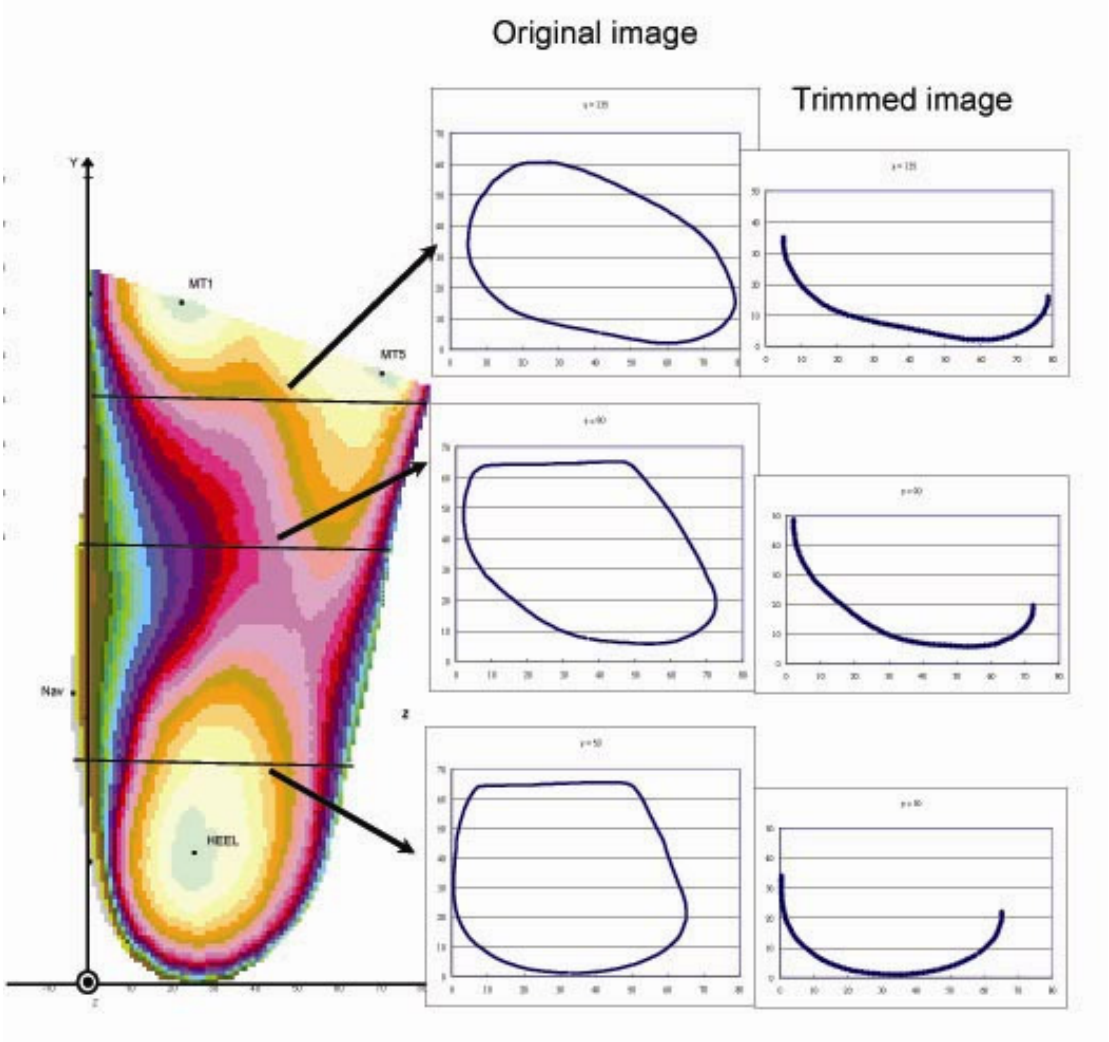

Figure 3.5.3-1 Modification of the scanned foot image:
The points above the turning points of the medial and lateral sides in each cross-section were not considered in the foot parameters calculation..

In plaster rectification procedure of the semi-rigid foot orthoses with full foot length, plaster would be added at the region anterior to the metatarsal heads to develop a flat forefoot plate. Similarly, the aligned foot image was modified so that all the data points anterior to the metatarsal line were changed to be zero in their z-coordinates. In addition, all the points above the turning point at the medial and lateral borders of

each x-z cross-section were removed (Figure 3.5.3-1). It is because the trimline of the total contact foot orthosis were just above the turning points of the medial and the lateral borders of the plaster model.

3.5.4. The Foot parameters

Based on the defined coordinates system and the reference points, three main groups of foot parameters were generated from the software. They were:

(i) Regional projection volume

(ii) Medial-lateral slopes, and

(iii) Dimensional Measurements: arch heights, navicular height and protrusion, and metatarsal width

3.5.4.1. Regional Projection Volume (Unit: mm^3)

The projection volume was the volume between the image and the supporting surface, i.e. the zero x-y plane. The image was divided into six regions in the x-y plane. The middle longitudinal axis joined the midpoint of the first and fifth metatarsal contact points (MT1 and MT5) and the heel contact point (HEEL). It divided the foot image into medial and lateral halves. The foot image was further divided into three parts which were perpendicular to the middle longitudinal axis and

according to the truncated foot length measured from the inked footprint (Figure 3.5.2.1-1 at page 80). These three parts were labeled as forefoot, midfoot and hindfoot regions. Therefore, there were six regional projection volumes in each foot image, they were

- $Volume_{MF}$ in the medial forefoot region,
- $Volume_{LF}$ in the lateral forefoot region,
- $Volume_{MM}$ in the medial midfoot region,
- $Volume_{LM}$ in the lateral midfoot region,
- $Volume_{MH}$ in the medial hindfoot region, and
- $Volume_{LH}$ in the lateral hindfoot region.

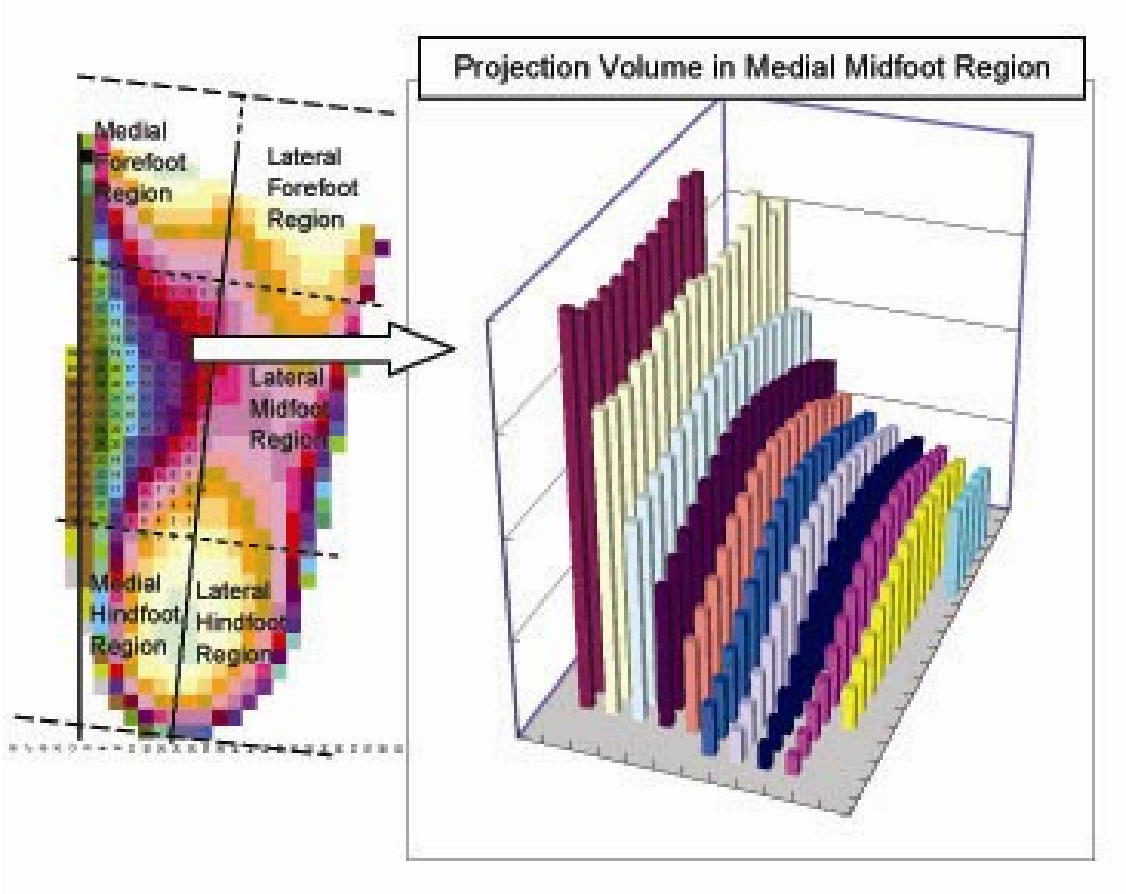

Figure 3.5.4.1-1 Calculation of the regional projection volume.
Using medial midfoot region as an example. Each point in the image was imagined as a column and hence the projection volume of each column = z-coordinates x 1 mm x 1 mm

During the calculation, the foot image was imagined to be constructed by numbers of rectangular columns of 1 mm wide and 1 mm long, and the location of each column was represented by the x- and y-coordinates. Thus the height of each column was the z-coordinates of the corresponding x- and y- coordinates. The volume of a particular region was calculated as the sum of the volume of the columns within the corresponding region. To simplify, the volume of the particular region was equal to

the sum of the z-coordinates of the points within the region x 1 mm x 1mm (Figure 3.5.4.1-1). The volume in specific regions would help to deduce the directional changes of the images. For example, the increase in the volume in the medial region implied that the foot image was more inverted.

3.5.4.2. Medial-lateral slopes (Unit: degree)

Foulston and his associates (1990) studied the plantar geometry in terms of medial-lateral slopes. Their reference axis was defined as the line joining the second metatarsal head and the heel center. Each cross-section was perpendicular to this reference axis (Figure 3.5.4.2-1). This study avoided using the marker system to define the anatomical landmarks and the second metatarsal head could not be defined on the geometrical shape on the plaster model. The method used by Foulston and his associates (1990) was modified.

In this study, the scanned foot image was evenly divided into 10 medial-lateral cross-sections from the metatarsal line to the back of the heel. Each cross-section was parallel to the metatarsal line and could be plotted as z-coordinates against x-coordinates (Figure 3.5.4.2-2).

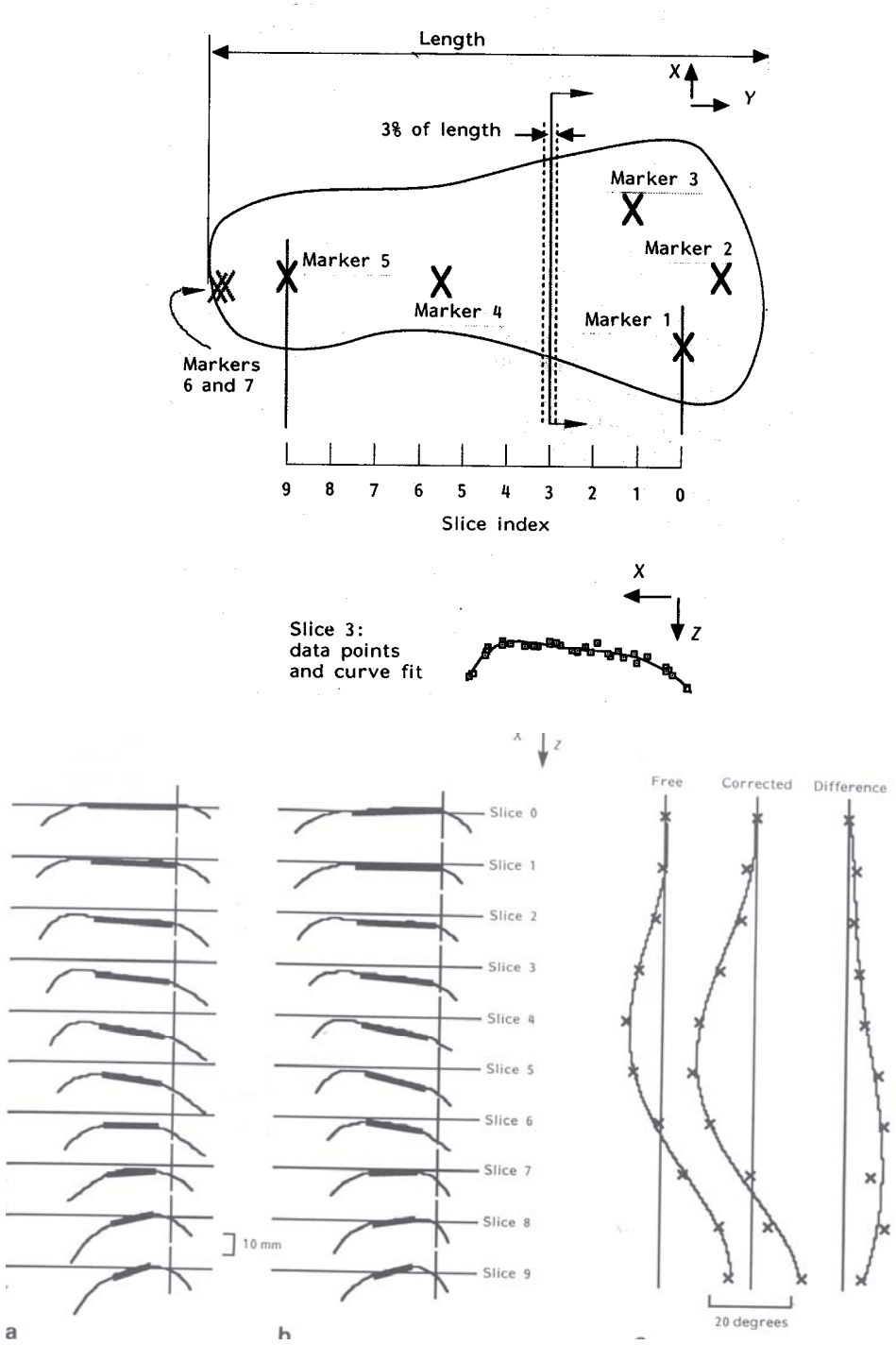

Figure 3.5.4.2-1 Three-dimensional analysis of plantar surface shape adopted by Foulston et al. (1990)

(Top) The plantar surface was divided into 10 cross-sections from 1st metatarsal head to the heel center.

(Bottom) The left diagram showed the contour of each cross-section with two different foot impression methods, and the right diagram showed the plots of the slopes of each cross-section.

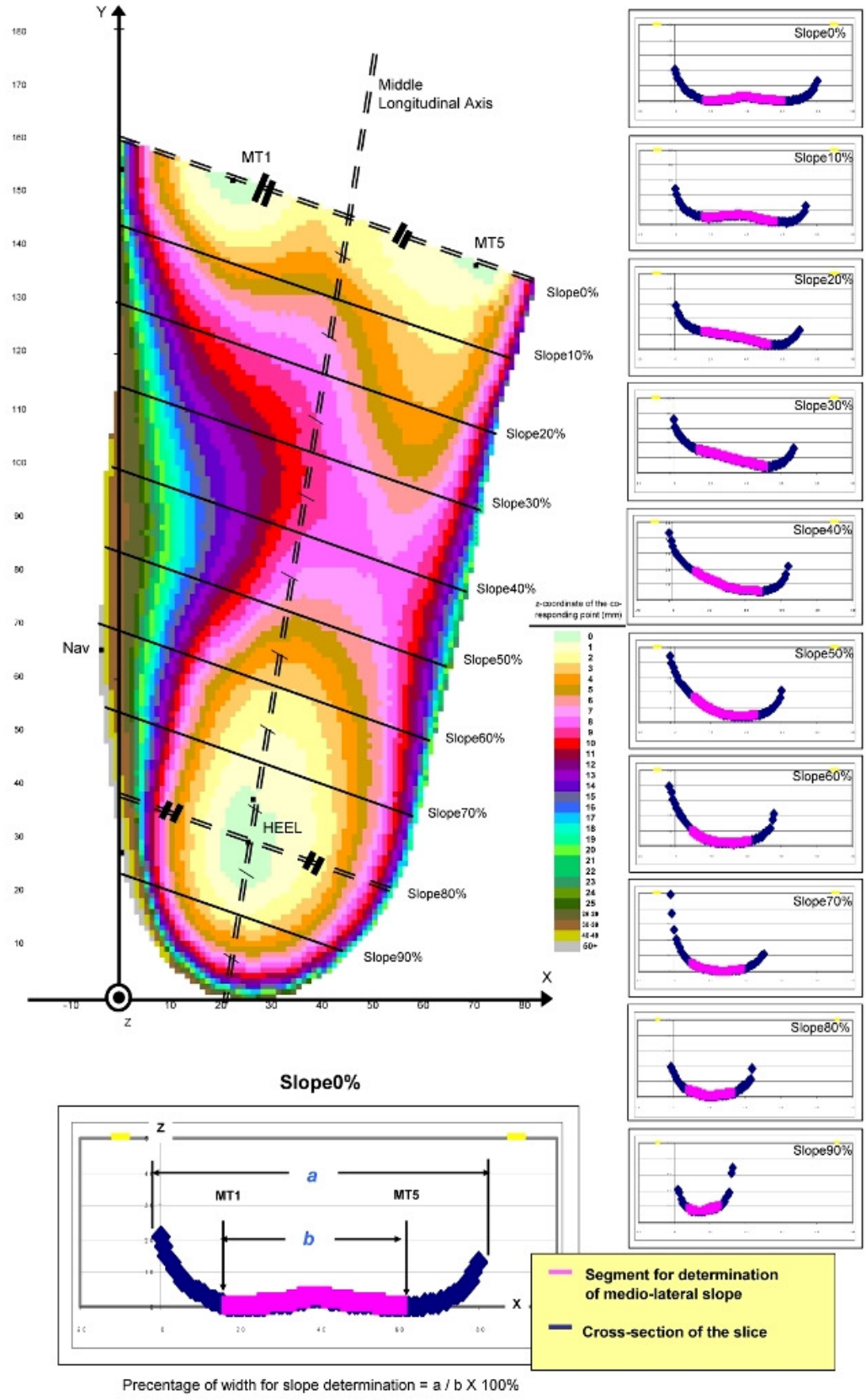

Figure 3.5.4.2-2 The definition of the medial-lateral slopes

The medial-lateral slop of each cross-section was determined by linear regression, by the formula:

$$slope = \frac{n\sum XZ - (\sum X)(\sum Z)}{n\sum X^2 - (\sum X)^2}$$

n = number of points selected in the slice

X = x-coordinates of the point

Z = z-coordinates of the point.

Using linear regression for calculating the slopes was also adopted in the study of Foulston and his associates (1990). The transverse curvatures of the plantar forefoot and midfoot have big radii and thus the linear approach was applied to compare the slopes among various regions.

As the points at both medial and lateral edges of each cross-section were curving, they deviated from the overall trend in the middle portion of the cross-section. In some orthotic design like posted foot orthosis (Figure 2.5-2 at page 47), the original shapes of these curving parts were modified by adding some plaster there. Therefore, these points were not included in the slope calculation. Only the central portions of the cross-sections were included in the slope calculation.

The number of points for slope calculation of each cross-section was determined by ***the percentage of width for slope determination***, which was defined as the percentage of the distance between the MT1 and MT5 over the width of that cross-section (Figure 3.5.4.2-2). The points under consideration for the slope calculation in the rest of the cross-sections were equal to the width of that cross-section times this percentage. The cross-section with the MT1 and MT5 was labeled as medial-lateral slopes at 0% of foot model length position (Slope0%), and the rest of the medial-lateral slopes were labeled as Slope10%, Slope20% … and Slope90% respectively. The positive slope meant the slope running up from the lateral region to the medial region.

3.5.4.3. Dimensional Measurements

The definitions of the dimensional measurements were illustrated in (Figure 3.5.4.3-1).

- Medial and lateral arch heights (Unit: mm)

  Two vertical cross sections were extracted from the image, starting from the first metatarsal contact point (MT1) to the heel contact point (HEEL) and from the fifth metatarsal contact point (MT5) to the heel contact point (HEEL). They

represented the medial and lateral longitudinal arches respectively. The z-coordinates of the highest point of the arches were defined as the medial and lateral longitudinal arch heights.

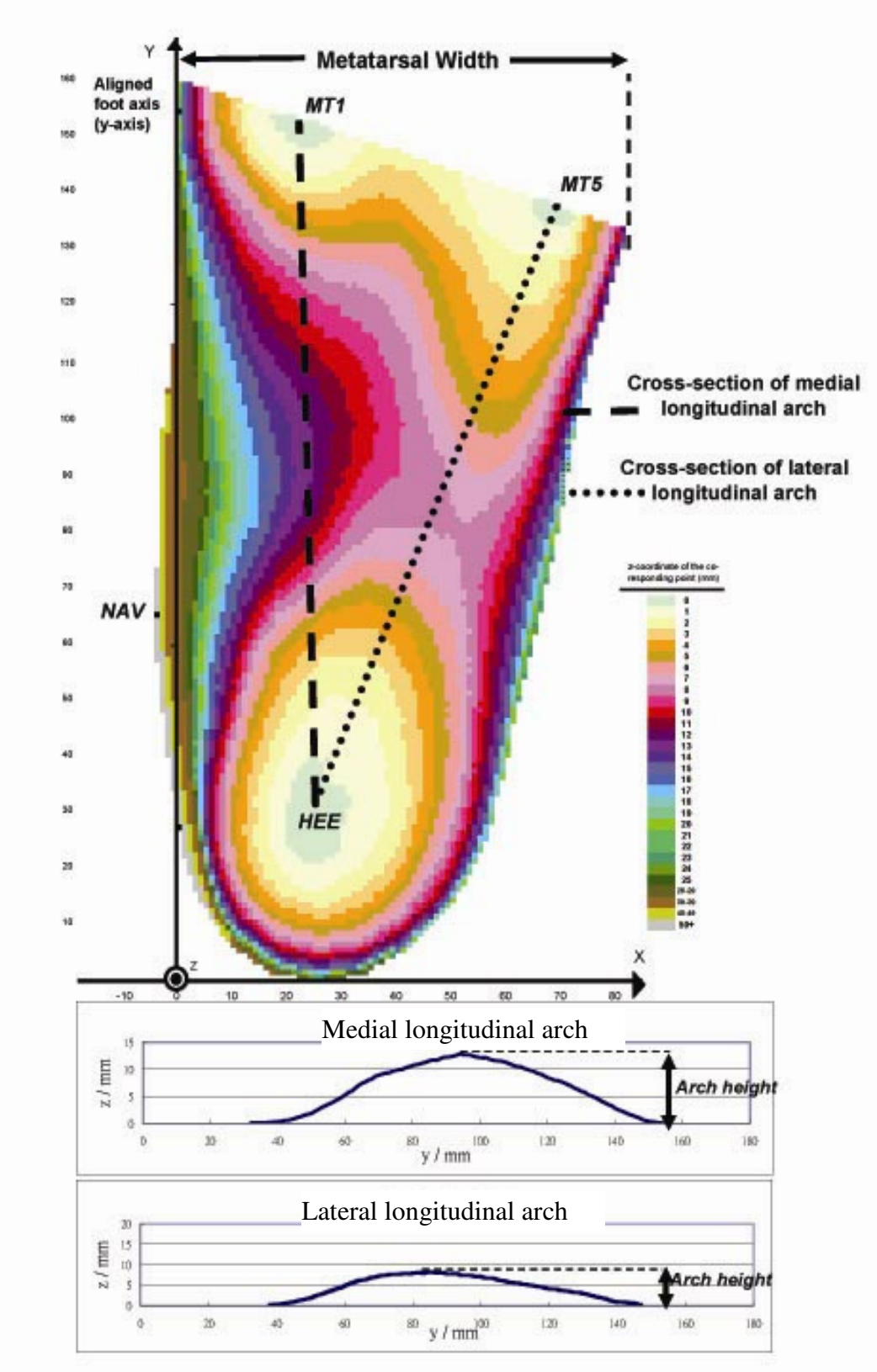

Figure 3.5.4.3-1 The definition of the medial and lateral longitudinal arch heights, navicular height, navicular protrusion and metatarsal width

- Navicular height and navicular protrusion (Unit: mm).

The Navicular (NAV) was defined as the most medial point of the image at the middle one third of the foot image in the x-y plane. Its x-coordinate was the navicular protrusion. The zero magnitude in x-coordinates was regarded as the navicular was located exactly on the medial reference axis (y-axis) while a positive value regarded as navicular protruding medially to the medial reference axis. The corresponding z-coordinate of that point was regarded as navicular height.

- Metatarsal Width (Unit: mm)

The metatarsal width was determined as the widest width of the image in the x-y plane parallel to the x-axis.

3.5.5. The accuracy and reliability of the INFOOT scanner

The accuracy of the foot parameters generated by the INFOOT laser scanner with the custom written software were tested through scanning of a rectangular block and also through scanning of a plaster foot model. As the plaster model of the human foot is irregular in shape, its dimensions measured by manual measurement would not be as accurate as those of a rectangular object. Therefore, a rectangular block was scanned

for preliminarily checking the accuracy of the scanner. The width and length of the rectangular block was closed to those in the x, y and z directions of human feet of smaller size. The accuracy test by scanning plaster foot model was also performed after that.

The rectangular block was scanned thrice. It was prepared by milling machine with the dimensions of 75 mm x 75 mm x 150 mm measured by mechanical caliper. It was then painted in white to match the same colour of plaster models. The resolution of scanning was set as 0.5 mm. For each scanning, the block was positioned, scanned and then removed. There was an L-frame which located the scanned object in a similar position for each scanning. The procedure of the scanning the rectangle block was as follow:

1. The glass of the scanning platform was cleaned and free from dust and plaster powder.
2. An L-frame was located on the scanning platform, with the corner of the frame matching with the left corner of the scanning platform.
3. The longer edge of the rectangular block was aligned with the longer edge of the L-frame and the shorter edge of the block was in contacted with the

shorter edge of the L-frame.

4. The L-frame was carefully removed from the scanning platform, without moving the rectangular block.
5. The glass of the scanning platform was checked again, to ensure that it was free from dust or plaster powder.
6. The cover of the INFOOT scanning was put back properly, to avoid any light source entering the scanning environment.
7. The rectangular block was scanned. The 3D image was checked immediately through the INFOOT software. If there were noises or irregularity on the image, the rectangular block should be scanned again, by removing the rectangular block on the scanner first and repeating steps 1-7.

The INFOOT scanner provided a consistent way for accurate measurement. The z-coordinates of the points on the bottom surface of the scanned image were first set zero. The image was then rotated anticlockwisely on the x-y plane until the longer edge aligned to the y-axis. The x-coordinates of the points on that surface of the image were set zero. The y-coordinates of the points on the surface orthogonal to the

y-z plane were set zero too. The widths, lengths, and heights obtained were the averaged x-, y- and z-coordinates of the points on the other three surfaces of the image respectively.

The consistency of the foot scanner was also tested. Four plaster models were scanned twice. The procedure of the scanning of the plaster model was similar to those stated as the point 10 of section 3.4.3 in the methodology session on page 74.

In the pilot study, the accuracy of the computer program was checked. It was by checked by manual measurement and manual calculation. In manual calculation, the horizontal labels of a excel spreadsheet represent the x-coordinates of the foot image and the vertical labels of the spreadsheet represent the y-coordinates of the foot image. Then the corresponding z-coordinates were input into the spreadsheet. The manual calculation should be the same as the values calculated by the computer program.

For manual measurement, there were about 0-3 mm differences between the manual measurement and calculated by the computer program. During the manual

measurement, the plaster models were aligned to the reference axes with the same definition as those the computer program. The differences might be resulted from the deviation of keeping the measuring tools (like ruler, set square, caliper) orthogonal to the reference axes.

To find the medial-lateral slopes, the plaster model was divided into ten cross-sections and marked. A small inclinometer was used to measure the slope of each section. As each cross-section was not completely straight and had a little curvature, there were about 0-5° difference between the manual measurement and by computer program.

To find the projection volume of the different foot regions, plastsil was inserted between the plaster model and the support surface. The difference between the volume of the plastsil and the calculated volume was within 0.5 cm^3.

The scanning resolution 0.5 mm was the finest available by the INFOOT scanner. Therefore it was chosen for the scanning process. In the pilot study, the calculation of the foot parameters for each foot using 0.5 mm resolution spent about twenty

minutes. Therefore the 1 mm resolution was used for calculation in order to shorten the time for the data processing.

* * * * * * * *

3.6. Data Analysis

The computer software, SPSS (Version 13.0) statistical package, was used for statistical analysis. Significant level of all the statistical tests was set as 0.05.

3.6.1. The reliability of the tibial and calcaneal bisecting and marking devices

The intraclass correlation coefficient ICC (3, 1) was used to determine the intra-rater reliability of the tibial stance and the relaxed calcaneal stance position (RCSP) marked by the devices and the clinical method which were performed by the same orthotist. The intraclass correlation coefficient ICC (2, 1) was used to determine the inter-rater reliability by the devices and the clinical method.

3.6.2. The reliability of the INFOOT laser scanner with the custom written software

The intraclass correlation coefficient ICC (3,1) was used to determine the reliability of the foot parameters generated by the INFOOT scanner with the custom written software between two scanning trials.

3.6.3. Data analysis of the foot parameters

There were eight conditions studied for each foot parameter:

- left feet with -4° inversion,
- left feet with -2° inversion,
- left feet with 0° inversion,
- left feet with 2° inversion,
- right feet with -4° inversion,
- right feet with -2° inversion,
- right feet with 0° inversion, and
- right feet with 2° inversion.

The Shapiro-Wilk normality test was carried out first. The Shapiro-Wilk test tests the null hypothesis that a sample comes from a normal distribution population. The result is shown in Appendices V-VII. The test rejects the null hypothesis if $p<0.05$. As over 90% of the parameters were supported by the null hypothesis, parametric test was applied in the rest of the study.

Two-way repeated measure analysis of variance (ANOVA) within-subject design was used to determine whether significant difference existed between different subtalar joint orientations of the individual foot parameters. Two within-subject factors were **left/right side factor** (2 levels: left and right feet) and **subtalar joint orientation** (4 levels: -4°, -2°, 0° and 2° inversion). If the statistically significance in main effect was found, post-hoc multiple comparison test, Bonferroni test, would be

performed to found out which pairs of subtalar joint orientations had that significant difference. No between-subject factor was set.

In order to investigate the linear relationship between the foot parameters, the Pearson's linear correlation coefficients were calculated by the SPSS software between selected pairs of the foot parameters.

Chapter 4. Results

This chapter presents the results of the investigation in the sequence as the followings:

- Subjects' particulars and foot types
- The reliability tests and the accuracy of the measuring devices and equipments used
- The effect of the subtalar joint orientations on the foot parameters
- The effect of the left/right side on the plantar foot geometry
- Correlations among the foot parameters

4.1. Subjects' particulars and foot types

Table 4.1-1 General information of the twenty subjects

Subject	Gender	Age	Weight (kg)	Height (m)
1	F	22	47.7	1.57
2	M	32	50.0	1.73
3	F	29	54.4	1.60
4	F	29	46.4	1.54
5	F	28	49.0	1.50
6	M	25	56.0	1.70
7	F	26	50.0	1.56
8	M	24	51.0	1.75
9	M	26	54.5	1.69
10	M	46	43.2	1.65
11	F	26	44.1	1.67
12	F	28	58.2	1.54
13	F	28	81.9	1.65
14	M	27	77.3	1.75
15	F	31	75.0	1.70
16	F	24	59.1	1.57
17	F	28	52.3	1.60
18	M	32	88.6	1.63
19	F	28	82.7	1.60
20	M	28	76.4	1.62
Mean	/	28.35	59.9	1.63
SD	/	4.77	14.17	0.07

There were 8 males and 12 females participated in the study. The mean age of the subjects was 28.4 years old (SD = 4.77). Their mean height was 1.63 m (SD = 0.07) and the mean weight was 59.89 kg (SD = 14.17). The general information of the twenty subjects is shown in Table 4.1-1.

Table 4.1-2 Relaxed calcaneal stance position (RCSP) and navicular drop of the subjects

Subject	RCSP* (°)		Navicular drop	
	Left	Right	Left	Right
1	-1.0	0.5	5.0	*5.0*
2	-1.5	-2.0	10.0	*10.0*
3	-1.5	-1.5	3.5	*5.5*
4	-2.0	-1.5	7.0	*6.5*
5	-1.5	-1.0	6.0	*8.0*
6	-0.5	-0.5	9.0	*7.5*
7	2.0	1.5	5.0	*3.0*
8	0.5	0.0	4.0	*5.5*
9	-1.5	-2.0	5.5	*6.0*
10	-2.0	-1.0	7.5	*6.0*
11	1.0	0.5	2.5	*3.0*
12	-1.0	-0.5	5.0	*2.5*
13	-1.5	-2.0	3.0	*5.5*
14	-1.5	-2.0	5.5	*2.5*
15	1.0	1.5	3.0	*3.0*
16	-0.5	-1.0	3.5	*7.5*
17	0.0	0.5	5.5	*9.0*
18	-2.0	-1.5	6.0	*4.5*
19	1.0	0.0	6.0	*6.5*
20	-1.5	-1.0	11.5	*11.5*
Mean	-0.7	-0.7	5.7	*5.9*
SD	*1.21*	*1.13*	*2.38*	*2.51*

*Remark: positive value indicates inversion

The relaxed calcaneal stance position (RCSP) and the navicular drop of each subject are shown in Table 4.1-2. The mean RCSP was 0.7 ± 1.21° eversion on the left side and 0.7 ± 1.13° eversion on the right side. The mean navicular drop was 5.7 ± 2.38 mm on the left side and 5.9 ± 2.51 mm on the right side.

4.2. The reliability tests and the accuracy of the measuring devices and equipments used

4.2.1. The reliability test of the tibial and the calcaneal bisection lines marking

Table 4.2.1-1 The intra-rater reliability of the tibial stance and the relaxed calcaneal stance position (RCSP) marked by clinical method and bisecting devices

	Clinical method				Bisecting and marking devices			
	Tibial stance (°)*		RCSP (°)*		Tibial stance (°)*		RCSP (°)*	
Subject	Trial 1	Trial 2	Trial 1	Trial 2	Trial 1	Trial 2	Trial 1	Trial 2
1	8	8	-3	-2	10	10	-3	-3
2	9	8	-2	-2	9	9	-3	-2
3	3	8	-8	-6	5	5	-2	-3
4	2	3	-3	-3	4	4	-2	-3
3	8	9	1	-4	8	10	-2	-2
6	8	12	2	0	10	10	-2	-2
7	5	5	6	6	3	3	2	3
8	8	6	0	-4	10	10	-2	-4
9	10	6	-10	-6	4	4	-6	-4
10	6	6	-2	-2	12	10	-2	-2
ICC (3,1)	0.64		0.88		0.98		0.91	

Remark: Positive value indicates inversion

The intra-rater reliability coefficient ICC (3,1) of the tibial stance and the relaxed calcaneal stance (RCSP) marked by the tibial and calcaneal bisecting and marking devices and the clinical method were compared (Table 4.2.1-1). With the tibial bisecting and marking devices, the ICC (3,1) of the tibial stance increased to 0.98 (95% CI 0.91 to 0.99), higher than that by clinical method (ICC(3,1) = 0.64, 95% CI to 0.46 to 0.91). The reliability of the RCSP marked with the calcaneal bisecting and

marking device, ICC (3,1) = 0.91 (95% CI 0.62 to 0.98), was close to that of the clinical method, ICC (3,1) = 0.88 (95% CI 0.52 to 0.97). The coefficient of reliability of both the tibial stance and the RCSP marked by the tibial and calcaneal bisecting devices exceeded 0.90. The devices were classified as having good reliability (Portney and Watkins, 1993) and were used in this study

Table 4.2.1-2 The inter-rater reliability of the tibial stance and the relaxed calcaneal stance position (RCSP) marked by clinical method and bisecting devices

Rater	Subject	Clinical method		Bisecting and marking devices	
		Tibial stance (°)*	RCSP (°)*	Tibial stance (°)*	RCSP (°)*
1	1	7	0	9	0
	2	7	-2	8	-1
	3	8	-2	8	-1
	4	8	0	7	0
	5	7	0	8	-1
2	1	7	1	9	0
	2	8	-1	7	-2
	3	7	-3	8	-1
	4	9	1	7	1
	5	8	2	9	-1
ICC (2,1)		0.20	0.71	0.71	0.73

The inter-rater reliability coefficient ICC (2,1) of the tibial stance and the relaxed calcaneal stance (RCSP) marked by the tibial and calcaneal bisecting and marking devices and the clinical method were compared (Table 4.2.1-2). With the tibial bisecting and marking devices, the ICC (2,1) of the tibial stance increased drastically,

from 0.20 (95% CI -0.69 to 0.87) by the clinical method to 0.71 (95% CI -0.43 to 0.97) by the devices. The reliability of the RCSP marked with the calcaneal bisecting and marking device, ICC (2,1) = 0.73 (95% CI -0.38 to 0.97), was close to that of the clinical method, ICC (2,1) = 0.71 (95% CI -0.32 to 0.97).

4.2.2. The accuracy and reliability of the INFOOT scanner with the custom written software

Table 4.2.2-1 The results of the three scanning trials of a rectangular block with known dimensions by the INFOOT scanner

	Trial 1	Trial 2	Trial 3	Mean (SD)	Actual value	Root mean square error	% difference from actual value
Length (mm) (x-axis)	74.1	74.3	75.5	74.65 (0.76)	75.0	0.71	0.95%
Width (mm) (y-axis)	149.9	148.8	149.1	149.28 (0.54)	150.0	0.49	0.33%
Height (mm) (z-axis)	76.3	75.4	75.5	75.72 (0.47)	75.0	0.47	0.86%

The accuracy of the INFOOT scanner was checked by scanning a rectangular block. The results of the three scanning trials are shown in Table 4.2.2-1. The percentage of deviation from the actual values was within 1% for all dimensions.

Table 4.2.2-2 The intraclass reliability ICC (3,1) of the scanning of plaster foot models

Foot Parameters	ICC(3,1)	95% Confidence interval		*p*-value
		Upper bound	Lower bound	
Projection volume under				
Medial Forefoot	0.99	0.92	1.00	0.00
Lateral Forefoot	1.00	0.98	1.00	0.00
Medial Midfoot	1.00	0.97	1.00	0.00
Lateral Midfoot	1.00	0.97	1.00	0.00
Medial Hindfoot	1.00	0.97	1.00	0.00
Lateral Hindfoot	0.96	0.49	1.00	0.01
Medial-lateral slopes at				
0% (Metatarsals)	0.99	0.86	1.00	0.00
10%	0.95	0.45	1.00	0.01
20%	1.00	0.96	1.00	0.00
30%	1.00	0.99	1.00	0.00
40%	0.97	0.58	1.00	0.00
50%	0.96	0.49	1.00	0.01
60%	0.98	0.77	1.00	0.00
70%	0.97	0.59	1.00	0.00
80%	0.93	0.27	1.00	0.01
90% (Heel)	0.09	-0.86	0.90	0.45
foot model length position				
Dimensional measurements				
Medial Arch Height	1.00	0.98	1.00	0.00
Lateral Arch Height	1.00	0.99	1.00	0.00
Navicular Protrusion	1.00	0.99	1.00	0.00
Navicular Height	0.95	0.41	1.00	0.01
Metatarsal width	1.00	1.00	1.00	0.00

The reliability of the foot parameters generated by the INFOOT scanner with the software was tested by scanning four plaster foot models twice. The intraclass correlation coefficient ICC (3,1) of all foot parameters were ranging from 0.93 to 1.00 (p = 0.00 to 0.01), except in the medial-lateral slopes at 90% of the foot model length position (Table 4.2.2-2).

4.2.3. Locations of the anatomical features on the foot model

The anatomical features of the foot, such as the navicular, the medial longitudinal arch and the heel contact point (i.e. heel center in clinical practice) were represented by the x-, y- and z-coordinates on the foot model. The relative position of these anatomical features along the foot model length (defined from the first metatarsal contact point MT1 to the back of the heel and parallel to the y-axis) were calculated. The midfoot region extended from 24.63 ± 3.98% to 62.14 ± 4.09% of the foot model length. The apical point of the medial longitudinal arch and the heel contact point (HEEL) were at 41.37 ± 2.96% and 78.75 ± 2.54 % of the foot model length positions respectively. The apical point of the medial arch was at the midway between the MT1 and the HEEL. The navicular (NAV) was positioned at 56.17 ± 3.41% of the foot model length.

* * * * * * * * * * *

4.3. The effect of the subtalar joint orientations on the foot parameters

4.3.1. The means and standard deviations of the foot parameters

4.3.1.1. The Projection Volume

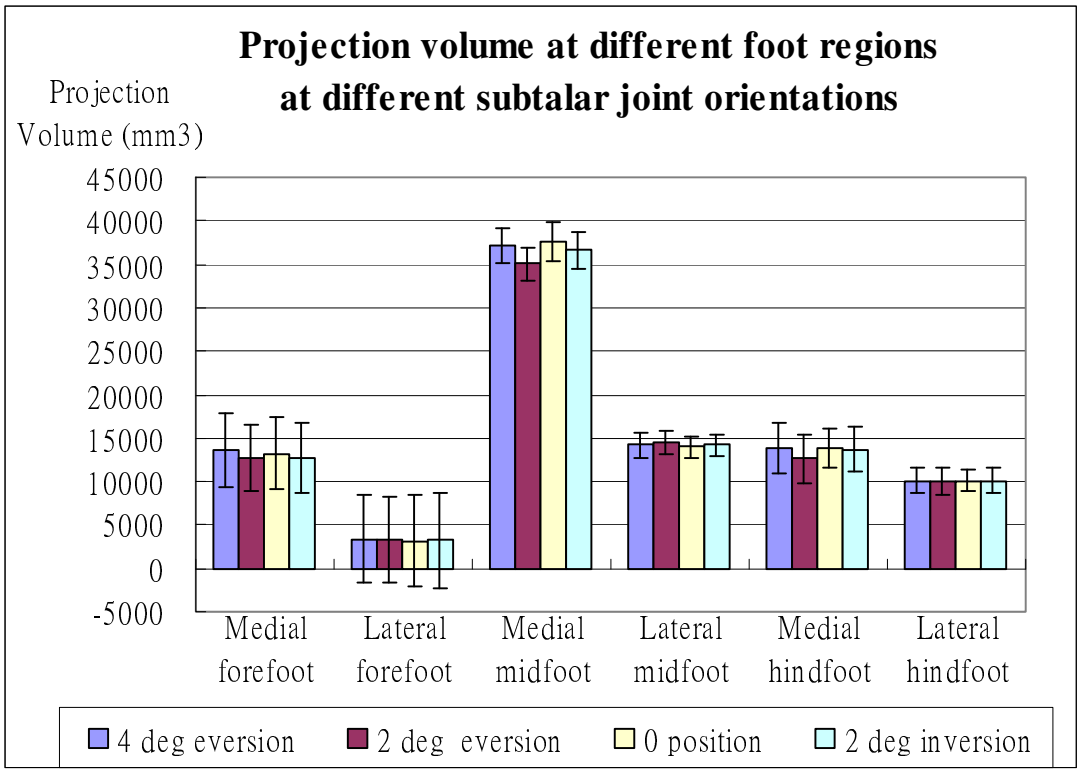

Figure 4.3.1.1-1 Projection volume (with ± 1 SD) in different foot regions at different subtalar joint orientations

Table 4.3.1.1-1 The mean and the standard deviation of the projection volume

Projection Volume (mm^3)		Subtalar joint orientations (positive as inversion)				Statistical analysis		
		-4°	-2°	0°	2°	F	*p*-value	Power
under medial forefoot ($Volume_{MF}$)	mean	13684.7	12676.6	13268.1	12796.8	12.33	*0.00**	0.98
	SD	4454.50	4275.46	4414.30	4347.40			
	SEM	945.6	850.5	909.5	904.2			
underlateral forefoot ($Volume_{LF}$)	mean	3384.9	3324.7	3133.9	3198.4	1.40	0.26	0.20
	SD	1559.61	1484.98	1312.98	1339.65			
	SEM	334.3	315.7	273.8	282.6			
under medial midfoot ($Volume_{MM}$)	mean	37111.6	35085.4	37657.0	36692.9	10.31	*0.00**	1.00
	SD	5534.23	5448.58	5436.70	5615.13			
	SEM	1135.9	1120.6	1166.4	1224.0			
Under lateral midfoot ($Volume_{LM}$)	mean	14225.1	14506.1	14012.9	14241.2	0.79	0.48	0.27
	SD	3197.87	3134.24	2619.58	2999.70			
	SEM	659.0	631.1	499.8	571.8			
under medial hindfoot ($Volume_{MH}$)	mean	13787.8	12655.3	13841.4	13641.9	5.62	*0.00**	0.93
	SD	2465.82	2123.33	2399.67	2293.36			
	SEM	451.4	429.1	489.8	477.0			
under lateral hindfoot ($Volume_{LH}$)	mean	10057.1	9982.5	10121.4	10067.5	0.44	0.73	0.14
	SD	1704.55	1754.48	1693.02	1820.71			
	SEM	326.9	336.3	286.9	320.0			

* *p*-value < 0.05

The mean and the standard deviation of the projection volume are shown in Figure 4.3.1.1-1and Table 4.3.1.1-1. The projection volume under the medial regions was bigger than that of the corresponding lateral regions in the forefoot, midfoot and hindfoot. The volume under the medial midfoot region was always at least one-fold bigger than the other regions. This reflected the location of the medial longitudinal arch.

4.3.1.2. The medial-lateral slopes

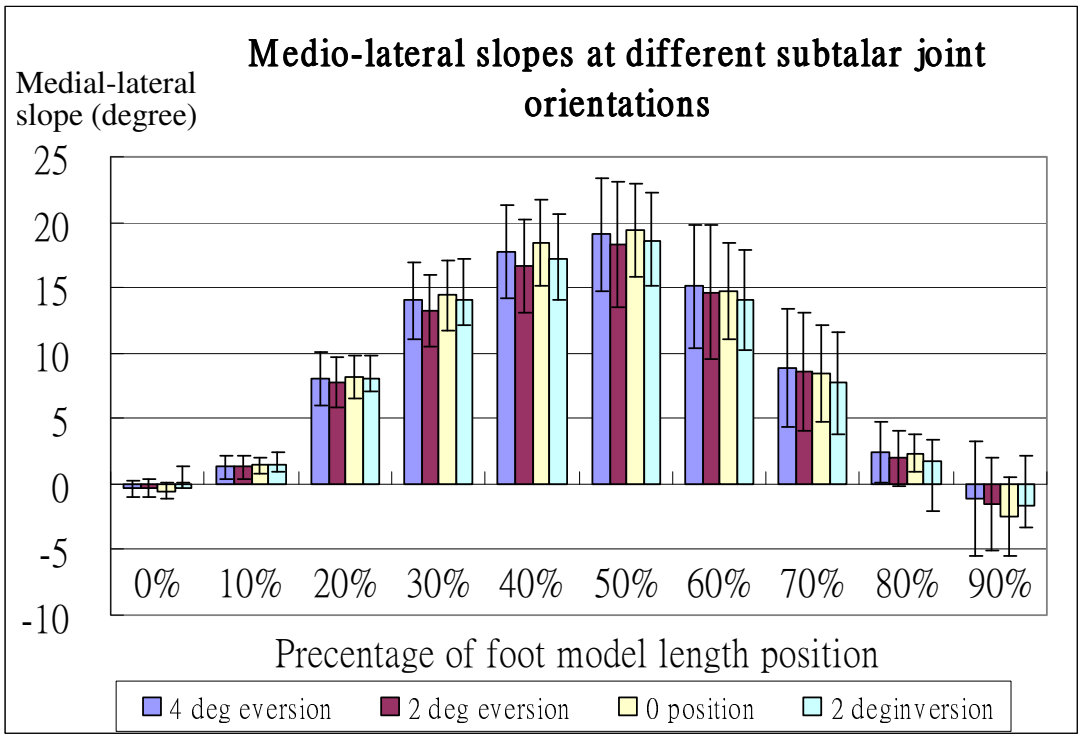

Figure 4.3.1.2-1 Medial-lateral slopes (with ± 1 SD) in different foot model length positions at different subtalar joint orientations

Table 4.3.1.2-1 The mean and the standard deviation of the medial-lateral slopes

Medial-lateral slopes (°)		Subtalar joint orientations				Statistical analysis		
		-4°	-2°	0°	2°	F	*p*-value	Power
At 0% foot model length position (Slope0%) (MT)	mean	-0.3	-0.3	-0.5	-0.3	1.16	0.33	0.30
	SD	0.74	0.77	0.84	0.67			
	SEM	0.1	0.2	0.1	0.1			
At 10% foot model length position (Slope10%)	mean	1.3	1.3	1.4	1.5	0.5	0.68	0.15
	SD	1.18	1.21	1.00	1.19			
	SEM	0.2	0.2	0.1	0.2			
At 20% foot model length position (Slope20%)	mean	8.1	7.8	8.1	8.0	0.82	0.45	0.22
	SD	2.33	2.20	2.21	2.64			
	SEM	0.5	0.4	0.4	0.4			
At 30% foot model length position (Slope30%)	mean	14.0	13.2	14.4	14.0	3.9	*0.02**	0.80
	SD	3.30	3.16	3.41	3.53			
	SEM	0.7	0.6	0.6	0.7			
At 40% foot model length position (Slope40%)	mean	17.7	16.7	18.4	17.2	3.82	*0.03**	0.79
	SD	3.84	3.82	4.57	4.27			
	SEM	0.8	0.8	0.7	0.8			
At 50% foot model length position (Slope50%)	mean	19.1	18.4	19.4	18.5	1.22	0.31	0.31
	SD	4.50	4.69	4.63	4.94			
	SEM	1	1.1	0.8	0.8			
At 60% foot model length position (Slope60%)	mean	15.1	14.7	14.8	14.0	0.97	0.39	0.25
	SD	4.83	5.21	4.91	5.10			
	SEM	1.1	1.1	0.8	0.9			
At 70% foot model length position (Slope70%)	mean	8.9	8.6	8.5	7.7	1.56	0.21	0.39
	SD	4.90	4.92	5.26	5.24			
	SEM	1.0	1.0	0.8	0.9			
At 80% foot model length position (Slope80%)	mean	2.5	2.0	2.3	1.8	1.23	0.31	0.31
	SD	2.65	2.39	2.66	2.65			
	SEM	0.5	0.5	0.3	0.4			
At 90% foot model length position (Slope90%) (Heel)	mean	-1.1	-1.5	-2.5	-1.6	0.89	0.45	0.23
	SD	5.34	4.99	3.98	5.27			
	SEM	1.0	0.8	0.7	0.8			

* *p*-value < 0.05

The mean and the standard deviation of the medial-lateral slopes are shown in Figure 4.3.1.2-1 and Table 4.3.1.2-1. The overall trend of the medial-lateral slopes increased

gradually from 0% foot model length position (at the metatarsal regions) and reached the steepest condition at 50% foot model length position (the middle of the medial longitudinal arch). Then the slopes gradually dropped towards 90% foot model length position (at the heel). The magnitudes of the slopes at the anterior part of the foot image (Slope0% - Slope50%) were not symmetrical to the slopes at the posterior part of the foot image (Slope50% - Slope90%). The differences between the maximum and the minimum slopes among the four subtalar joint orientations in each of the ten cross-sections studied were less than 2°.

4.3.1.3. The dimensional parameters

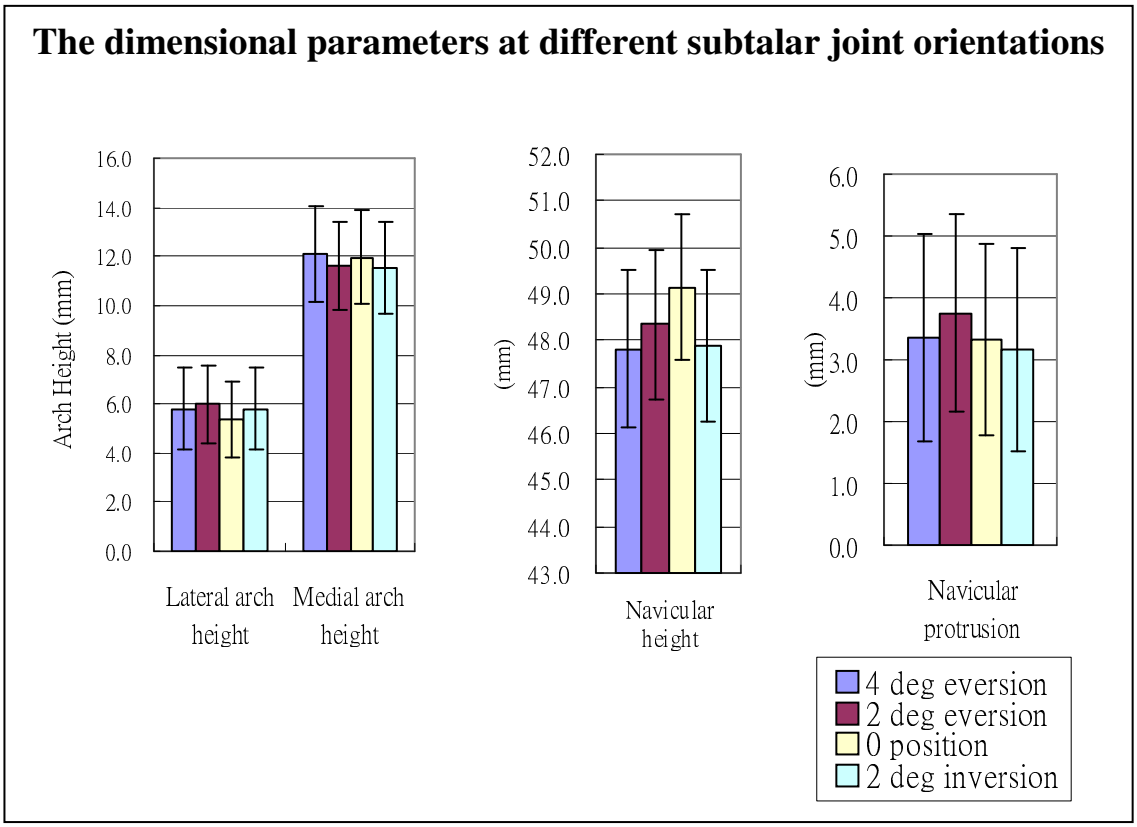

Figure 4.3.1.3-1 The dimension measurements (with ± 1 SD) at different subtalar joint orientations

Table 4.3.1.3-1 The mean and the standard deviations of the dimensional measurements

Dimensional measurements (mm)		Subtalar joint orientations				Statistical analysis		
		-4°	-2°	0°	2°	F	*p*-value	Power
Medial Arch Height	mean	12.1	11.6	12.0	11.5	2.84	0.05	0.65
	SD	2.1	2.1	2.1	2.1			
	SEM	0.4	0.4	0.4	0.4			
Lateral Arch Height	mean	5.8	6.0	5.4	5.8	4.07	*0.01**	0.82
	SD	4.1	3.5	4.0	3.8			
	SEM	0.4	0.4	0.3	0.4			
Navicular Protrusion	mean	3.4	3.8	3.3	3.2	1.38	0.26	0.35
	SD	2.50	2.31	2.46	2.56			
	SEM	0.5	0.5	0.4	0.5			
Navicular Height	mean	47.8	48.4	49.1	47.9	0.70	0.55	0.19
	SD	6.96	7.53	6.00	6.02			
	SEM	1.2	1.4	1.0	1.1			
Metatarsal Width	mean	86.6	86.8	87.0	87.0	0.23	0.80	0.09
	SD	7.63	7.76	7.46	7.24			
	SEM	1.71	1.72	1.58	1.52			

* *p*-value < 0.05

The mean and the standard deviations of the dimensional parameters are shown in Figure 4.3.1.3-1 and Table 4.3.1.3-1.

Besides, the statistical results of the pairwise comparisons of the two-way repeated measure ANOVA statistical test between different subtalar joint orientations of the foot parameters are attached in Appendices VIII-XI.

4.3.2. Changes in plantar foot geometry at individual subtalar joint orientations

The foot parameters reflected the changes in the plantar foot geometry. The changes were summarized according to individual subtalar joint orientations.

4.3.2.1. Foot impressions originated at 4° eversion

The projection volume under the medial forefoot region ($Volume_{MF}$) at 4° eversion (mean = 13684.7 mm^3, SD = 4454.5) was the biggest among all the subtalar joint orientations such that it was 3.0%, 8.0% and 6.9% bigger than those at 0° position, 2° eversion and at 2° inversion respectively ($p = 0.00$). Referring to the data of the individual subjects (n = 20 and bilateral feet were investigated), there were 20 feet having the highest projection volume under the medial forefoot region at 4° eversion. The result of the two-way repeated measures ANOVA showed that significant differences were found between:

(a) 4° eversion and 2° eversion (mean difference =1008.12 mm^3, 95% confidence interval between 322.9 and 1693.35, $p = 0.00$),

(b) 4° eversion and 2° inversion (mean difference = 887.96 mm^3, 95% confidence interval between 376.60 and 1399.32, $p = 0.00$).

Referring to the definitions of the foot parameters in this study, **the medial-lateral slopes at 10% and 20% of foot model length positions (Slope10% and Slope20%)** were also located at the forefoot region. However, the Slope10% and Slope20% remained constant at different subtalar joint orientations, in which the changes were under 0.3°.

The projection volume under the lateral forefoot ($Volume_{LF}$) at 4°eversion (mean = 3384.9 mm^3, SD = 1559.61) was similar to that at 2° eversion and was higher than that at 0° condition and 2° inversion for about 5%. The projection volume under the lateral forefoot region trended to increase with more eversion subtalar joint orientations. However, there was no significant difference noted in the two-way repeated measures ANOVA test.

* * * * * * * * *

4.3.2.2. Foot impression originated at 2° eversion

The projection volume under the medial forefoot region ($Volume_{MF}$) at 2° eversion (mean = 12676.6 mm^3, SD = 4275.46) was just 0.7% higher than that at 2° inversion. Both of them were the lowest among the four subtalar joint orientations. Referring to the data of individual subjects (n = 20, both feet investigated), there were 12 feet having the minimum projection volume under medial forefoot region at 2° eversion.

The projection volume under the medial midfoot region ($Volume_{MM}$) (mean = 35085.4 mm^3, SD = 5448.58) at 2° eversion was the lowest such that those at 4° eversion, 0° position and 2° inversion were 6.1%, 7.5% and 4.9% larger than that at 2° eversion respectively. Referring to the data of the individual subjects, there were 22 feet having the minimum volume at 2° eversion. The result of the two-way repeated ANOVA showed that significant difference was found between the projection volume under the medial midfoot region at 2° eversion and the other three subtalar joint orientations as the following:

- with 4° eversion, mean difference = -2026.2 cm^3, 95% confidence interval between -3574.37and -447.96, p = 0.00;

- with 0° position, mean difference = -2571.6 cm^3, 95% confidence interval between -3800.93 and -1342.24, $p = 0.00$; and
- with 2° inversion, mean difference = -1607.6 cm^3; 95% confidence interval between -2918.78 and -296.32, $p = 0.01$.

The projection volume under the medial hindfoot region ($Volume_{MH}$) at 2° eversion (mean = 12655.3 mm^3, SD = 2123.33) was the lowest too, such that those at 4° eversion, 0° condition and 2° inversion were 8.3%, 9.0% and 7.4% higher than that at 2° eversion respectively. Referring to the data of individual subjects, there were 18 feet having the minimum volume 2° eversion. The result of the two-way repeated measures ANOVA showed that significant difference was found between the projection volume under the medial hindfoot region at 2° eversion with other three subtalar joint orientations respectively. These were summarized as:

- comparing to 4° eversion, mean difference = -1132.4 cm^3, 95% confidence interval between -3574.37 and -477.96, $p = 0.01$;
- comparing to 0°condition, mean difference = -1186.0 cm^3, 95% confidence interval between -1342.24 and -388.93, $p = 0.01$; and
- comparing to 2°inversion, mean difference = -986.55 cm^3, 95% confidence

interval between -2918.78 and -296.32 and, $p = 0.00$.

The projection volume under the lateral forefoot region ($Volume_{LF}$) at 2°eversion was similar to that at 4°eversion and were relatively larger than that at 0° condition and 2° inversion for about 5%. However, there was no significant difference noted in the 2-way repeated measures ANOVA test (p =0.92 to 1.00)**.**

The reduction in the projection volume implies that the plantar foot surface is closer to the support surface. Particularly, the reduction in the projection volume under the medial forefoot, midfoot and hindfoot regions ($Volume_{MF}$, $Volume_{MM}$ and $Volume_{MH}$) at 2° eversion implied the collapse of the medial longitudinal arch. The lowest geometrical shape of the medial longitudinal arch observed in foot impressions originated at 2° eversion was also supported by the measurements of (i) the lowest medial-lateral slopes at forefoot regions, (ii) the lower medial longitudinal arch height, (iii) the highest lateral longitudinal arch height and (iv) the highest navicular protrusion.

The medial-lateral slopes at 20% to 50% foot model length positions (Slope20% to Slope50%) reached the minimum at 2°eversion. It was smaller than those at other subtalar joint orientations by 0.2 to1.2°. The Slope30% at 2° eversion (mean = 13.2°, SD = 3.16) was lower than those of other three subtalar joint orientations by 6.1% to 9.1% (p = 0.02 to 0.04) while Slope40% at 2° eversion (mean =16.7°, SD = 3.82) was lower than those at 4° eversion and zero positions by 6.0% to 12.0% (p = 0.02 to 0.04). Referring to the data of the individual subjects (n = 20, both feet studied), there were 12 feet and 16 feet having the smallest value at 2°eversion in the Slope30% and Slope40% respectively. The two-way repeated measures ANOVA showed that the Slope30% at 2°eversion was significantly smaller than the other three subtalar joint orientations. These were summarized as:

- comparing to 4° eversion (mean difference = -0.79°, 95% confidence interval between -1.58 and 0.00, p = 0.04);
- comparing to 0° position (mean difference = -1.2°, 95% confidence interval between -2.28 and -0.13, p = 0.02); and
- comparing to 2° inversion (mean difference = -0.8°, 95% confidence interval between -1.5 and -0.08, p = 0.02).

The result of the two-way repeated measures ANOVA showed that the Slope40% at 2°eversion was also significantly smaller than the other two subtalar joint orientations. These were summarized as:

- comparing to 4° eversion (mean difference = -0.99°, 95% confidence interval between -1.87 and -0.12, $p = 0.02$) and
- comparing to 0° position (mean difference = -0.79°, 95% confidence interval between -3.29 and -0.05, $p = 0.04$).

The medial longitudinal arch height at 2° eversion (mean = 11.6 mm, SD = 2.1) was just 0.9%higher than that at 2° inversion and 3.4% and 4.3% lower than those at 0° position and 4° eversion respectively, but no significant difference was noticed ($p = 0.29$ to 1.00).

The lateral longitudinal arch height at 2° eversion (mean = 6.0 mm, SD = 3.5) was found to be the highest among the four subtalar joint orientations and that at 2° inversion was the lowest. Significant difference was found with these two conditions ($p = 0.00$) in which that at 2° inversion was 10% lower than that at 2° eversion. The mean difference was 0.60 mm (95% CI 0.19 to 1.01).

The navicular protrusion at 2°eversion (mean = 3.8mm, SD = 2.3) reflected that the navicular tuberosity displaced most medially among the four subtalar joint orientations, and was at least 10% more in magnitude than those measured in other three subtalar joint orientations. However, no significant difference was found in this parameter (p = 0.46 to 1.00).

* * * * * * * * *

4.3.2.3. Foot impressions originated at zero position

The projection volume under the medial forefoot region ($Volume_{MF}$) (mean = 13268.1 mm^3, SD = 4414.3) at the zero position was in the middle of the range among the four subtalar joint orientations investigated. It was smaller than that at 4° eversion by 3.0%, but higher than those at 2° eversion and 2° inversion by 4.6% and 3.6% respectively. The result of the two-way repeated measures ANOVA showed that significant differences were found between 0° position and 2° inversion (mean difference = 471.29 mm^3, 95% confidence interval between 80.06 and 862.52, p = 0.01).

The geometrical shape of the medial longitudinal arch was highest at 0° position, reflected by the measurements of (i) the highest mean medial-lateral slopes at 30% and 40% foot model length positions, (ii) the highest projection volume under medial midfoot region ($Volume_{MM}$) and (iii) the lowest lateral arch height. Significant differences were found in these parameters between the impressions originated at 0° position and 2° eversion (which had the lowest geometrical shape of the arch), but not with 4° eversion and 2° inversion. The details are as summarized below:

(a) **The medial-lateral slopes at 30% foot model length position** (mean = 13.2°, SD = 3.2°) **and medial-lateral slopes at 40% foot model length position** (mean = 16.7°, SD = 3.8°) at 0° position were 2.8 to 5.7% higher than those at 4° eversion and 2° inversion and 9.0 to 10.0% higher than those at 2° eversion. Referring to the data of the individual subjects (n=20, bilateral feet were investigated), there were 16 and 17 feet having the highest value of the Slope30% and Slope40% at 0° position respectively.

(b) **The mean projection volume under medial midfoot region** (37657.0 mm^3, SD = 5436.7) at 0° position was slightly higher (1.4 to 2.6%) than those at 4° eversion and 2° inversion and was 7.3% higher than those at 2°

eversion.

(c) **The mean lateral arch height (5.4mm, SD = 4.0)** at 0° position was 6.9% lower than those at 4°eversion and 4°eversion and was 10% lower than that at 2° eversion.

* * * * * * * * *

4.3.2.4. Foot impressions originated at 2° inversion

The projection volume under the medial forefoot region ($Volume_{MF}$) at 2° eversion was just 0.7% higher than that at 2° inversion. Both of them were the lowest among all the four subtalar joint orientations. Referring to the data of individual subjects (n = 20, both feet investigated), there were 10 feet having the minimum projection volume under medial forefoot region at 2° inversion.

According to **the projection volume under the medial midfoot region ($Volume_{MM}$)**, the medial-lateral slopes at 30% to 40% of foot model length positions and the medial and lateral arch heights, the geometrical shape of the medial longitudinal arch of the impressions originated from 2° inversion was similar to

those from 4° eversion. It was lower than that at 0° position but significantly higher then that at 2° eversion.

* * * * * * * * *

Some parameters remained relatively constant upon the change of the subtalar joint orientations, fore example, the projection volume under the lateral midfoot region (mean = 14012.9 to 14506.1 mm^3) and at lateral hindfoot region (mean = 9982.5 to 10121.4 mm^3), the medial-lateral slope at 0%-10% (mean of Slope0% = 0.3 to 0.5° and mean of Slope10% = 1.3 to 1.5°), the medial-lateral slope at 50 to 90% of foot model length positions (mean difference ranging from 0.7°to 1.4°), the navicular height (mean = 47.8 to 49.1 mm), the navicular protrusion (mean = 3.2 to 3.8 mm)and the metatarsal width (mean = 86.6 to 87.0). The *p*-values of these parameters were quite high and closed to 1.00. This implied that the effect of the subtalar joint orientations on the plantar foot geometry at the area other than the medial longitudinal arch was minimal.

There were five statistical elements concerned for the power analysis of the statistical test. They were: the significance criterion (α), the sample size (n), sample variance (s^2), effect size (ES) and power ($1-\beta$). According to the observed power of the two-way repeated measure ANOVA statistical tests (also shown in Appendices VIII-XI), only the powers of the projection volume under the medial foot regions, the lateral arch height and the medial-lateral slopes at 30-40% foot model length positions were over 0.8.

4.4. The effect of the left/right side on the plantar foot geometry

Table 4.4-1 The mean and the standard deviations of the projection volume of the left and right sides

Projection Volume (mm^3)			Subtalar joint angle			
			4° eversion	2° eversion	0°	2° inversion
Under medial forefoot region ($Volume_{MF}$)	L	Mean	14198.17	12805.17	13756.00	12884.76
		SD	4249.68	3946.58	4256.63	4051.35
	R	Mean	13389.76	13179.77	13353.63	13281.17
		SD	4740.57	4676.73	4668.36	4722.11
Under lateral forefoot region ($Volume_{LF}$)	L	Mean	3288.68	3148.42	3027.83	3130.77
		SD	1579.88	1384.55	1320.65	1357.67
	R	Mean	3471.79	3538.42	3326.23	3282.84
		SD	1574.52	1590.40	1321.97	1352.17
Under medial midfoot region ($Volume_{MM}$)	L	Mean	37246.64	34394.43	36987.32	36389.76
		SD	5888.38	5101.01	5337.89	5571.69
	R	Mean	37459.41	35994.23	38651.16	37466.02
		SD	5307.59	5793.88	5542.65	5750.26
Under lateral midfoot region ($Volume_{LM}$)	L	Mean	13831.10	14066.10	13646.15	14278.78
		SD	3480.85	3140.53	2816.45	3298.14
	R	Mean	14659.91	14849.90	14598.22	14295.75
		SD	2917.71	3158.76	2382.45	2755.38
Under medial hindfoot region ($Volume_{MH}$)	L	Mean	13539.06	12639.23	13726.91	13637.53
		SD	2241.14	2010.14	2175.07	2323.84
	R	Mean	14117.14	12910.13	14121.41	13799.95
		SD	2698.51	2274.88	2647.09	2319.84
Under lateral hindfoot region ($Volume_{LH}$)	L	Mean	10161.90	10178.00	10258.65	10342.60
		SD	1799.73	1888.55	1682.87	1805.24
	R	Mean	10059.65	9978.95	10336.25	10167.65
		SD	1649.06	1652.57	1745.93	1878.69

Table 4.4-2 The mean and the standard deviation of the medial-lateral slopes of the left and right sides

Medial-lateral slopes (°)			Subtalar joint angle			
			4° eversion	2° eversion	0°	2°inversion
At 0% foot model length position (Slope0%) (MT level)	L	Mean	-0.20	-0.16	-0.39	-0.12
		SD	0.76	0.74	0.72	0.57
	R	Mean	-0.49	-0.46	-0.62	-0.47
		SD	0.72	0.79	0.94	0.73
At 10% foot model length position (Slope10%)	L	Mean	1.79	1.65	1.67	1.56
		SD	1.23	1.02	1.09	1.06
	R	Mean	0.84	0.93	1.17	1.37
		SD	0.93	1.30	0.87	1.32
At 20% foot model length position (Slope20%)	L	Mean	8.57	7.87	8.40	7.66
		SD	2.23	2.14	1.60	2.05
	R	Mean	7.60	7.65	7.88	8.39
		SD	2.38	2.30	2.70	3.14
At 30% foot model length position (Slope30%)	L	Mean	14.47	13.25	14.77	13.78
		SD	2.95	3.38	2.75	3.03
	R	Mean	13.59	13.23	14.07	14.19
		SD	3.65	3.03	4.00	4.04
At 40% foot model length position (Slope40%)	L	Mean	18.01	16.69	18.09	16.84
		SD	3.30	3.99	3.87	3.64
	R	Mean	17.43	17.01	18.10	17.70
		SD	4.39	3.74	5.28	4.88
At 50% foot model length position (Slope50%)	L	Mean	19.15	17.98	18.78	18.34
		SD	3.80	4.25	4.20	4.23
	R	Mean	19.14	18.83	9.68	19.14
		SD	5.21	5.16	5.10	5.65
At 60% foot model length position (Slope60%)	L	Mean	14.71	13.90	14.08	13.38
		SD	4.38	4.24	3.47	3.79
	R	Mean	15.35	15.12	15.56	14.73
		SD	5.35	6.08	6.01	6.17
At 70% foot model length position (Slope70%)	L	Mean	8.64	8.50	7.58	7.37
		SD	3.57	4.23	4.48	4.88
	R	Mean	9.17	8.79	9.32	8.02
		SD	6.03	5.63	5.94	5.68
At 80% foot model length position (Slope80%)	L	Mean	2.03	1.56	1.91	1.18
		SD	2.44	2.23	2.64	2.60
	R	Mean	2.92	2.39	2.75	2.42
		SD	2.83	2.54	2.69	2.62
At 90% foot model length position (Slope90%) (Heel level)	L	Mean	-1.28	-1.74	-1.86	-0.55
		SD	4.70	4.92	4.59	5.43
	R	Mean	-1.00	-1.31	-3.16	-2.74
		SD	6.03	5.18	3.26	5.00

Table 4.4-3 The mean and the standard deviation of the dimensional measurements of the left and right sides

Dimensional Measurements (mm)			Subtalar joint angle			
			4° eversion	2° eversion	0°	2° inversion
Lateral Arch Height	L	Mean	5.70	5.90	5.20	5.70
		SD	1.89	1.48	1.79	1.78
	R	Mean	5.90	6.05	5.55	5.90
		SD	1.71	1.96	1.64	1.71
Medial Arch Height	L	Mean	12.75	11.95	12.15	11.90
		SD	2.17	2.04	2.13	2.36
	R	Mean	11.45	11.25	11.80	11.15
		SD	1.85	2.05	2.02	1.84
Metatarsal Width	L	Mean	86.98	87.02	86.42	87.24
		SD	7.47	7.30	7.16	6.66
	R	Mean	86.31	86.55	87.60	86.69
		SD	7.96	8.38	7.88	7.94
Navicular Protrusion	L	Mean	-3.25	-3.74	-3.23	-3.12
		SD	2.61	2.40	2.65	2.45
	R	Mean	-3.46	-3.78	-3.40	-3.21
		SD	2.45	2.28	2.33	2.74
Navicular Height	L	Mean	47.03	46.95	48.94	47.68
		SD	7.55	8.55	6.40	5.73
	R	Mean	48.59	49.75	49.35	48.11
		SD	6.43	6.27	5.72	6.45

The mean and the standard deviation of the foot parameters for the left and right sides are shown in Table 4.4-1 to Table 4.4-3.

Table 4.4-4 The statistical result of the left/right side factor and the interaction between left/right side factor and the subtalar joint orientations factor of the 2-way repeated measure ANOVA

Parameters		Left/right side factor			Interaction between left/right side factor and subtalar joint orientation factor		
		F	*p*-value	Power	F	*p*-value	Power
Projection volume under different foot regions#	$Volume_{MF}$	0.86	0.14	0.14	2.25	0.09	0.37
	$Volume_{LF}$	1.77	0.20	0.24	0.35	0.79	0.11
	$Volume_{MM}$	1.07	0.31	0.17	1.30	0.28	0.25
	$Volume_{LM}$	1.58	0.22	0.22	0.76	0.52	0.15
	$Volume_{MH}$	0.26	0.62	0.08	0.31	0.82	0.11
	$Volume_{LH}$	1.06	0.32	1.00	0.56	0.64	0.14
Medial-lateral slopes at different % of foot model length position^	Slope0% (MT)	5.82	*0.03**	0.63	0.08	0.92	0.06
	Slope10%	8.8	*0.01**	0.80	1.29	0.29	0.33
	Slope20%	0.23	0.63	0.08	2.29	0.13	0.55
	Slope30%	0.2	0.66	0.07	1.34	0.27	0.34
	Slope40%	0	0.96	0.05	0.88	0.42	0.23
	Slope50%	0.77	0.39	0.13	0.22	0.81	0.09
	Slope60%	1.49	0.24	0.21	0.37	0.78	0.12
	Slope70%	0.5	0.49	0.10	0.47	0.71	0.14
	Slope80%	4.43	0.05	0.52	0.07	0.98	0.06
	Slope90% (Heel)	0.36	0.56	0.09	1.48	0.23	0.37
Dimensional measurements	Medial Arch Height	10.81	*0.00**	0.88	1.25	0.30	0.07
	Lateral Arch Height	1.25	0.28	0.19	0.12	0.95	0.32
	Navicular Protrusion	0.07	0.79	0.06	0.03	0.99	0.05
	Navicular height	1.00	0.33	0.16	0.54	0.66	0.15
	Metatarsal Width	0.04	0.85	0.05	1.28	0.29	0.32

Foot regions: MF = medial forefoot; LF = lateral forefoot; MM = medial midfoot; LM = lateral midfoot; MH = medial hindfoot; LH = lateral hindfoot

^ Slope10% = medial-lateral slope at 10% of the foot model length position

The symmetry of plantar foot geometry of the left and right feet were compared by the two-way repeated measures ANOVA and the result is shown Table 4.4-4.

It was found that the medial arch height of the left feet were significantly higher that of the right feet by 0.78 mm (95%CI 0.28 to 1.26, p = 0.00). The medial-lateral slopes at 0 % and 10% of foot model length positions of the right feet were significantly higher than those of the left feet by 0.3° (95% CI 0.04 to 0.54, p = 0.01) and 0.6° (95% CI 0.17 to 1.00, p-value = 0.03) respectively. There was no interaction between the left/right side factor and the subtalar joint orientation factor in the two-way repeated measures ANOVA test.

4.5. Correlations among the foot parameters

4.5.1. Correlations among medial longitudinal arch related parameters

Table 4.5.1-1 The correlation matrix of parameters related to the medial longitudinal arch

	Subtalar joint orientation (+ve as inversion)	Medial Arch Height		Projection Volume under Medial Midfoot Region		Navicular Height		Navicular Protrusion		Slope50%*		Slope40%#	
		Left	Right	Left	Right	Left	Right	Left	Right	Left	Right	Left	Right
Medial Arch Height	-4	1.00	1.00	***0.48***	***0.61***	0.23	0.09	0.17	0.16	***0.47***	***0.65***	***0.59***	***0.63***
	-2	1.00	1.00	***0.62***	***0.43***	0.13	-0.12	0.33	0.28	***0.39***	***0.58***	***0.52***	***0.46***
	0	1.00	1.00	0.19	***0.59***	0.10	***0.42***	-0.08	***0.45***	0.03	***0.61***	0.10	***0.63***
	2	1.00	1.00	0.33	***0.79***	0.11	0.13	-0.20	***0.43***	0.14	***0.65***	0.17	***0.75***
Projection Volume under Medial midfoot region	-4			1.00	1.00	***-0.50***	-0.37	***0.68***	0.32	***0.41***	***0.59***	0.32	***0.56***
	-2			1.00	1.00	-0.24	-0.24	***0.51***	0.16	***0.56***	***0.53***	***0.62***	***0.47***
	0			1.00	1.00	-0.34	0.11	0.15	***0.37***	***0.40***	***0.68***	0.34	***0.67***
	2			1.00	1.00	-0.20	-0.25	0.11	***0.51***	0.21	***0.48***	0.19	***0.56***
Navicular Height	-4					1.00	1.00	***-0.49***	***-0.46***	0.03	-0.05	0.22	0.08
	-2					1.00	1.00	***-0.39***	***-0.38***	-0.10	-0.32	-0.01	-0.22
	0					1.00	1.00	-0.24	-0.05	-0.04	0.05	-0.06	0.18
	2					1.00	1.00	-0.18	***-0.48***	-0.16	0.15	0.00	0.20
Navicular Protrusion	-4							1.00	1.00	0.05	0.28	-0.09	0.28
	-2							1.00	1.00	0.32	***0.51***	0.31	***0.54***
	0							1.00	1.00	-0.16	***0.54***	-0.29	***0.64***
	2							1.00	1.00	-0.20	***0.39***	-0.29	***0.42***
Slope50%*	-4									1.00	1.00	***0.92***	***0.91***
	-2									1.00	1.00	***0.92***	***0.93***
	0									1.00	1.00	***0.93***	***0.91***
	2									1.00	1.00	***0.92***	***0.93***
Slope40%#	-4											1.00	1.00
	-2											1.00	1.00
	0											1.00	1.00
	2											1.00	1.00

* slope50%: Medial-lateral slope at 50% foot model length position

\# slope40%: Medial-lateral slope at 40% foot model length position

Remarks: for r > 0.378, the value is bolded and italiced.

Table 4.5.1-2 Averaged correlation matrix of the medial arch related parameters

	Medial Arch Height	Projection volume under medial midfoot region	Navicular Height	Navicular Protrusion	Slope50%*	Slope40%#
Medial Arch Height	1.00	***0.51***	0.14	0.19	***0.44***	***0.48***
Projection volume under Medial midfoot region		1.00	-0.25	0.35	***0.48***	***0.47***
Navicular height			1.00	-0.33	-0.06	0.05
Navicular Protrusion				1.00	0.22	0.19
Slope50%*					1.00	***0.92***
Slope40%#						1.00

* slope50%: Medial-lateral slope at 50% foot model length position

slope40%: Medial-lateral slope at 40% foot model length position

Remarks: for r > 0.378, the value is bolded and italiced.

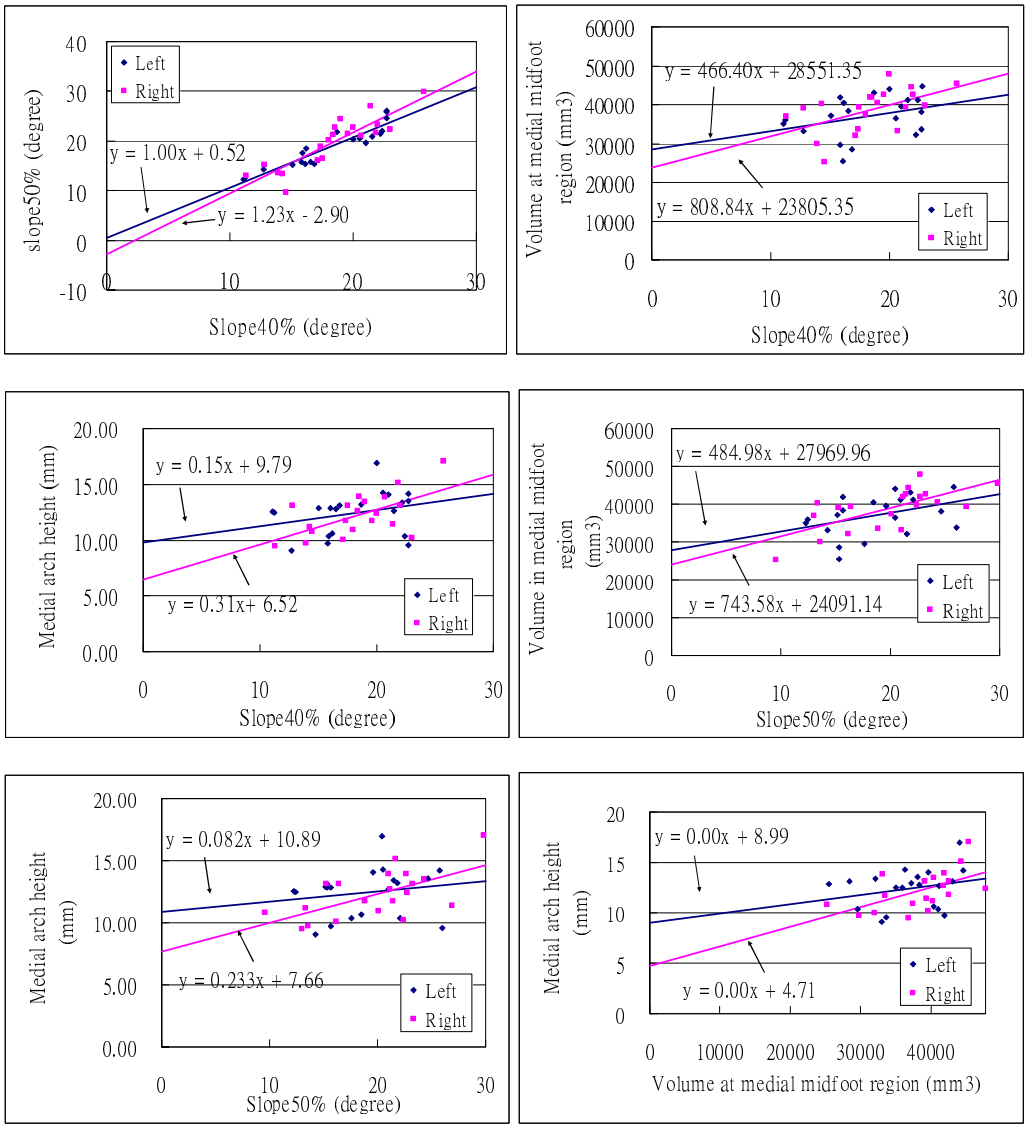

Figure 4.5.1-1 Scatter Diagrams of the correlation between the projection volume under medial midfoot region, medial arch height and slope at 40% and 50% of foot model length positions.

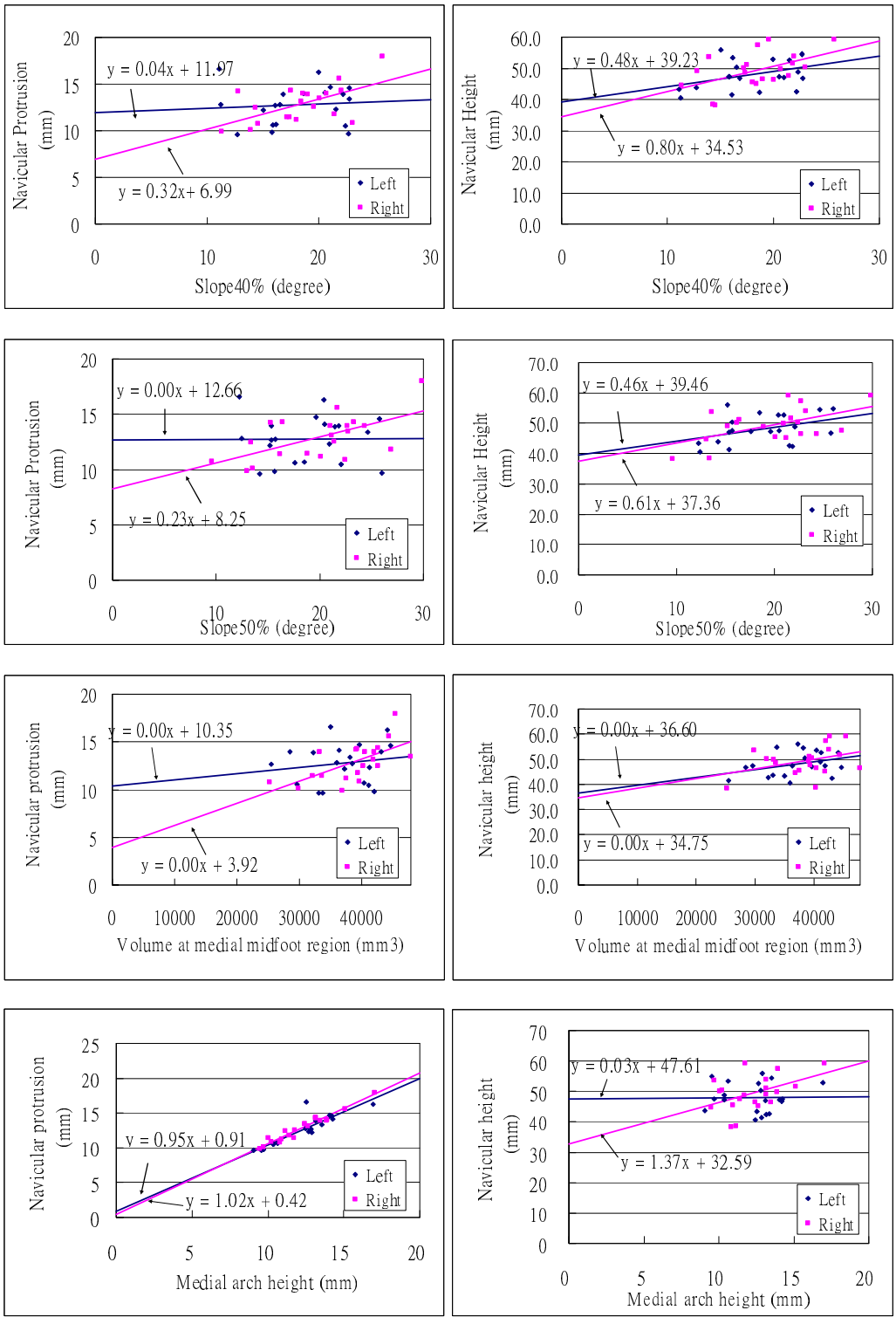

Figure 4.5.1-2 Scatter Diagram of the correlation between the navicular height and protrusion with other medial arch related parameters

The correlation matrix of the Pearson correlation coefficients (r) of the parameters related to the medial longitudinal arch was shown in Table 4.5.1-1. The medial longitudinal arch related parameters included the projection volume in the medial midfoot region, the medial longitudinal arch height, the navicular height and protrusion, and medial-lateral slopes at 40-50% of foot model length positions. As each foot parameter had the components of the left/right sides and the four subtalar joint orientations, the correlation coefficients of each foot parameter were averaged among these eight components for the ease of comparison (Table 4.5.1-2). The scatter diagrams of the medial arch related parameters at 0° condition were plotted to show the relationship between the parameter pair (Figure 4.5.1-1 and Figure 4.5.1-2).

With a sample size of 20 and a predetermined level of significance $\alpha = 0.05$, the critical value to reject the null hypothesis of no correlation is $r = 0.378$ (Portney and Watkins, 1993). If the observed value of r is less than this critical value ($r = 0.378$), the null hypothesis of no correlation ($r = 0$) would not be rejected. Therefore the null hypothesis of $r = 0$ was rejected between the following pairs of foot parameters:

- Projection volume under the medial midfoot region and medial arch height ($r = 0.51$)

- Medial arch height and Slope40% and Slope50% respectively (r = 0.48 and 0.44 respectively)
- Projection volume under medial midfoot region and Slope40% and Slope50% respectively (r = 0.47, 0.48 respectively)
- Slope40% and 50% (r = 0.92).

There were linear correlations between these parameter pairs. According to the classification of the correlation by Colton (1974), fair correlation (r = 0.25 to 0.50) was found among the medial longitudinal arch, the projection volume under the medial midfoot region and the medial-lateral slopes at 40% and 50% of foot model length positions; good to excellent correlation (r > 0.75) was found between Slope40% and Slope50%.

The mean correlation coefficient of the navicular height with other medial arch related parameters were ranging from 0.19 to 0.35. The mean correlation coefficient (absolute value) of the navicular protrusion with other medial arch related parameters were ranging from 0.05 to 0.25. According to the cut-off value of the

correlation coefficient (cut-off r = 0.378), there was no correlation between the navicular height and protrusion with the medial arch related parameters.

4.5.2. Correlations among the medial-lateral slopes

Table 4.5.2-1 Averaged correlation matrix of the medial-lateral slopes

	Slope0%	Slope10%	Slope20%	Slope30%	Slope40%	Slope50%	Slope60%	Slope70%	Slope80%	Slope90%
Slope0%	1.00	**0.03**	-0.06	-0.03	-0.16	-0.18	-0.29	-0.38	-0.25	-0.16
Slope10%		1.00	**0.71**	0.44	0.34	0.31	0.30	0.18	0.07	0.04
Slope20%			1.00	**0.82**	0.69	0.60	0.32	0.10	0.15	0.16
Slope30%				1.00	**0.90**	0.77	0.45	0.26	0.35	0.24
Slope40%					1.00	**0.92**	0.63	0.42	0.49	0.30
Slope50%						1.00	**0.77**	0.53	0.53	0.25
Slope60%							1.00	**0.82**	0.58	0.16
Slope70%								1.00	**0.67**	0.18
Slope80%									1.00	**0.35**
Slope90%										1.00

Remark: Slope10% represents the medial-lateral slope at 10% of the foot model length position

The correlation matrix of the medial-lateral slopes is shown in Table 4.5.2-1.The correlation coefficients of adjacent medial-lateral slopes within the range of 20-80% of the foot model length positions were good to excellent (r = 0.67 to 0.92), according to Colton's scale. However the correlation of the slopes at 90% of the foot model length position with adjacent slope (Slope80%) was poor (r = 0.35).

4.5.3. Correlations between the left and right sides of the foot parameters

Table 4.5.3-1 The mean Pearson's correlation coefficients (r) of the foot parameters between the left and right sides
(Averaged from the four subtalar joint orientations)

	Parameters	Pearson's correlation coefficients (r)		Range of r among 4 subtalar joint orientations	
				From	to
Projection volume under different foot regions#	$Volume_{MF}$	0.73	>0.378	0.68	0.78
	$Volume_{LF}$	0.77	>0.378	0.73	0.80
	$Volume_{MM}$	0.72	>0.378	0.66	0.80
	$Volume_{LM}$	0.48	>0.378	0.07	0.70
	$Volume_{MH}$	0.54	>0.378	0.32	0.61
	$Volume_{LH}$	0.47	>0.378	0.39	0.56
Medial-lateral slopes at different % of foot model length position^	Slope0% (MT)	0.38	>0.378	0.05	0.76
	Slope10%	0.18		-0.12	0.46
	Slope20%	0.27		-0.03	0.54
	Slope30%	0.39	>0.378	0.13	0.61
	Slope40%	0.37		0.07	0.71
	Slope50%	0.45	>0.378	0.05	0.78
	Slope60%	0.43	>0.378	0.07	0.79
	Slope70%	0.34		-0.05	0.77
	Slope80%	0.10		-0.41	0.54
	Slope90% (Heel)	0.12		-0.03	0.31
Dimensional measurements	Medial Arch Height	0.72	>0.378	0.57	0.87
	Lateral Arch Height	0.72	>0.378	0.64	0.75
	Navicular Protrusion	0.40	>0.378	0.10	0.65
	Navicular height	0.22		0.06	0.38
	Metatarsal Width	0.85	>0.378	0.73	0.95

Foot regions: MF = medial forefoot; LF = lateral forefoot; MM = medial midfoot; LM = lateral midfoot; MH = medial hindfoot; LH = lateral hindfoot

^ Slope10% = medial-lateral slope at 10% of the foot model length position

The Pearson's correlation coefficients between the left and right sides of the parameters are shown in Table 4.5.3-1. The left and right feet were correlated linearly in the foot parameters of projection volume under all foot regions, the

medial-lateral slopes at 0%, 30%, 50% and 60% of the foot model length positions, the medial and lateral arch heights, the navicular protrusion and the metatarsal widths ($r = 0.38$ to 0.85).

Chapter 5. Discussion

The orientation of the subtalar joint mainly affected the foot parameters in the medial longitudinal arch and the medial forefoot regions. The geometrical shape of the medial longitudinal arch attained the lowest at 2° eversion and was significantly different from all other three subtalar joint orientations. The changes in the geometrical shape of the medial arch were supported by the parameters of the projection volume under the medial midfoot region (p = 0.00 to 0.01), the medial-lateral slopes at 30% and 40% foot model length positions (p = 0.02 to 0.05), the lateral longitudinal arch height (p = 0.00). The projection volume under the medial forefoot was the biggest at 4° eversion and was significantly different from that at 2° eversion and 2° inversion (p = 0.00).

5.1. Interpretations of the changes in the plantar foot geometry observed

The subtalar joint motion is triplanar and its pronation and supination motions are usually quantified by the everison and inversion components in the frontal plane respectively. In this study the forefoot-to-rearfoot angle was kept zero and the subtalar joint orientations was varied in 2° interval (-4°, -2°, 0° and 2° inversion), The observed change in the geometrical shape of the medial longitudinal arch was

neither an increasing nor a decreasing trend. The geometrical shape of the medial longitudinal arch was the highest at the subtalar joint zero position. It decreased upon subtalar pronation and supination. The increase in the medial forefoot projection volume at 4° eversion was due to the result of the foot alignment control to keep a zero forefoot-to-rearfoot angle. This would be explained in the later sections.

The function of the subtalar joint and the midtarsal joint have been widely investigated since last century through the dissection of cadavers, motion analysis with skin surface markers and Magnetic Resonance Imaging technique, the movements of the tarsal bones and other foot bones are not clearly understood (Mattingly et al., 2006; Nester and Findlow, 2006; Payne et al., 2000). The interpretation of the changes in the plantar geometry as presented in sections, sections 5.1.1 and 5.1.2, would be relied on the manipulation of a foot bone model, in which the joint movement depends on the shape of the articulation surfaces. The tension of the ligaments and the muscle tones of the foot affect bone movement. The bone movement might also be masked by the relatively thick plantar soft tissue such as the plantar muscles, the plantar fascia and the fat pad under the heel.

5.1.1. Decrease in the medial longitudinal arch during impression procedure with subtalar supinated

The navicular is regarded as the apical bone of the medial longitudinal arch and the navicular height is sometimes used to indicate the arch height. When the subtalar joint supinates during standing, the medial longitudinal arch would become higher. However, this was not observed during impression procedure with subtalar joint supinated. This is because the forces applied to the foot and the control of the forefoot-to-rearfoot angle were different during standing and the foot impression procedure.

During standing, the floor and the foot form a closed kinetic chain condition of the subtalar joint. The calcaneus is relatively stable and inverts, and the mobile talus dorsiflexes and abducts. The inversion of the entire foot is compensated by pronating the forefoot to make the first metatarsal head contact with the ground. The forefoot-to-rearfoot angle is in inversion in this scenario. As the navicular articulates with the talus posteriorly, the dorsiflexion of the talus would move the navicular upwards. Thus an increase in arch height is observed during subtalar supination during standing (Figure 5.1.1-1).

Figure 5.1.1-1 The medial longitudinal arch at (a) pronated, (b) neutral and (c) supinated positions (The navicular was indicated with a “x”)

Although the condition of the subtalar joint during the foot impression procedure is also a closed kinetic chain condition, the application of the force by the hand of the orthotist was different to the ground reaction force during standing. Even though the manipulation technique was described in the section 3.4.3 of the methodology, this section further elaborate the consequences of the joints movements due to the manipulation force.

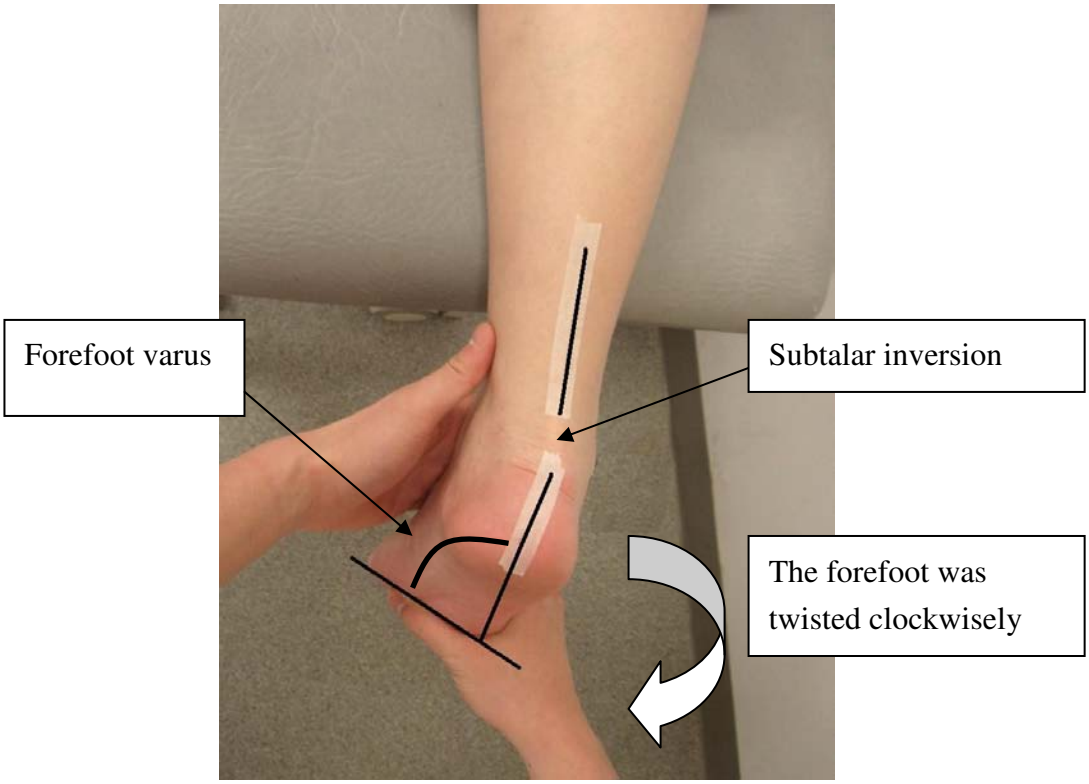

Figure 5.1.1-2 Controlling force applied during impression procedure with the subtalar joint supinated

In order to manipulate the subtalar joint of the right foot to an inversion orientation, a clockwise twisting force was applied at the forefoot by the right hand of the orthotist (Figure 5.1.1-2). As the midtarsal joint was closer to the forefoot, the twisting force applied might affect the midtarsal joint more than the subtalar joint. A larger degree of varus might happen between the forefoot and the rearfoot (the forefoot-to-rearfoot angle). In order to control the forefoot-to-rearfoot angle zero, a plantarflexion force was applied by pushing the first metatarsal head downward from the dorsal surface by the index finger and a dorsiflexion force was applied by pushing the lesser

metatarsal heads upwards from the plantar foot surface by the thumb. The medial cuneiform articulates with the first metatarsal anteriorly and with the navicular posteriorly. The plantarflexion force applied at the first metatarsal head would transfer to the medial cuneiform and then the navicular through the sliding movement among the articulation surfaces.

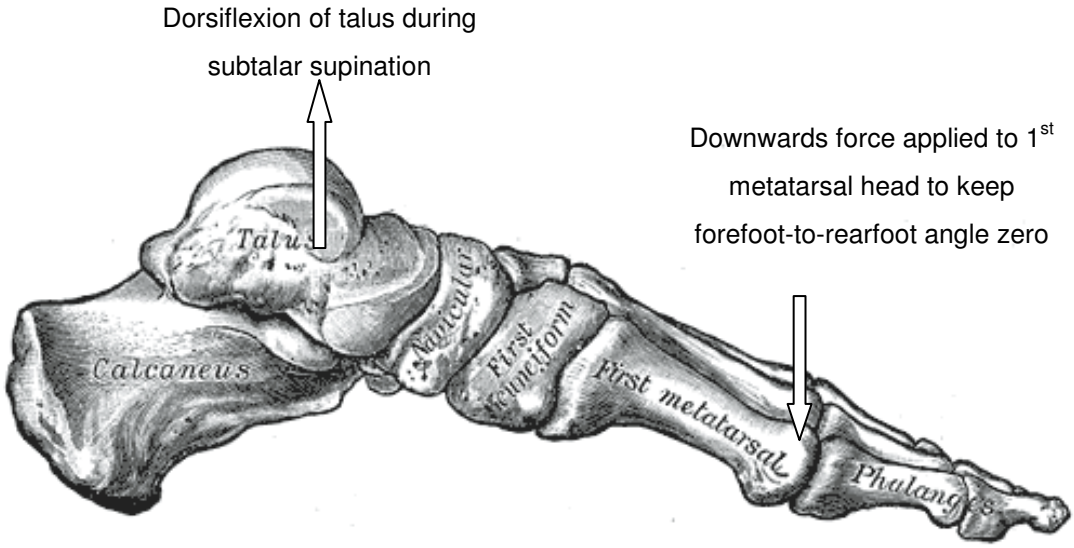

Figure 5.1.1-3 Upward and downward moment experienced by the navicular during the impression procedure with the subtalar supinated

As a result, the navicular experienced an upward moment by the dorsiflexion of the talus during subtalar supination and a downward moment induced by the plantarflexion force applied at the first metatarsal heads when the subtalar joint was

supinated and the forefoot-to-rearfoot angle was kept at zero degree (Figure 5.1.1-3). Referred to the results, the geometrical shape of the medial longitudinal arch at 2° subtalar inversion was lower than that at subtalar zero position. It was deduced that the downward moment dominated at 2° inversion. However, the magnitudes of these upward and downward moments were unknown.

5.1.2. Decrease in the medial longitudinal arch height during impression procedure with subtalar pronated

Similarly, during the impression procedure of a pronated right feet, an anti-clockwise force should be applied on the forefoot region of the right feet. The subtalar and midtarsal joint were pronated by the anti-clockwise force. The forefoot-to-rearfoot angle became valgus (Figure 5.1.2-1). In order to manipulate the forefoot-to-rearfoot angle to a zero position, a dorsiflexion force was applied by pushing the first metatarsal heads upward and a plantarflexion force applied by pushing the lesser metatarsal heads downward.

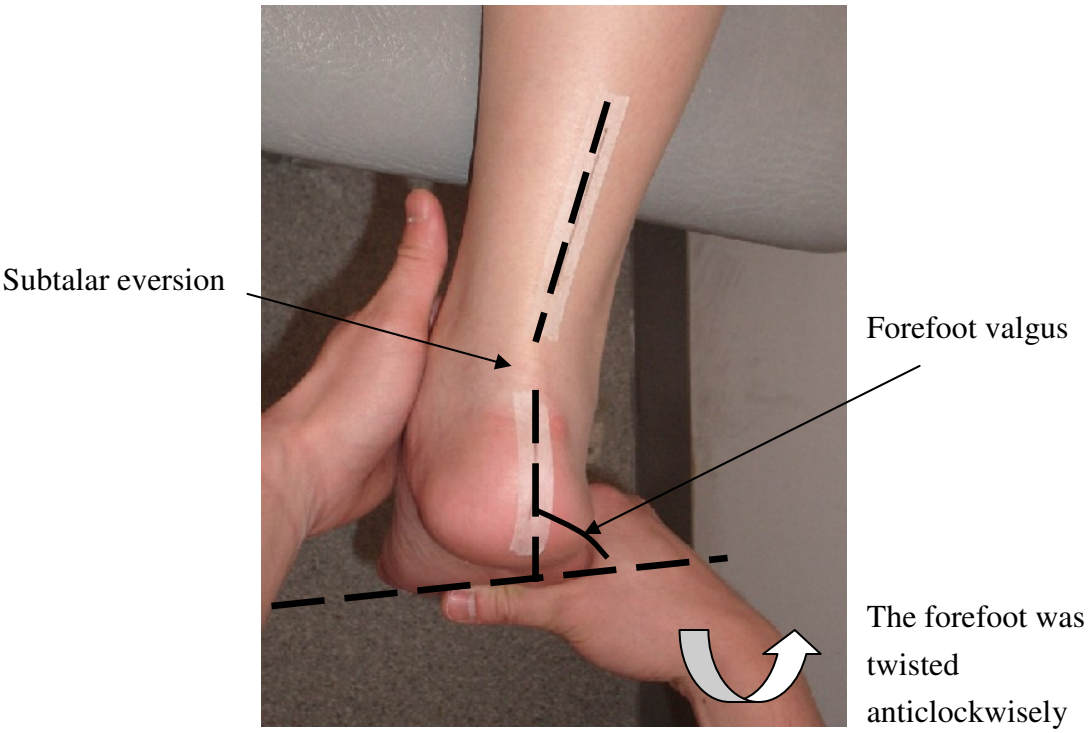

Figure 5.1.2-1 Controlling force applied during impression procedure with the subtalar joint pronated

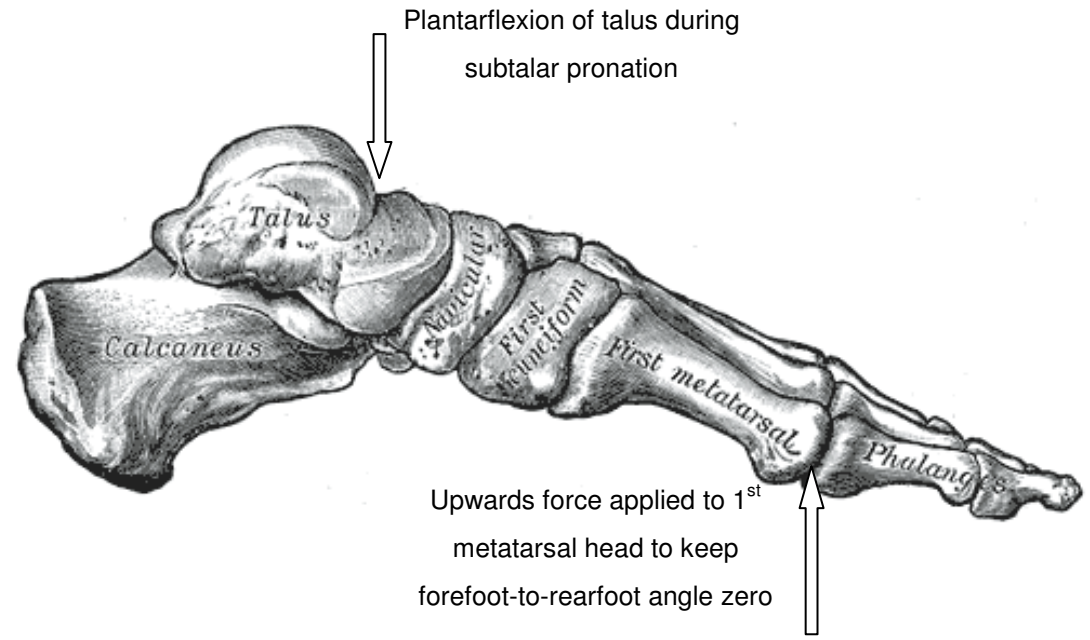

Figure 5.1.2-2 Upward and downward moment experienced by the navicular during the impression procedure with the subtalar pronated

It was assumed that there was a downward moment exerted on the navicular as the talus plantarflexed upon subtalar pronation. An upward moment which was transferred from the dorsiflexion force at the first metatarsals was also expected to exert on the navicular (Figure 5.1.2-2). The result of this study showed that the geometrical shape of the medial longitudinal arch was lower at 2° eversion than that at the zero position. It implied that the upward moment applied to the navicular was not dominated. Since the foot structure becomes more flexible upon subtalar pronation to serve for the shock absorption during walking (Perry et al., 1995; Mannon et al., 1997; Torburn et al., 1998), it was suspected that some of the upward force transferred from the forefoot was absorbed by the articulation between the first metatarsal and the medial cuneiform and were not transferred to the navicular.

The navicular becomes prominent and the forefoot abducts when the medial longitudinal arch is pronated (Dahle et al, 1991; Aquino and Payne, 2001). It is because the talus adducts upon subtalar pronation and thus the navicular moves medially. This explained why the maximum navicular protrusion was observed in 2° subtalar eversion. However, there was no significant difference found.

* * * * * * * * *

The geometrical shape of the medial longitudinal arch at 4° subtalar eversion was higher than that at 2° subtalar eversion. It was suspected as a result of the large anti-clockwise controlling force required to achieve the 4° subtalar eversion. The large anti-clockwise controlling force also introduced a larger extent of forefoot valgus in at 4° subtalar eversion. The eversion of the forefoot to the rearfoot increased exponentially as the subtalar joint moved from its fully supinated position to its fully pronated position (Philips and Philips, 1983). In order to align the forefoot-to-rearfoot angle to zero degree at 4° subtalar eversion, a greater dorsiflexion force was applied at the first metatarsal head. This force might cause the significantly increase of projection volume under the medial forefoot region and also transferred to the navicular to increase the geometrical shape of the medial longitudinal arch. Consequently, the first ray dorsiflexed and further affected the contour of the medial forefoot region. The mean area of the medial forefoot region at 4° subtalar eversion was 1305.71 mm^2 and the maximum mean difference of the projection volume in that region among the four subtalar joint orientations was

1008.3 mm^3. The averaged height increased over the medial forefoot region was 1.3 mm.

The slope10% and slope20% did not reflect the change medial to the first metatarsal contact point (MTI). These slopes did not increased when the projection volume under the medial forefoot region was increased at 4° subtalar eversion. This might caused by the change medial to the first metatarsal contact point (MTI).

Although the change of the geometrical shape of the medial forefoot region at 4° subtalar eversion was small, this was not recommended because of the possibility of inhibiting the windlass effect in walking (Hicks, 1954; Aquino and Payne, 2001; Scherer et al., 2006). The plantar aponeurosis is attached proximally to the calcaneus and distally to the proximal phalanx of the hallux. At heel-off, the first metatarsophalangeal joint dorsiflexes and the aponeurosis winds on the first metatarsal head. This results in tightening of the plantar aponeurosis and hence elevating the arch and supinating the subtalar joint. The foot is stabilized to facilitate push-off. Roukis and his associates (1996) found that the first metatarsalphalangeal joint dorsiflexion decreased 19% as the first metatarsal was posited in a dorsiflexion

orientation by putting a 4mm wedge under the first metatarsal head. Functional and structural deformities such as functional hallux limitus, hallux abductory eversion and hallux rigidus would be developed secondary to lack of motion at the first metatarsophalangeal joint.

5.2. The magnitude of the changes in the foot parameters

5.2.1. Comparison of the changes in the foot parameters with previous studies

The foot impressions are affected by the foot alignment control, weightbearing conditions and impression materials used. The magnitudes of the changes in the foot parameters obtained in this study were compared with those in the literature, so as to understand the importance of the subtalar joint control in the foot impression procedure.

5.2.1.1. The medial-lateral slopes

The forefoot-to-rearfoot angle was kept zero in this study. Significant difference of the medial-lateral slopes among different subtalar joint orientations was found at 30% and 40% of the foot model length positions. Among all the ten foot model length positions studied, the biggest amount of the changes (i.e. the difference between the maximum mean slopes and the minimum mean slopes) was observed at the slope at 40% of foot model length position, which was equal to 1.2°.

Foulston and his associates (1990) investigated the effect of the forefoot alignment control on the plantar foot geometry. They compared the difference between the

controlled forefoot alignment (with the plane of forefoot parallel to the plane of the heel) and the uncontrolled forefoot alignment (where the forefoot was in natural inversion) in terms of the medial-lateral slopes. The mean forefoot-to-rearfoot angles of the plaster models were 3° inversion in the controlled condition and 8° inversion in the uncontrolled condition. Significant differences were found in the medial-lateral slopes located between the first metatarsal head and the midfoot.

The effect of the forefoot alignment control on the medial-lateral slopes (about 5° change) was much bigger than that of the subtalar joint orientation control in this study (changes about 1.2° change). The forefoot alignment control mainly affected the metatarsals and the apical region of the medial longitudinal arch while the subtalar joint orientation control mainly affected the apical region of the medial longitudinal arch.

5.2.1.2. The medial longitudinal arch height

The arch height in this study was measured at about 49.13% of the distance from the first metatarsal contact point (MT1) to the heel contact point (HEEL). The mean arch height was 11.5 to 12.1 mm (SD = 2.1mm). This value was lower than the arch

height of the non-weightbearing foot impressions reported by Payne and his associates (2001) (14.88 mm, SD = 3.43). The difference between the arch height found in this study and that by Payne and his associates (2001) might be due to race difference. Moreover, they observed that the arch height of the impressions taken at the weightbearing condition was 9.39 mm (SD = 2.61).

Laughton and his associates (2002) investigated the arch height of the digitized image of (i) non-weightbearing impression with subtalar joint neutral, (ii) semi-weightbearing impression by foam impression, (iii) partial and (iv) non-weightbearing impressions by laser scanning. They defined the arch height as the highest soft-tissue margin in the arch area. The mean arch heights of different impression method ranged from 20.5 to 38.6 mm. Thus the effect of the above conditions on the arch height was much bigger than that of the subtalar joint orientation control.

5.2.1.3. The navicular Height

In this study, the navicular height, which was defined as the most prominent point on the midfoot region of the plaster model, was 47.8 to 49.1 mm (SD = 6.00 to 7.53)

among the non-weightbearing impressions in different subtalar orientations. The navicular height measured directly on the subjects' feet during double leg standing, the mean "navicular height" was 43 mm (SD = 6.00). The lower value of the navicular height measured on the subjects' feet might be resulted from the slightly compression of the plantar soft tissue in standing. The deformation of the plantar soft tissue was minimal during the non-weightbearing impression procedure.

The effect of the subtalar joint orientations on the mean navicular height was within 1.33 mm in this study. Leung and his associates (2004) measured the navicular height to study the reliability of the foot impression method using Orfit^{TM} low-temperature thermoplastic. Since children were recruited, their result was not comparable to this study. There are no other studies investigating the navicular height on plaster models. Besides, Williams and McClay (2000) and Vinicombe and his associates (2001) measured the navicular height by palpation of the navicular tuberosity of the subjects without foot related disorder. It was 51 mm and 95 mm at the semi-weightbearing and non-weightbearing conditions respectively. Therefore, the effect of the subtalar joint orientations to the navicular height might be smaller than the effect of the weightbearing conditions.

5.2.1.4. The navicular Protrusion

The effect of the subtalar joint orientations on the mean navicular protrusion was within 0.6 mm in this study. The clinical measurement of the navicular drift is defined as the medial displacement of the position of the navicular tuberosity from minimal weightbearing condition to 50% weightbearing condition. Vinicombe and his associates (2001) found that the navicular drift of subjects without foot related disorder was 7.0 mm. Therefore, the effect of the subtalar joint orientations to the navicular protrusion was smaller than the effect of the weightbearing conditions.

5.2.1.5. The metatarsal width

The metatarsal width increased 4.33 mm from 0% to 100% body weight in subtalar neutral position (Houston et al. 2006). The forefoot width increased 5.69 mm from non-weight bearing condition to full weight bearing condition in Chinese population (Tsung et al., 2003). Laughton and his associates (2002) compared the forefoot width resulted from the non-weight bearing foot impression procedure done with plaster bandages and laser scanning. The forefoot width of the impression taken by plaster bandage and by laser scanning were 2.0 mm and 1.7 mm wider than that using clinical measurement respectively.

The effect of the subtalar joint orientations on the metatarsal width was within 0.4 mm in this study and was smaller than the effects of different weightbearing conditions and different impression or imaging methods used.

5.2.1.6. The projection volume

Although there was no literature using the projection volume to quantify the plantar foot geometry, the effect of the subtalar joint orientations on the projection volume was small too. The medial midfoot region had the biggest changes in projection volume among the six regions studied. The differences of the projection volume in this region among different subtalar joint angles were within 2571.59 mm^3 and the mean area of the region was 1132.01 mm^2. If that change was evenly distributed over that region, the average height changed in that region was 2.27 mm.

5.2.2. The importance of the subtalar joint orientation in the foot impression procedure

To conclude, the effect of the subtalar joint orientations on the plantar foot geometry much smaller than the effect of the weightbearing conditions, the effect of the forefoot alignment control and the effect of the impression materials used. The

magnitude of change of the foot parameters due to the subtalar joint orientations was within 2.5 cm^3 in projection volume in the medial midfoot, within 1.7° in medial-lateral slopes and within 1.4 mm in dimensional measurements.

5.3. Symmetry of the left and right feet

Gheluwe (2002) suggested that if the correlation of the measurements between the left and right sides are low or insignificant, the left and right measurements could be pooled, effectively doubling the statistical population. Otherwise, it is necessary to carry out the statistical analysis separately for left and right lower extremities. In their study the goniometric measurements of the left and right sides (such as the forefoot varus, neutral calcaneal stance position, relaxed calcaneal stance position and etc) were significantly correlated. In this study, the left and right sides had moderate to high correlations for the projection volume in all foot regions, medial-lateral slopes at 30%, 50% and 60% foot model length positions, medial and lateral arch heights, navicular protrusion and metatarsal width (r = 0.38-0.85) (see Table 4.5.3-1, page 143). Only the medial arch height and the slopes at 80% and 90% of the foot models length positions were significant different between the left

and right sides (p = 0.00-0.03) (see Table 4.4-4, page 133). Since most of the parameters were moderately to highly correlated for the left and right sides (r = 0.38-0.85), the statistical analysis was carried out for left and right side respectively, but not combining the data of the left and right sides into one group.

Previous studies found no significant difference between the left and the right feet by measuring the arch index from the ink footprint (Kanatli et al., 2001) and electronic footprint (Chu et al., 1995) and the goniometric measurements of hindfoot motions (Ball and Johnson, 1996). Only Garbalosa and his associates (1994) observed that the forefoot varus measured between the left and right legs was statistically significant (p = 0.01). Therefore it is suggested that further studies related to the foot impression procedure could investigate either the left or the right feet only.

5.4. Evaluation of the tibial and calcaneal bisecting and marking devices

With the aid of the tibial bisecting and marking devices, both the inter-rater (Table 4.2.1-1, page 106) and intra-rater reliability (Table 4.2.1-2, page 107) of the tibial stance were improved, compared with the clinical method using the rules alone. In contrast, the inter-rater and intra-rater reliability of the calcaneal bisection line

marking using the calcaneal bisecting and marking device was similar to that by the clinical method. Improvements were not found in the reliability of marking of the calcaneal bisection line might be due to the shorter distance between the two bisection points on the calcaneus and relatively lighter softer tissue at the medial and lateral borders of the calcaneus. These would facilitate the consistence of the two bisection points marking between different measurements. However, as there are plenty of soft tissue on the lower one third of the tibia and dividing the relatively long tibia to locating the bisection point at the lower one third of the tibia by the visual observation would make it less consistent for the tibial bisection line marking. The distance of the two dividers on the tibial bisecting and marking device were fixed and thus improved the reliability.

5.5. Evaluation of the custom written software for quantifying the plantar foot geometry

Only a few studies (Foulston et al. 1990; Laughton et al. 2002; Tsung et al. 2003) utilized a computer system to quantify and compare the plantar geometry of foot impressions. Different parameters were used in these studies to quantify the plantar

foot geometry. This makes the comparison among different studies difficult. This study attempted to include most of the parameters used in the previous studies, to investigate the relationships among them, and to shorten the list of the parameters for further related studies.

5.5.1. Suggestions on the foot parameters for quantifying the plantar foot geometry in further studies

The noises, such as light source or dust from the surroundings during the foot model scanning would affect the accuracy. Although the scanned image could be previewed immediately by the software provided by the INFOOT scanner, a single point of noise might not be displayed as the resolution of the previewed image of the scanned foot models (1 mm) was not as fine as the scanned resolution (0.5 mm). The existence of the noise of the scanned image might not be noticed by studying some parameters like the volume and the slopes. The inclusion of dimensional parameters to quantify foot geometry, such as the metatarsal width (defined as the widest width along the x-axis) and the arch heights, would help to cross-check the accuracy of the scanned image by comparing with the actual measurements or with the parameters of other scanned image of the same subject. If there were deviations found, the x, y, and

z-co-ordinates of that foot model would be plotted to locate the noise point(s). Alternatively, the plaster foot models might be needed to scan again.

The changes in the foot parameters related to the medial longitudinal arch were consistent with each other**.** For example, the lowest of the geometrical shape of the medial longitudinal arch at 2° eversion among four subtalar joint orientations was reflected by the lowest magnitude in projection volume under the medial midfoot regions, the medial-lateral slopes at the 30% and 40% of the foot model length positions, and the highest magnitude in the lateral arch height and the navicular protrusion. There were moderate correlations among these parameters (r = 0.44-0.51) (Table 4.5.1-2, page 136).

The projection volume under various foot regions are recommended as representation of plantar foot geometry due to the following considerations:

(1) The projection volume describes the foot geometry under different foot regions: medial/lateral part of the forefoot/midfoot/hindfoot. Using these anatomical regions to describe the location of the change happened would be more

meaningful than interpreting the geometrical shape of the foot impression in terms of the cross-sections, for example the medial-lateral slopes at 30% foot model length position. Moreover, similar definitions of foot regions of the foot are utilized in plantar pressure measurement, for example, the F-Scan® system.

(2) Some of the foot parameters like the medial longitudinal arch height, navicular height and etc only concentrated to a particular part of the foot. Other areas of the foot were not taken into consideration during the calculation. Studying these parameters alone might ignore other foot regions, especially when investigating different manipulation methods during impression taking. For example, dorsiflexing the first metatarsophalangeal joint during the foot impression procedure might alter the plantar contour at the medial forefoot region in a greater extent than the medial midfoot region. Therefore, the projection volume under different foot regions was recommended as it considers the geometry of the entire foot impression.

(3) As the projection volume is the summation of the data points in the corresponding regions, the effect of the errors at individual data points (if any) would be averaged by other data points and thus the influence by the error data point(s) would be smaller. On the contrary, the medial and lateral arch height

and navicular height and navicular protrusion depended on the single points while the medial-lateral slopes were considering the points in a cross-section line (usually about 40 points on average in the apical arch cross-section). Any errors in the data points would affect the accuracy of these parameters a lot.

5.5.2. Suggestions on modifying the interval of the medial-lateral slopes studied

If the effect of the plantar geometry of the posted foot orthosis style is studied, the medial-lateral slopes would be suitable to quantify the plantar geometry. Additional plaster would be added to the medial and lateral borders of the plaster models and hence only the central portion of the plaster model kept the original shape. The medial-lateral slopes are only calculated according to the data points in the center of the foot image.

The reliability of the scanning of the slopes at 90% of the foot model length position (Slope90%) was poor (ICC(3,1) = 0.09, p = 0.45) and its correlation with adjacent slope (slope80%) was little (r = 0.35). Referring to individual data of the Slope90%, there was only 5 to 10 mm of the data point in that cross-section taken into account in for the slope calculation. Also, there was a relatively drastic change in the contour at the back of the hindfoot. As the cross-sections at the heel regions are not linear, it would be more suitable to calculate the slopes at the heel by polynomial. These made the measurement of the Slope90% not consistent between measurements. It is not recommended to analysis Slope90% in further studies.

On the other hand, the correlation coefficients of adjacent medial-lateral slopes between 20 to 80% foot model length position were good to excellent (r = 0.71 to 0.92), according to Colton's scale. It is suggested that the interval of the medial-lateral slopes could be changed to 20% for future study.

5.5.3. Poor correlation of the navicular height and protrusion with the medial arch related parameters

The correlation coefficient of the navicular height with other medial arch related parameters ranged from 0.19 to 0.35. The correlation coefficient (absolute value) of the navicular protrusion with other medial arch related parameters ranged from 0.05 to 0.25. According to the cut-off value of the correlation coefficient (cut-off r = 0.378), there was no correlation between the navicular height and protrusion with the medial arch related parameters.

The measurement of the navicular height and protrusion of this study was based on the geometry of the rigid plaster models taken in non-weight bearing condition, rather than through palpating of the bony prominence under the soft tissue. It was

suspected that the little movement of the navicular (if any) might be hidden by the soft tissue which would be easier to detect through palpation but not by the geometry of the plaster model. Therefore, it is suggested that these two parameters would not be effective to reflect the change in the plantar geometry.

5.6. Possible errors

The errors of the study might be resulted from the following aspects.

1. The measurement of subtalar joint angles

In the evaluation of reliability of the tibial and calcaneal bisecting and marking devices for ten subjects, the standard error of measurement of subtalar angle during relaxed standing was 0.7°. The subtalar joint orientation studied were -4°, -2°, 0° and 2° inversion, a goniometer with integral degree was utilized because this study aimed at developing a common clinical method for evaluating the subtalar joint angle in the clinical environment. A more precise device could be electronic goniometer, electromagnetic transducer or reflective markers system. In order to measure the subtalar orientation, the devices should be located on the lower one third of the tibia and the heel. In contrast, the foot impression procedure of this study aimed to capture the original contour of the entire heel region. The volume of these devices would affect the contour of the foot impression. If this technical problem is solved, the reliability of the device will be improved.

2. The foot impression procedure

The foot impression method using Orfit^{TM} low-temperature thermoplastic was documented by Leung and his associates (2004). The standard errors of measurements of the forefoot width and the navicular height of the plaster models taken by this material were 2 mm and 1 mm respectively.

3. Quantifying the plantar geometry by scanning the plaster models and the calculation of the foot parameters by the custom written program.

The accuracy of the INFOOT scanner with our custom written software was close to those with the build-in software. The manufacturer reported that the difference between the actual and measured dimensions of an object was 0.9% (Kouchi and Mochimaru 2001) while the difference found in this study was within 1.0%. The possible error might be introduced by the noises such as light source in the room and the slight scratch on the glass scanning platform. The reliability of the foot parameters generated between two scanning on the same plaster foot model was good. The intra-rater reliability ICC (3,1) of all foot parameters (except the medial-lateral slopes at 90% of foot model length position) between two scans of a plaster foot model was 0.93-1.00. The scanning of each plaster foot model was within one minute. However,

calibration conducted by the distributor is required if the scanner was relocated from one site to another.

Theoretically, calculating the volume using a smooth surface approach would be more accurate than using a column counting approach, thus calculating the volume using columns was one of the possible errors of this study. The changes of the volume in this study were coherent with the change of the medial-lateral slopes. Moreover, the z-coordinate of each point (height of each column) generated by the INFOOT scanner was closed to 0.1 mm. It was not rounded off during volume calculation. In addition, the resolution of the points in each region concerned was 1 mm x 1 mm increments. For example, there were about 1180 points in the medial midfoot region. These two factors minimized the inaccuracy due to the volume comprised of columns

5.7. Limitations of the study

The limitations of this study mainly including the following aspects:

1. **The interpretation of the results was relied on the foot bone model.** The influence of the muscles, ligaments and other soft tissues attached to the bones were ignored.

2. **There was no direct measure to evaluate the changes in the foot structure, for example, bones, soft tissue and ligament.** The effect of the plantar pressure distribution of the foot orthosis originated from different subtalar joint orientations could not be reflected by the changes in the plantar foot geometry. The plantar surface of the foot bones were covered by a relatively thick layer of soft tissue. Upon loading, the soft tissue would be deformed while the alignment of the bone would be change due to the differences in the tissue properties. Plantar pressure analysis or finite element modeling should be carried to investigate the plantar pressure distribution.
3. **Assumption of the foot orthosis design for the foot parameters:** different types of foot orthoses have different trimelines and/or plaster modification procedure. The foot models and the foot parameters of this study were concentrated to the total contact foot orthosis design. The effect of the subtalar joint orientations of other types of the foot orthoses might vary.
4. **Subject group:** the feet of all subjects were normal and free from the foot deformities. Other foot types, such as excessively pronated foot or excessively supinated foot, may involve different extent of the tightness or laxity of the

ligament. The result of the study on these groups of subjects might be different to the normal group.

Besides, some subjects were obese or overweight. The body weight would have an effect on the foot shape. There would be excessive soft tissue at the plantar foot surface of the obese people, especially at the heel region. The soft tissue properties of this fat pad would affect the result of this study.

5. **Sample size:** the data analysis was not further differentiated for subjects with different genders due to limited number of subjects that unable to make powerful conclusion.

Chapter 6. Conclusion

6.1. Conclusion

Subtalar joint neutral position is widely adopted in the measurement of foot angles and in the foot impression procedure. In this study, the effect of the subtalar joint orientations on the plantar foot geometry was investigated through a three-dimensional analysis of the scanned image of positive plaster foot models. Only the non-weightbearing foot impression condition was studied. The foot models with the subtalar orientations ranged from 4° eversion to 2° inversion were obtained and scanned. This range of angles included the mean subtalar joint neutral position and the mean relaxed standing position as reported in the literature.

The results of this study provided a guideline on the acceptable range of the subtalar joint orientation during the foot impression procedure for the foot orthotic intervention. The projection volume and the medial-lateral slopes at the medial longitudinal arch were the lowest at 2° eversion, with significant differences noticed. Although the projection volume under the medial midfoot regions of the other subtalar joint orientations were about 4.9-7.5% larger than that at 2° inversion, the decrease in medial longitudinal arch height at 2° inversion was about 0.1-0.6 mm. This implied that the changes mainly happened at the soft tissue margin of the

medial longitudinal arch and just slightly affected the overall arch height. Since the subtalar joint neutral positions reported in previous studies were included in the range of the subtalar joint orientations studied, it is suggested that the control of the subtalar joint neutral position need not be over emphasized in foot orthotic intervention.

Comparing with previous studies on foot impression procedure, the effect of the subtalar joint orientations on the plantar geometry found in this study was much smaller than the effects of the forefoot alignment control, the weightbearing conditions and the materials used. It is suggested to concentrate on the control of the forefoot-to-rearfoot angle during the foot impression procedure, which induces more obvious foot geometry and alignment changes. Besides, the calculation of the foot parameters was based on the original shape of the scanned plantar foot geometry and would be applicable to the total contact foot orthosis design. The effect of the subtalar change of the subtalar angle orientation during impression might even become less significant to the plantar foot orthotic design such as posted foot orthosis that applied modifications along the medial and lateral borders as well as the posterior heel area.

6.2. Suggestions to further study

In order to enhance the biomechanical function and the user compliance of foot orthoses, the following factors should be considered for further investigations of the impression procedure of foot orthoses:

1. The subject group recruited in this study was regarded as normal arch according to the definition of Song and his associates (1996). The excessively pronated feet sometimes involve ligament laxity while the excessively supinated feet sometimes involve ligament tightness (Rule et al., 1993; Van Boerum and Sangeorzan, 2003). Therefore, it is suggested to conduct the same study on the people with different foot types, to verify whether the same results would be obtained.
2. The effect of the subtalar joint orientation during weight bearing condition is suggested to conduct. The results might not be the same as those at non-weightbearing condition, as the foot structure was in closed kinetic chain condition and is affected by the ground reaction force and the muscle pulls during movement. The projection volume of the foot impression resulted from loaded condition would be lower. The medial-lateral slopes would be gentler. The navicular height and the arch heights would be lower and the navicular

protrusion would be increased.

3. Previous studies on impression procedures comparing the difference in foot alignment control, materials used and weightbearing conditions through two-dimensional analysis (McPoil et al. 1989; Payne et al. 2001; Laughton et al. 2002; Chuter et al. 2003), the three-dimensional approach should be continued for future study.

4. Foulston and his associates (1989) observed that the medial-lateral slopes increased significantly in the uncontrolled forefoot condition than the controlled forefoot condition during the impression procedure. The biomechanical effect of varying the forefoot-to-rearfoot angle should be further investigated though three-dimensional gait and plantar pressure analyses.

References

1. **Aquino A and Payne C (2001)**. Function of the windlass mechanism in excessively pronated feet. *Journal of the American Podiatric Medical Association, 91(5): 245-250*.
2. **Aquino A and Payne C (1999)**. Function of the plantar fascia. *The Foot, 9: 73-78.*
3. **Astrom M and Arvidson T (1995)**. Alignment and joint motion in normal foot. *The Journal of Orthepdic and Sports Physical Therapy, 22(5): 216-222.*
4. **Ball KA and Afheldt MJ (2002).** Evolution of foot orthotics - Part 1: coherent theory or coherent practice. *Journal of Manipulative and Physiological Therapeutics, 25(2): 116-121.*
5. **Ball KA and Afheldt MJ (2002).** Evolution of foot orthotics - Part 2: research reshapes long-standing theory. *Journal of Manipulative and Physiological Therapeutics, 25(2): 125-134.*
6. **Ball P and Johnson GR (1993).** Reliability of hindfoot goniometry when using a flexible electrogoniometer. *Clinical Biomechanics*, 8: 13-19.
7. **Basque MG, Nasadowski R, Johnson RE (1989).** Neutral position casting techniques: results of a survey. *Journal of the American Podiatric Medical Assoication, 79(7): 330-335.*
8. **Baltimore MD (1993).** Chapter five: casting technique. In: Foot orthoses and other forms of conservative foot care. Michaud TC. 193-195.
9. **Bleck EE and Berzins UJ (1977).** Conservative management of pes valgus with plantar flexed talus, flexible. *Clinical Orthopaedic Related Research* 122: 85-94.
10. **Benink RJ (1985).** The constraint mechanism of the human tarsus. *Acta Orthop Scand 56 (suppl)*: 215.
11. **Blackwood CB, Yuen TJ, Sangeorzan BJ, Ledoux WR (2005).** The midtarsal joint locking mechanism. *Foot and Ankle International 26(12)*:1074-1080.
12. **BodyFix Clinic.** 4Cycling [homepage on internet]. California: BodyFix clinic; [Updated 2006; cited 2008 Jan 13]. Available from

http://bodyfix.net/4cycling.html.

13. **Brody D (1982).** Techniques in evaluation and treatment of the injured runner. *Orthop Clin North Am* 13, 541-558.
14. **Brown D, Smith C (1976).** Vacuum casting for foot orthoses. *Journal of the American Podiatry Association* 66: 582-587.
15. **Bruckner J (1987).** Variations in the human subtalar joint. *The Journal of Orthopaedic and Sports Physical Therapy* 8: 489-494.
16. **Burns MJ (1977).** Non-weightbearing cast impressions for the construction of orthotic devices. *Journal of the American Podiatry Association* 67: 790-795.
17. **Cavanagh PR (1980).** The Running Shoe Book. View CA: Anderson World Inc.
18. **Cavanagh PR, Rodgers MM (1987).** The arch index: a useful measure from footprints. Journal of Biomechanics 20: 547.
19. **Chen WP, Chia WJ and Tang FT (2003).** Effects of total contact insoles on the plantar stress redistribution: a finite element analysis. *Clinical Biomechanics* 18: S17-S24.
20. **Chu WC, Lee SH, Chu W, Wang TJ, Lee MC (1995).** The use of arch index to characterize arch height: a digital image processing apporach. *CIEEE Transactions on Biomedical Enginerrings* 42(11): 1088-1093.
21. **Chuter V, Payne C and Miller K (2003).** Variability of neutral-position casting of the foot. *Journal of the American Podiatric Medical Association, 93(1:, 1-5.*
22. **Clarke HH (1933).** An objective method of measuring the height of the longitudinal arch in foot examinations. *Research Quarterly* 4: 99.
23. **Colton T (1974).** Statistics in Medicine. Boston, Little, Brown.
24. **Cornwall MW and McPoil TG (1992).** Effect of rearfoot posts in reducing forefoot forces: a single-subject design. *The Journal of the American Podiatric Medical Association* 82: 371.
25. **Cox RA, Ingrando CR, Park SC and Lake DA (1999).** Comparison of forefoot varus measurements obtained from nonweightbearing, partial weighting, and full weightbearing orthotic casting techniques. *The Journal of Orthopedic and Sports Physical Therapy, 29(1): A-5.*
26. **Dahle Lk, Mueller M, Delitto A and Diamond JE (1991).** Visual Assessment

of foot type and relationship of foot type to lower extremity injury. *The Journal of Orthopedic and Sports Physical Therapy, 14(2): 70-74.*

27. **Elfman H (1960).** The transverse tarsal joint and its controls. *Clinical Orthopaedi*cs 16: 41-45.
28. **Elveru RA, Rothstein JM, Lamb RL and Riddle DL (1988).** Goniometric reliability in a clinical setting - subtalar and ankle joint measurement. *Physical Therapy, 68(5): 672-677.*
29. **Evans AM, Copper AW, Scharfbilling RW, Scutter SD and Williams MT (2003)**. Reliability of the foot posture index and traditional measurement of foot position. *Journal of the American Podiatric Medical Association, 93(3):, 203-213.*
30. **Faculty of Podiatry, La Trobe University.** Midtarsal Joint [homepage in internet]. Australia: Faculty of Podiaty, La Trobe University. [Updated 2002 Aug 20; cited 2008 Jan 13]. Available from http://www.latrobe.edu.au/podiatry/Midtarsaljoint.html.
31. **Foulston, Lord and West (1990).** Changes in plantar surface shape induced by corrective forefoot eversion. *Clinical Biomechanics, 5(4): 229-235.*
32. **Franco AH (1987).** Pes cavus and pes planus. *Physcial Therapy 67(5): 688-694.*
33. **Garbalosa JC, McClure MH, Catllin PA and Wooden M (1994).** The frontal plane relationship of the forefoot to the rearfoot in an asymptomatic population. *Journal of Orthopedic and Sports Physical Therapy, 20(4): 200-206.*
34. **Gheluwe B, Kirby K, Roosen P and Phillips R (2002)**. Reliability and accuracy of biomechanical measurements of the lower extremities. *The Journal of the American Podiatric Medical Association, 92(6): 317-326.*
35. **Guldemond NA, Leffers P, Sanders AP, Emmen H, Schaper NC and Walenkamp GHIM (2006). Casting methods and plantar pressure.** *The Journal of the American Podiatric Medical Association, 96(1): 9-18.*
36. **Hamill J, Bates BT, Knutzen KM and Kirkpatrick GM (1989).** Relationship between selected static and dynamic lower extremity measures. *Clinical Biomechanics, 4(4): 217-225.*
37. **Hawes MR, Nachbauer W, Sovak D, Nat S, Nigg BM and Nat S (1992).**

Footprint parameters as a measure of arch height. *Foot & Ankle, 13(1): 22-26.*

38. **Henderson and Campbell (1969).** UCBL shoe insert--casting and fabrication. *Bull Pros Res:* Spring:215-35.
39. **Hicks JH (1954).** The mechanics of the foot: part II . The plantar aponeurosis and the arch. *Journal of Anatomy, 88: 25.*
40. **Houston VL, Luo G, Mason CP, Mussman M, Garbarini M and Beattie AC (2006).** Changes in male foot shape and size with weightbearing. *Journal of the American Podiatric Medical Association, 96(4): 330-343.*
41. **Inman (1976).** The Joint of the Ankle. Williams & Wilkins. Baltmore.
42. **Irwin LW (1937).** A study of the tendency of school chldren to develop flat-footedness. *Res. Q., 8: 46-53.*
43. **Johanson MA, Donatelll R, Wooden MJ, Andrew PD and Cummings GS (1994).** Effects of three different posting methods on controlling abnormal subtalar pronation. *Physical Therapy. 74(2): 149-158.*
44. **Kanatli U, Yetkin H, Cila E (2001).** Footprint and radiographic analysis of the feet. *Journal of Pediatric Orthopaedics 21:* 225-228.
45. **Kirby KA (1989).** Rotational equilibrium across the subtalar joint axis. *Journal of the American Podiatric Medical Association 79:* 1.
46. **Kitaoka HB, Luo ZP, An KN (1997).** Analysis of longitudinal arch support in stabilizing the arch of the foot. *Clinical Orthopaedics and Related Research, 341: 250-256.*
47. **Kogler GF, Solomonidis SE and Paul JP (1995).** In vitro method for quantifying the effectiveness of the longitudinal arch support mechanism of a foot orthosis. *Clinical Biomechanics, 10(5): 245-252.*
48. **Kogler GF, Veer FB, Solomonidis SE and Paul JP (1998).** The influence of medial and lateral orthotic wedges on loading of the plantar aponeurosis: in vitro study. *Book of Abstracts from 9th Word Congress of the International Society For Prosthetics and Orthotics 1998 , 579-581.*
49. **Kouchi M and Mochimaru M (2001).** Development of a low cost foot-scanner for a custom shoe marking system. *Proceeding of the 5th Symposium on Footwear Biomechanics: Zuerich, Switzerland. Eds:/ Hennig E, Stacoff A.*

50. **LaPointe SJ, Peebles C, Nakra A and Hillstrom H (2001).** The reliability of clinical and caliper-based calcaneal bisection measurements. *Journal of the American Podiatric Medical Association, 91(3): 121-126.*

51. **Lattanza L, Gray GW and Kantner RM (1988).** Closed versus open kinematic chain measurements of subtalar joint eversion: implication for clinical practice. *The Journal of Orthopeadic and Sports Physical Therapy, 9(9): 310-314.*

52. **Lau CP, Leung KL.** Calcaneal Bisector. US Patent No.: US 7, 331117B2

53. **Laughton C, Davis IM and Williams DS (2002).** A comparison of four methods of obtaining a negative impression of the foot. *Journal of the American Podiatric Medical Association, 92(5): 216-258.*

54. **Ledoux WR and Hillstrom HJ (2001).** Acceleration of the calcaneus at heel strike in neutrally aligned and pes planus feet. *Clinical Biomechanics, 16: 608-613.*

55. **Ledoux WR and Hillstrom HJ (2002).** The distributed plantar vertical force of neutrally aligned and pes planus feet. *Gait and Posture, 15: 1-9.*

56. **Leung AKL, Cheng JC, Mak AF (2004).** Orthotic design and foot impression procedures to control foot alignment. Prosthetics and Orthotics International 28(3): 254-62

57. **Leung AK, Mak AF, Evans JH (1998).** Biomedical gait evaluation of the immediate effect of orthotic treatment for flexible flat foot. *Prosthetics and Orthotics International* 22 (1): 25-34.

58. **Liu W, Miller J, Stefanyshyn D and Nigg BM (1999).** Accuracy and reliability of a technique for quantifying foot shape, dimensions and structural characteristics. *Ergonomics, 42(2): 346-358.*

59. **Lundberg A, Svensson OK (1993).** The axes of rotation of the talocalcaneal and talonavicular joints. *The Foot 3:* 65.

60. **Mannon K, Anderson T, Cheetham P, Cornwall MW and McPoil TG (1997**). A comparison of two motion analysis systems for the measurement of two-dimensional rearfoot motion during walking. *Foot and Ankle International, 18(7): 427-431.*

61. **Manter JT (1941).** Movements of the subtalar and transverse tarsal joints. *Anat.*

Rec. 80: 397-409.

62. **Mathieson I, Upton D and Prior TD (2004).** Examining the validity of selected measures of foot type: a preliminary study. *Journal of American Podiatric Medial Association, 94(2): 275-281.*

63. **Mattingly B, Talwalkar V, Tylkowski C, Stevens DB, Hardy PA and Pienkowski D (2006).** Three dimensional in vivo motion of adult hindfoot bones. *Journal of Biomechanics, 39: 726-733.*

64. **McClay I and Manal K (1998).** A comparison of three-dimensional lower extremity kinematics during running between excessive pronators and normals. *Clinical Biomechanics, 13(3): 195-203.*

65. **McPoil TG and Cornwall NW (1996a).** Relationship between three static angles of the rearfoot and the pattern of rearfoot motion during walking. *Journal of Orthopedic and Sports Physical Therapy, 23(6): 370-375.*

66. **McPoil TG and Cornwall MW (1995).** Footwear and foot orthotic effectiveness research: a new approach. *The Journal of Orthopedic and Sports Physical Therapy, 21(6): 337-344.*

67. **McPoil TG and Cornwall MW (1996b)**. The relationship between static lower extremity measurements and rearfoot motion during walking. *The Journal of Orthopedic and Sports Physical Therapy, 24(5): 309-314.*

68. **McPoil TG and Cornwall NW (1994).** The relationship between static measurements of the lower extremity and the pattern of rearfoot motion during walking. Physical Therapy 74: 141.

69. **McPoil TG and Hunt GC (1995).** Evaluation and management of foot and ankle disorders: present problems and future directions. *The Journal of Orthopedic and Sports Physical Therapy, 21(6): 381-388.*

70. **McPoil TG and Knecht HG (1985).** Biomechanics of the foot in walking: a function approach. *The Journal of Orthopaedic and Sports Physical Therapy, 7(2):69-72.*

71. **McPoil TG, Knecht HF and Schuit D (1988).** A survey of foot types in normal females between agnes of 18 and 30 years. *The Journal of Orthopaedic and Sports Physical Therapy, 9(12): 406-409.*

72. **McPoil TG, Schult D and Knecht HG (1989).** Comparison of three methods used to obtain a neutral plaster foot impression. *Physical Therapy, 69(6): 448-452.*

73. **Menz HB (1997).** Clinical measurement of the lower extremity - where to from here. *Australasian Journal of Podiatric Medicine, 31(3): 95-99.*

74. **Menz HB (1998).** Alternative techniques for the clinical assessment of foot pronation. *Journal of the American Podiatric Medical Association, 88(3): 119-129.*

75. **Mueller MJ (1994).** Effects of three different posting methods on controlling abnormal subtalar pronation. Invited Commentary. *Physical Therapy* 74(2): 158-159.

76. **Mündermann A, Nigg BM, Humble RN and Stefanyshyn DJ (2003).** Foot orthotics affect lower extremity kinematics and kinetics during running. *Clinical Biomechanics, 18: 254-262.*

77. **Mündermann A, Nigg BM, Humble RN and Stefanyshyn DJ (2003).** Orthotic comfort is related to kinematics, kinetics, and EMG in recreational runner. *Medicine and Science in Sports and Exercise:*: 1710-1719.

78. **Nester CJ, Bowker P and Bowden P (2002).** Kinematics of the midtarsal joint during standing leg rotation. *Journal of the American Podiatric medical Association* 92(2): 77-81.

79. **Nester CJ and Findlow AH (2006).** Clinical and experiemntal models of the midtarsal joint: proposed terms of reference and associated terminology. *Journal of the American Podiatric Medical Assoication, 96(1): 24-31.*

80. **Nester CJ, Linden ML and Bowker P (2003).** Effect of foot orthoses on the kinematics and kinetics of normal walking gait. Gait and Posture, 17: 180-187.

81. **Nigg BM (2000).** The role of impact forces and foot pronation: a new paradigm. *Clinical Journal of Sport, 11: 2-9.*

82. **Norkin CC and Levangie PK (1983).** Joint Structure and Function. F.A. Davis: Philadelphia, PA.

83. **Payne CB (2000).** The role of theory in understanding the midtarsal joint. *Journal of the American Podiatric Medial Assoication, 90(7): 377-379.*

84. **Payne C and Chuter V (2001).** The clash between theory and science on the kinematic effectiveness of foot orthoses. *Clinics in Podiatric Medicine and Surgery, 18(4): 705-713.*

85. **Payne C, Chuter V, Oates M and Miller K (2001).** Introductory evaluation of a weightbearing neutral position casting device. *Australasian Journal of Podiatric Medicine, 35(3): 65-71.*

86. **Payne C and Richardson M (2000).** Changes in the measurement of neutral and relaxed calcaneal stance positions with experience. *The Foot, 10: 81-83.*

87. **Perry SD and Laotune MA (1995).** Influences of inversion/eversion of the foot upon impact loading during locomotion. *Clinical Biomechanics, 10(5): 253-257.*

88. **Phillips RD and Phillips RL (1983).** Quantitative analysis of the locking position of the midtarsal joint. *Journal of the American Podiatry Association* 73(10): 518-522.

89. **Philps JW (1995).** The functional foot orthoses. 2nd edition. Singapore: Churchill Livingstone.

90. **Pierrynowski MR and Smith SB (1996).** Rear foot inversion/eversion during gait relative to the subtalar joint neutral position. *Foot and Ankle International, 17(7): 406-412.*

91. **Razeghi M and Batt ME (2002).** Foot type classification: a critical review of current methods. G*ait and Posture, 15: 281-291.*

92. **Richie DH (2007).** Effects of Foot Orthoses on Patients with Chronic Ankle Instability. Journal of the American Podiatric Medical Association 97(1): 19-30

93. **Robinson JR and Frederick EC (1989).** Scaling of foot dimensions. *The XII international Congress of Biomechanics. Abstract #127.*

94. **Root ML, Weed JH and Orien WP (1971).** *Neutral Position Casting Techniques. Los Angeles: Clinical Biomechanics Corporation.*

95. **Root ML, Orien WP and Weed JH (1977).** Clinical Biomechanics: Normal and Abnormal Function of Foot (Volume 2). Los Angeles: Clinical Biomechanics Corp.

96. **Roukis TS, Scherer PR, Anderson DF (1996).** Position of the first ray and motion of the first metatarsophalangeal joint. *Journal of the American Podiatric*

Medical Association, 86(11): 538-546.

97. **Rule J, Yao L and Seeger LL (1993).** Spring ligament of the ankle: normal MR anatomy. *American Journal of Roentgenology, 161(6):1241-1244.*
98. **Saltman CL, Nawoczenski DA and Talbot KD (1995).** Measurement of the medial longitudinal arch. *Archives of Physical Medicine and Rehabilitation, 76: 45-49.*
99. **Scherer PR, Sanders J, Eldredge DE, Duffy SJ and Lee RY (2006).** Effect of functional foot orthoses on first metatarsophalangeal joint dorsiflexion in stance and gait. *Journal of the American Podiatric Medical Association, 96(6): 474-481.*
100. **Schuter RO (1976).** Neutral plantar impression cast - method and rationale. *Journal of the American Podiatric Medical Association, 66(6): 422-426.*
101. **Sell KE, Verity TM, Worrell TW, Pease BJ and Wigglesworth J (1994).** Two measurement techniques for assessing subtalar joint position: a reliability study. *The Journal of Orthopedic and Sports Physical Therapy, 19(3): 162-167.*
102. **Scientific Research Institute for the Shoe Making Industry of the China National Light industry Council 輕工業部制鞋工業科學研究所 (1984)**. Chinese shoe size and shoe last design 中國鞋號及鞋楦設計. Beijing :Light Industry Publisher 北京: 輕工業出版社. (Chinese reference)
103. **Simkin A, Leichter I, Giladi M, Stein M, Milgrom C (1989).** Combined effect of foot arch structure and an orthotic device on stress fractures. *Foot and Ankle* 10 (1): 25-29.
104. **Smith-oricchio K and Harris BA (1990).** Inter-rater reliability of subtalar neutral, calcaneal inversion and eversion. *The Journal of Orthopedic and Sports Physical Therapy, 12(1): 10-15.*
105. **Sobel E and Levitz SJ (1997).** Reappraisal of the negative impression cast and the subatalar joint neutral position. *Journal of the American Podiatric Medical Association, 87(1): 32-33.*
106. **Sobel E, Levitz SJ, Caselli MA, Tran M, Lepore F, Lilja E, Sinaie M and Wain E (1999).** Reevaluation of the relaxed calcaneal stance position. *Journal of the American Podiatric Medical Association, 89(5): 258-264.*

107. **Song J and Hillstrom H (1997).** Effects of foot type on diabetic neuropathic foot function. *Gait and Posture, 5(2): 169-170.*

108. **Song J, Hillstrom H and Secord D (1995).** Foot type determinant of static and dynamic foot function, *Gait and Posture. 3(2): 93.*

109. **Song J, Hillstrom HJ, Secord D and Levit J (1996).** Foot type biomechanics: comparison of planus and rectus foot types. *Journal of the American Podiatric Medical Association, 86(1): 16-23.*

110. **Subotnick SI (1980).** The cavus foot. *Physician and Sportsmedicine* 8: 53-55.

111. **Subotnick SI (1981).** The flat foot. *Physician and Sportsmedicine* 9: 85-91.

112. **Thompson D**. Subtalar joint motion [homepage in internet]. USA: The University of Oklahoma. [Updated 2007 Oct 19; cited 2008 Jan 13]. Available from http://moon.ouhsc.edu/dthompso/gait.

113. **Tillman MD, Chiumento AB, Trimble MH, Bauer JA, Cauraugh JH, Kaminski TW and Hass CJ (2003).** Tibiofemoral rotation in landing: the influence of medially and laterally posted orthotics. *Physical Therapy in Sport, 4: 34-39.*

114. **Tiberio D (1987).** The effect of excessive subtalar pronation on patellofemoral mechanics: a theoretical model. *The Jounral of Orthopaedic and Sports Physical Therapy* 9 (4): 160-165.

115. **Torburn L, Perry J and Gronley JK (1998).** Assessment of rearfoot motion: passive positioning, one-legged standing, and gait. *Foot and Ankle International, 19(10): 688-693.*

116. **Tsung BYS, Zhang M, Fan YB and Boone DA (2003).** Quantitative comparison of plantar foot shapes under different weight-bearing conditions. *Journal of Rehabilitation Research and Development*, 40(6): 517-526.

117. **Valmassy RL (1979).** Advantages and disadvantages of various casting techniques. *Journal of the American Podiatric Medical Association, 69(12): 707-712.*

118. **Van Boerum DH and Sangerozan BJ (2003).** Biomechanics and pathophysiology of flat feet. *Foot and Ankle Clinic, 3: 419-430.*

119. **Van Langelaan EJ (1983).** A kinematical analysis of the tarsal joints: an X-ray

photogrammetric study. *Acta Orthop Scand* 54 (suppl):204.

120. **Vinicombe A, Raspovic A and Menz HB (2001).** Reliability of navicular displacement measurement as a clinical indicator of foot posture. *Journal of the American Podiatric Medical Association, 91(5): 262-268.*
121. **Walter JH JR, Ng G, Stoltz JJ (2004).** A patient satisfaction survey on prescription custom-molded foot orthoses. *Journal of the American Podiatric Medical Association,* 94:363-367.
122. **Wernick J and Langer S (1972).** *A Practical Manual for a Basic Approach to Clinical Biomechanics. New York: Langer Acrylic Laboratory.*
123. **Williams DS and McClay IS (2000)**. Measurements of used to characterize the foot and the medial longitudinal arch: reliability and validity. *Physical Therapy, 80(9): 864-871.*
124. **Wright DG and Desai SM and Henderson WH (1964)**. Action of the subtalar and ankle-joint complex during the stance phase of walking. *The Journal of Bone and Joint Surgery, 46-A (2): 361-382.*

Appendix I The consent form

CONSENT FORM

I _____ (name), hereby consent to participate as a subject for the project entitled "**The Effect of the Subtalar orientations on the Plantar Foot Geometry**".

Project Leader: Dr. Leung Kam Lun, Aaron

I have read and understood the information presented to me.

I have an opportunity to ask questions about the study.

I realize I may not benefit personally from taking part in the study.

I realize I can withdraw from the study at any time with no penalty.

I realize that the results of this study may be published, but that my own results will be kept and processed in accordance with the provision of the Personal Data (Privacy) Ordinance, and that I will not be identified personally in any published work.

I realize that the results of this study will be the properties of the Jockey Club Rehabilitation Engineering Centre (REC) of The Hong Kong Polytechnic University.

Signature _____ Date _____
( )

Witness Signature _____ Date _____
( )

Appendix II The information sheet

THE HONG KONG
POLYTECHNIC UNIVERSITY
香港理工大學

INFORMATION SHEET

The Effect of the Subtalar orientations on the Plantar Foot Geometry

You are invited to participate on a study conducted by LEE Ka Lai, who is a post-graduate of the Jockey Club Rehabilitation Engineering Centre in The Hong Kong Polytechnic University.

The aim of this study is investigating the changes in the contour of the plantar foot surface with different manipulations applied during foot impression procedure. The study will involve a preliminary assessment and measurements of the foot conditions. Then four pairs of foot impressions will be taken with different joint angles manipulated. It is hoped that this information will help to understand the foot alignment control during impression procedure in order to develop better orthotic treatments for foot problems.

The testing should not result in any undue discomfort, but your feet will need to be impressed with low-temperature thermo-plastic (about 40-50°C when contact with skin). All information related to you will remain confidential, and will be identifiable by codes only known to the researcher.

You have every right to withdrawn from the study before or during the measurement without penalty of any kind. The whole investigation will take about 3 hours.

If you have any complaints about the conduct of this research study, please do not hesitate to contact Mr Eric Chan, Secretary of the Human Subjects Ethics Sub-Committee of The Hong Kong Polytechnic University in person or in writing (c/o Human Resources Office of the University).

If you would like more information about this study, please contact Dr. Aaron Leung on tel. no. 2766-7676.

Thank you for your interest in participating in this study.

Dr. Aaron LEUNG

Principal Investigator

Appendix III The procedure of preparing a standing template

A standing template (modified from that of McPoil et al. (1988)) was used to standardize the toe-out angle and the heel distance between different trials of each subject. The procedures are as follow:

1. Each subject, with mineral oil soaked feet, was asked to walk across a four-meter long facsimile paper. There was another two-meter long space at the further end of the paper for the achieving of an average gait pattern.
2. The last four footprints on the paper were outlined with a marker before the mineral oil dried.

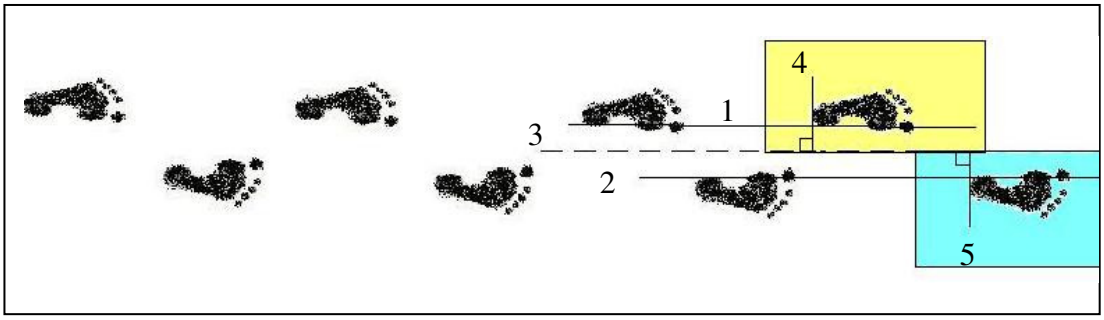

Figure 1 The last left and right footprints were cut along the midline

3. A straight line, line 1 was drawn tangential to the medial heel borders of the two left footprints (Figure 1). A similar approach was done for the right side (line 2) (Figure 1).
4. A midline (line 3), was drawn to equally bisect the space between line 1 and line 2 (Figure 1).
5. Line 4 and line 5 were drawn perpendicular to line 3 and contacted with the most posterior part of the last left and right footprints respectively (Figure 1).
6. Then the last left and right footprints were cut along line 3.

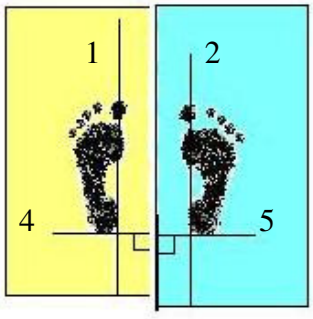

Figure 2 The left and right footprint were matched together to form the standing template

7. They were then put together along line 3, with lines 4 and line 5 connected as a straight line to form the standing template (Figure 2).

Appendix IV The procedure of calculating the truncated foot length

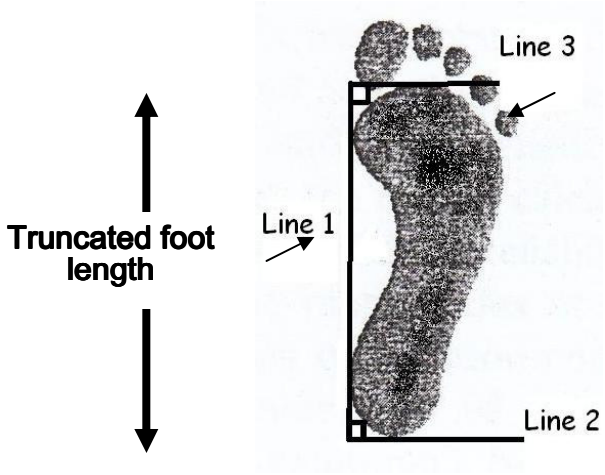

Figure 1 The truncated foot length

1. The subject was asked to walk neutrally along a 2-meter walking path. In the first walking trial, the position of the third step was marked. The imprinter was then placed at the position of the third step. The subject was asked to walk again and the inked footprint of one foot was obtained.
2. The procedure was repeated for the other foot.
3. Some reference lines were drawn on the inked footprint for the determination of the truncated foot length (Figure 1):
    i. the most medial points of the metatarsal and the heel regions were connected by a straight line, which was labeled as Line 1.
    ii. A line (labeled as Line 2) perpendicular to Line 1 was drawn which pass through the most posterior point of the heel.
    iii. Another line (labeled as Line 3) perpendicular to Line 1 was drawn which pass through the most anterior point of the forefoot with the toes were neglected.
    iv. The distance between Lines 2 and 3 was the truncated foot length.

Appendix V Result of the Shapiro-Wilk test (W) for projection volume at different foot regions

Projection volume	Subtalar joint orientation (positive as inversion)	Left		Right	
		W	*p*-value	W	*p*-value
Under medial forefoot region ($Volume_{MF}$)	-4°	0.98	0.90	0.97	0.77
	-2°	0.95	0.41	0.96	0.60
	0°	0.97	0.74	0.96	0.53
	2°	0.97	0.69	0.95	0.39
Under lateral forefoot region ($Volume_{LF}$)	-4°	0.95	0.43	0.97	0.71
	-2°	0.96	0.48	0.95	0.41
	0°	0.96	0.47	0.96	0.48
	2°	0.94	0.29	0.95	0.45
Under medial midfoot region ($Volume_{MM}$)	-4°	0.97	0.81	0.95	0.41
	-2°	0.96	0.45	0.93	0.19
	0°	0.96	0.61	0.97	0.66
	2°	0.97	0.65	0.94	0.24
Under lateral midfoot region ($Volume_{LM}$)	-4°	0.96	0.58	0.90	***0.04****
	-2°	0.96	0.47	0.93	0.15
	0°	0.94	0.28	0.96	0.51
	2°	0.98	0.88	0.97	0.84
Under medial hindfoot region ($Volume_{MH}$)	-4°	0.97	0.73	0.88	***0.02****
	-2°	0.96	0.47	0.97	0.72
	0°	0.96	0.52	0.96	0.53
	2°	0.98	0.95	0.94	0.23
Under lateral hindfoot region ($Volume_{LH}$)	-4°	0.95	0.38	0.95	0.40
	-2°	0.96	0.49	0.95	0.32
	0°	0.97	0.70	0.96	0.51
	2°	0.92	0.11	0.96	0.59

p-value < 0.05

Appendix VI Result of the Shapiro-Wilk test (W) for medial-lateral slopes

Medial-lateral slopes at different % of foot model length position	Subtalar joint orientation (positive as inversion)	Left		Right	
		W	*p*-value	W	*p*-value
Slope0%	-4°	0.84	***0.00****	0.90	0.05
	-2°	0.95	0.36	0.90	0.05
	0°	0.95	0.34	0.82	*0.00**
	2°	0.88	***0.02****	0.91	0.07
Slope10%	-4°	0.91	0.06	0.98	0.97
	-2°	0.96	0.51	0.94	0.30
	0°	0.97	0.81	0.95	0.39
	2°	0.93	0.14	0.98	0.88
Slope20%	-4°	0.97	0.74	0.89	***0.03****
	-2°	0.94	0.19	0.90	0.05
	0°	0.96	0.53	0.94	0.26
	2°	0.95	0.45	0.89	0.03
Slope30%	-4°	0.92	0.11	0.94	0.20
	-2°	0.96	0.45	0.95	0.42
	0°	0.95	0.44	0.97	0.73
	2°	0.96	0.60	0.97	0.83
Slope40%	-4°	0.96	0.62	0.96	0.46
	-2°	0.91	0.05	0.93	0.19
	0°	0.98	0.86	0.94	0.24
	2°	0.99	0.99	0.98	0.95
Slope50%	-4°	0.96	0.56	0.98	0.86
	-2°	0.93	0.13	0.97	0.67
	0°	0.97	0.74	0.96	0.50
	2°	0.97	0.72	0.97	0.72
Slope60%	-4°	0.94	0.24	0.95	0.35
	-2°	0.97	0.77	0.96	0.57
	0°	0.95	0.32	0.96	0.59
	2°	0.91	0.07	0.97	0.68
Slope70%	-4°	0.91	0.05	0.92	0.12
	-2°	0.93	0.15	0.95	0.44
	0°	0.88	***0.02****	0.92	0.11
	2°	0.97	0.69	0.92	0.10
Slope80%	-4°	0.95	0.37	0.97	0.76
	-2°	0.98	0.89	0.94	0.25
	0°	0.96	0.60	0.95	0.40
	2°	0.95	0.37	0.98	0.90
Slope90%	-4°	0.91	0.07	0.97	0.75
	-2°	0.90	0.04	0.97	0.85
	0°	0.95	0.34	0.97	0.66
	2°	0.96	0.64	0.97	0.84

Remark: slope10% stands for medial-lateral slopes at 10% of foot model length position

* *p*-value < 0.05

Appendix VII Result of the Shapiro-Wilk test (W) for dimensional parameters

Dimensional parameters	Subtalar joint orientation (positive as inversion)	Left		Right	
		W	*p*-value	W	*p*-value
Navicular Protrusion	-4°	0.97	0.84	0.97	0.83
	-2°	0.99	1.00	0.98	0.89
	0°	0.95	0.33	0.97	0.77
	2°	0.96	0.58	0.98	0.89
Navicular Height	-4°	0.91	0.08	0.96	0.58
	-2°	0.86	***0.01****	0.94	0.28
	0°	0.97	0.75	0.96	0.56
	2°	0.96	0.63	0.91	0.07
Metatarsal width	-4°	0.91	0.07	0.91	0.06
	-2°	0.89	***0.03****	0.86	***0.01****
	0°	0.89	***0.02****	0.88	***0.02****
	2°	0.98	0.95	0.92	0.11
Lateral Arch Height	-4°	0.94	0.30	0.87	***0.01****
	-2°	0.92	0.10	0.86	***0.01****
	0°	0.97	0.67	0.92	0.08
	2°	0.90	***0.04****	0.90	***0.04****
Medial Arch Height	-4°	0.95	0.43	0.95	0.31
	-2°	0.92	0.10	0.95	0.33
	0°	0.93	0.15	0.92	0.09
	2°	0.93	0.17	0.86	***0.01****

* *p*-value < 0.05

Appendix VIII Pairwise comparison of the 2-way repeated measure ANOVA statistical test between two subtalar joint orientations for the projection volumes

Projection volume	Subtalar angle (I)	Subtalar angle (J)	Mean Difference (I-J)	Std. Error	*p*-value	95% Confidence Interval	
						Lower bound	Upper bound
Under medial forefoot region ($Volume_{MF}$)	-4°	-2°	1008.12	232.7	0.00 *	322.90	1693.35
	-4°	0°	416.67	152.6	0.08	-32.64	865.99
	-4°	2°	887.96	173.7	0.00 *	376.60	1399.32
	-2°	0°	-591.45	217.6	0.08	-1232.25	49.35
	-2°	2°	-120.16	187.8	1.00	-673.02	432.69
	0°	2°	471.29	132.9	0.01 *	80.06	862.52
Under lateral forefoot region ($Volume_{LF}$)	-4°	-2°	60.23	93.41	1.00	-214.75	335.21
	-4°	0°	250.99	184.4	1.00	-292.04	794.03
	-4°	2°	186.44	126.2	0.94	-185.28	558.15
	-2°	0°	190.77	128.0	0.92	-186.29	567.83
	-2°	2°	126.21	120.7	1.00	-229.17	481.59
	0°	2°	-64.56	151.2	1.00	-509.69	380.58
Under medial midfoot region ($Volume_{MM}$)	-4°	-2°	2026.17	525.9	0.01 *	477.96	3574.37
	-4°	0°	-545.42	384.5	1.00	-1677.50	586.67
	-4°	2°	418.62	562.6	1.00	-1237.68	2074.92
	-2°	0°	-2571.59	417.5	0.00 *	-3800.93	-1342.24
	-2°	2°	-1607.55	445.4	0.01 *	-2918.78	-296.32
	0°	2°	964.04	559.2	0.61	-682.22	2610.29
Under lateral midfoot region ($Volume_{LM}$)	-4°	-2°	-280.98	221.6	1.00	-933.61	371.65
	-4°	0°	212.25	398.6	1.00	-961.18	1385.68
	-4°	2°	-16.13	314.2	1.00	-941.35	909.10
	-2°	0°	493.23	329.6	0.91	-477.28	1463.75
	-2°	2°	264.85	312.8	1.00	-656.03	1185.74
	0°	2°	-228.38	322.9	1.00	-1179.08	722.32
Under medial hindfoot region ($Volume_{MH}$)	-4°	-2°	1132.43	316.0	0.01 *	201.95	2062.91
	-4°	0°	-53.65	421.3	1.00	-1294.02	1186.73
	-4°	2°	145.88	315.3	1.00	-782.53	1074.28
	-2°	0°	-1186.08	299.6	0.01 *	-2068.31	-303.84
	-2°	2°	-986.55	235.0	0.00 *	-1678.52	-294.59
	0°	2°	199.52	376.3	1.00	-908.32	1307.36
Under lateral hindfoot region ($Volume_{LH}$)	-4°	-2°	74.65	115.0	1.00	-264.05	413.35
	-4°	0°	-64.30	136.7	1.00	-466.77	338.17
	-4°	2°	-10.42	108.8	1.00	-330.94	310.09
	-2°	0°	-138.95	130.5	1.00	-523.29	245.39
	-2°	2°	-85.08	125.6	1.00	-455.05	284.90
	0°	2°	53.88	112.5	1.00	-277.41	385.16

* *p*-value < 0.05

Appendix IX Pairwise comparison of the 2-way repeated measure ANOVA statistical test between two subtalar joint orientations for the medial-lateral slopes at 0-40% of foot model length positions

	Subtalar angle (I)	Subtalar angle (J)	Mean Difference (I-J)	Std. Error	*p*-value	95% Confidence Interval	
						Upper bound	Lower bound
Slope0% (MT)	-4°	-2°	-0.04	0.10	1.00	-0.24	0.32
	-4°	0°	0.16	0.15	1.00	-0.59	0.28
	-4°	2°	-0.05	0.12	1.00	-0.31	0.42
	-2°	0°	0.20	0.13	0.80	-0.57	0.17
	-2°	2°	-0.01	0.13	1.00	-0.38	0.40
	0°	2°	-0.21	0.13	0.77	-0.18	0.60
Slope10%	-4°	-2°	0.03	0.17	1.00	-0.52	0.47
	-4°	0°	-0.11	0.17	1.00	-0.39	0.60
	-4°	2°	-0.15	0.19	1.00	-0.40	0.71
	-2°	0°	-0.13	0.16	1.00	-0.34	0.60
	-2°	2°	-0.18	0.18	1.00	-0.36	0.72
	0°	2°	-0.04	0.15	1.00	-0.38	0.47
Slope20%	-4°	-2°	0.33	0.21	0.78	-0.94	0.28
	-4°	0°	-0.06	0.30	1.00	-0.82	0.93
	-4°	2°	0.07	0.36	1.00	-1.12	0.99
	-2°	0°	-0.38	0.19	0.33	-0.17	0.93
	-2°	2°	-0.26	0.24	1.00	-0.44	0.97
	0°	2°	0.12	0.26	1.00	-0.89	0.65
Slope30%	-4°	-2°	0.79	0.27	0.05 *	-1.58	0.00
	-4°	0°	-0.41	0.42	1.00	-0.83	1.65
	-4°	2°	-0.01	0.36	1.00	-1.05	1.06
	-2°	0°	-1.20	0.37	0.02 *	0.13	2.28
	-2°	2°	-0.80	0.24	0.02 *	0.08	1.51
	0°	2°	0.41	0.46	1.00	-1.76	0.94
Slope40%	-4°	-2°	0.99	0.30	0.02 *	-1.87	-0.12
	-4°	0°	-0.68	0.57	1.00	-1.00	2.35
	-4°	2°	0.50	0.47	1.00	-1.89	0.90
	-2°	0°	-1.67	0.55	0.04 *	0.05	3.29
	-2°	2°	-0.50	0.46	1.00	-0.87	1.86
	0°	2°	1.17	0.67	0.57	-3.14	0.80

Remark: slope10% stands for the medial lateral slope at 10% of foot model length position

* *p*-value < 0.05

Appendix X Pairwise comparison of the 2-way repeated measure ANOVA statistical test between two subtalar joint orientations for the medial-lateral slopes at 50-90% of foot model length positions

	Subtalar angle (I)	Subtalar angle (J)	Mean Difference (I-J)	Std. Error	*p*-value	95% Confidence Interval	
						Upper bound	Lower bound
Slope50%	-4°	-2°	0.72	0.40	0.5	-1.89	0.45
	-4°	0°	-0.33	0.67	1.0	-1.64	2.31
	-4°	2°	0.56	0.62	1.0	-2.40	1.28
	-2°	0°	-1.05	0.73	1.0	-1.11	3.22
	-2°	2°	-0.16	0.68	1.0	-1.85	2.17
	0°	2°	0.89	0.59	0.8	-2.63	0.85
Slope60%	-4°	-2°	0.47	0.47	1.0	-1.85	0.91
	-4°	0°	0.36	0.68	1.0	-2.36	1.65
	-4°	2°	1.13	0.58	0.4	-2.85	0.60
	-2°	0°	-0.11	0.87	1.0	-2.44	2.66
	-2°	2°	0.66	0.74	1.0	-2.82	1.51
	0°	2°	0.77	0.64	1.0	-2.66	1.12
Slope70%	-4°	-2°	0.26	0.36	1.0	-1.31	0.79
	-4°	0°	0.45	0.52	1.0	-1.99	1.09
	-4°	2°	1.16	0.63	0.4	-3.03	0.70
	-2°	0°	0.19	0.61	1.0	-1.99	1.61
	-2°	2°	0.90	0.62	0.9	-2.73	0.93
	0°	2°	0.71	0.59	1.0	-2.44	1.01
Slope80%	-4°	-2°	0.50	0.36	1.0	-1.56	0.57
	-4°	0°	0.14	0.45	1.0	-1.47	1.18
	-4°	2°	0.67	0.39	0.6	-1.83	0.48
	-2°	0°	-0.35	0.43	1.0	-0.92	1.62
	-2°	2°	0.18	0.38	1.0	-1.30	0.95
	0°	2°	0.53	0.35	0.8	-1.54	0.49
Slope90%	-4°	-2°	0.39	0.88	1.0	-2.99	2.21
	-4°	0°	1.37	1.13	1.0	-4.69	1.96
	-4°	2°	0.50	1.00	1.0	-3.45	2.44
	-2°	0°	0.98	0.77	1.0	-3.26	1.30
	-2°	2°	0.12	0.63	1.0	-1.97	1.74
	0°	2°	-0.86	0.65	1.0	-1.05	2.78

Remark: slope50% stands for the medial lateral slope at 50% of foot model length position

Appendix XI Pairwise comparison of the 2-way repeated measure ANOVA statistical test between two subtalar joint orientations for the dimensional measurements

	Subtalar angle (I)	Subtalar angle (J)	Mean Difference (I-J)	Std. Error	*p*-value	95% Confidence Interval	
						Upper bound	Lower bound
Medial Arch Height	-4°	-2°	0.50	0.24	0.2	-0.20	1.20
	-4°	0°	0.13	0.22	1.0	-0.51	0.76
	-4°	2°	0.58	0.25	0.2	-0.17	1.32
	-2°	0°	-0.38	0.20	0.4	-0.96	0.21
	-2°	2°	0.08	0.22	1.0	-0.58	0.73
	0°	2°	0.45	0.28	0.7	-0.37	1.27
Lateral Arch Height	-4°	-2°	-0.18	0.15	1.0	-0.61	0.26
	-4°	0°	0.43	0.20	0.3	-0.17	1.02
	-4°	2°	0.00	0.20	1.0	-0.59	0.59
	-2°	0°	0.60	0.14	0.0 *	0.19	1.01
	-2°	2°	0.18	0.20	1.0	-0.40	0.75
	0°	2°	-0.43	0.18	0.1	-0.94	0.09
Navicular Protrusion	-4°	-2°	0.40	0.21	0.4	-0.23	1.03
	-4°	0°	-0.04	0.32	1.0	-0.97	0.89
	-4°	2°	-0.19	0.33	1.0	-1.15	0.77
	-2°	0°	-0.44	0.31	1.0	-1.35	0.47
	-2°	2°	-0.59	0.33	0.5	-1.55	0.37
	0°	2°	-0.15	0.32	1.0	-1.09	0.79
Navicular height	-4°	-2°	-0.54	0.92	1.0	-3.24	2.16
	-4°	0°	-1.34	0.99	1.0	-4.26	1.59
	-4°	2°	-0.08	0.90	1.0	-2.74	2.58
	-2°	0°	-0.79	1.23	1.0	-4.42	2.84
	-2°	2°	0.46	1.17	1.0	-2.98	3.90
	0°	2°	1.25	0.93	1.0	-1.49	3.99
Metatarsal width	-4°	-2°	-0.14	0.33	1.0	-1.12	0.84
	-4°	0°	-0.37	0.41	1.0	-1.58	0.84
	-4°	2°	-0.32	0.58	1.0	-2.04	1.39
	-2°	0°	-0.23	0.51	1.0	-1.72	1.26
	-2°	2°	-0.18	0.65	1.0	-2.11	1.74
	0°	2°	0.05	0.47	1.0	-1.34	1.44

* *p*-value < 0.05